Marquette University
e-Publications@Marquette

Dissertations (2009 -) | Dissertations, Theses, and Professional Projects

Sensorimotor Control of 3D Arm Movement and Stability in Post-Stroke Hemiparesis

Kakanand Alfonsomarie SrungBoonmee
Marquette University

Recommended Citation
SrungBoonmee, Kakanand Alfonsomarie, "Sensorimotor Control of 3D Arm Movement and Stability in Post-Stroke Hemiparesis" (2011). *Dissertations (2009 -)*. Paper 142.
http://epublications.marquette.edu/dissertations_mu/142

SENSORIMOTOR CONTROL OF 3D ARM MOVEMENT AND STABILITY IN POST-STROKE HEMIPARESIS

by

Kakanand A. SrungBoonmee, M.Eng.

A Dissertation submitted to the Faculty of the Graduate School,
Marquette University,
in Partial Fulfillment of the Requirements for
the Degree of Doctor of Philosophy

Milwaukee, Wisconsin

August 2011

ABSTRACT
SENSORIMOTOR CONTROL OF 3D ARM MOVEMENT AND STABILITY IN POST-STROKE HEMIPARESIS

Kakanand A. SrungBoonmee, M.Eng.

Marquette University, 2011

Deficits of the affected arm in people with post-stroke hemiparesis have been generally associated with decreased strength and increased spasticity. These deficits are varied in proximal (shoulder) and distal (elbow) joints which results in an overall impairment during movement or during stabilization of hand position in space. In this study, reaching of the hemiparetic arm in 3D workspace was characterized by a curved and non-smooth endpoint trajectory and a reduced functional range of motion, compared to the unimpaired arm. Smoother trajectories were observed in the acceleration phase more than the deceleration phase, which was common to both the stroke subjects and the neurologically intact controls. Decreased range of motion of the paretic arm in the proximal joint was associated with shoulder weakness, whereas limited range of motion in the elbow appeared to be due to increased antagonist muscle activation. In a task requiring subjects to stabilize their hand at different positions in space, arm weakness and movement synergy constraints may have contributed to stroke survivors generally decreasing the plane of elevation in order to maintain stable arm postures during movement and then stabilize the hand in space. The degree of decreased plane of elevation was negatively correlated with the Fugl-Meyer score. For a task when fine control movement was required simultaneously with a stable arm posture, stroke subjects demonstrated an inability to grade fine muscle control, resulting in larger range of the plane of elevation movements and larger endpoint error. These findings suggest that shoulder strength training might have important implications to the recovery of movement and ability to stabilize the hemiparetic arm during functional tasks.

ACKNOWLEDGMENTS

Kakanand A. SrungBoonmee, M.Eng.

Writing my dissertation has been both the most trying and most rewarding experience for me. I am both proud and humble by the final product, as it tremendously contributes to our knowledge on the movement of hemiparetic arm, and to the advancement of science in general. Throughout these years I have faced many challenges and obstacles, but I finally overcame them. I could not have done it alone, and owe endless thanks to many people that have, in one way or many, helped me through many tough times.

I am most grateful to my advisor, Dr. Brian Schmit, for his excellent support and incomparable mentorship. His guidance has helped me overcome countless obstacles throughout my dissertation.

Special thanks are owed to all my committee members—Dr. Robert Scheidt, Dr. Scott Beardsley, Dr. Na Jin Seo and Dr. Allison Hyngstrom. They have all taken time to read my drafts and give me the suggestions and feedback. Their involvement is not only during the research stage of my PhD. Program, but also throughout all the years at Marquette. I would like to specially thank Dr. Hyngstrom for all the Fugl-Meyer score assessment that she has done for me, in addition to the mental support and various suggestions in experiments. I am also grateful to Dr. Robert Scheidt who let me use his OPTOTRAK system throughout all my studies.

The members of the Integrative Neural Engineering & Rehabilitation Laboratory have also played a vital role in my PhD career in providing their very helpful feedbacks during my presentation. Each one of them contributed to help me in different ways. Ryan, Ben and Eric helped me figure out the signal processing problems. Ryan and Tanya read my drafts. Tanya has also lent me her car seat for me to use as a comfortable experiment chair.

This project could not have been completed without the stroke and control subjects who volunteered to participate in all my studies. Their time and cooperation are greatly appreciated. To them I also owe special thanks. Financial support for my study comes from the NIH grant # R01-NS052509 and the Royal Thai government scholarship.

I would like to thank my family for all their love and support, especially my brother, Ty, who is with me all the years at Marquette, to my dad who inspires me to pursue the PhD, to my mom and my brother, Piyes, for constant mental support.

Finally, I would like to thank God for everything that He had given me.

TABLE OF CONTENTS

LIST OF TABLES

LIST OF FIGURES

LIST OF ABBREVIATIONS

2D	two-dimensional
3D	three-dimensional
AC	acromion
ADT	anterior deltoid
ANOVA	the analysis of variance
BI	(long head of) biceps
BRD	brachioradialis
CCW	counterclockwise
CW	clockwise
D	dominant arm
ECR	extensor carpi radialis
EL	the lateral epicondyles of the humerus
EM	the medial epicondyles of the humerus
EMG	electromyography
EMG_{avg}	average electromyographic value
EMG_{rms}	the root-mean-square of the filtered electromyographic data
F	female
FCR	flexor carpi radialis
FM	Fugl-Meyer
fps	frame per second
GH	glenohumeral joint rotation center
Hz	Hertz

IRED	infrared emitting diode
l	movement amplitude
L	left
LED	light-emitting diode
M	male
MVC	isometric maximum voluntary contractions
ND	nondominant arm
NJS	normalized jerk score
NP	nonparetic arm
NS	not significant
P	paretic arm
PDT	posterior deltoid
PECS	pectoralis major
R	right
$RMSE_{xy}$	root-mean-square error of laser pointer and desired cursor positions
RS	the styloid processes of the radius
SE	standard error of the sample mean
t	movement time
t_{off}	the movement offset
t_{on}	the movement onset
TRI	(lateral head of) triceps
US	the styloid processes of the ulna
Vavg	average tracking velocity
V_{max}	peak tangential velocity
Vstd	standard deviation of the tracking velocity

CHAPTER 1: LITERATURE REVIEW

1.1 INTRODUCTION

Stroke is a leading-cause of disability due in part from the sharp decrease in death rate from stroke in the United States. According to the American Heart Association, the drop in death rate from stroke was 33.5% in 10 years, from 1996 to 2006, leaving over 3.5 million stroke survivors (Patten, Lexell & Brown, 2004). Approximately one fourth of newly diagnosed stroke patients develop hemiparesis (Zorowitz, Chen, Tong, & Laouri, 2009), which interferes with daily living activities. Diverse rehabilitation methods have been implemented to help regain normal functional movement in people with post-stroke hemiparesis. The important factor in developing effective rehabilitation strategies is knowledge of underlying mechanisms and characteristics of sensorimotor impairment post stroke. This dissertation aimed to characterize and understand the deficits in control of arm movement in people with post-stroke hemiparesis by performing a comprehensive analysis of different three-dimensional movement tasks and determining the commonality of the impairments. The ultimate goal was to provide a better understanding of the characteristics of upper-extremity hemiparesis.

This chapter provides literature reviews on the research and state-of-the-art knowledge of control of arm movement in post-stroke hemiparesis, based on the impairment characteristics and possible underlying mechanisms. Sensory augmentation that has been used to improve movement and stability post stroke is also reviewed. Finally the aims of overall study are summarized.

1.2 ARM MOTION IN POST-STROKE HEMIPARESIS

Deficits of multijoint reaching movements in people with post-stroke hemiparesis are primarily associated with spasticity (Mottram, Suresh, Heckman, Gorassini, & Rymer, 2009), weakness (Mercier & Bourbonnais, 2004), and an inability to isolate individual joint movements (Zackowski, Dromerick, Sahrmann, Thach, & Bastain, 2004) as summarized in the following paragraphs.

Following stroke, corticospinal drive is decreased due to the injury and the descending motor commands rely more on reticular pathways, which are not inhibited following a cortical injury (Gracies, 2005). The combined decrease in descending corticospinal inhibition and increase in reticulospinal drive could contribute to the hyperexcitability of stretch reflexes that is observed in stroke survivors. Spasticity is defined as a velocity-dependent increase in tonic stretch reflexes (Lance, 1990) and is believed to result from hyperexcitability of the tonic stretch reflex (Schmit, Dhaher, Dawald, & Rymer, 1999). In the arm flexor muscles, the hyperexcitability appears to be linked to an abnormal enhanced synaptic input to motoneurons of the biceps, rather than increased persistent inward currents (Mottram et al., 2009). It has also been shown that spasticity is more pronounced in distal musculature (Nielsen & Sinkjar, 1996).

Weakness, as opposed to strength, is defined as a decrease in maximal voluntary torque or force generation compared to the normal (Bohannon, 1995). It is a direct effect following decreased descending drive post stroke. Both structural and neural factors contribute to upper-extremity weakness post-stroke although all of the mechanisms are not well-understood. Structural factors contributing to post-stroke weakness relate to

muscle atrophy, which is associated with a reduction in the paretic arm motion and muscle activity (Patten et al., 2004). Strong evidence for an additional contribution of neural factors is supported by observations that weakness is also found in the less affected arm (Andrews & Bohannon, 2000). Not only are the magnitude of force and torque generation impaired post stroke, the time to generate force and torque is also impaired (McCrea, Eng, & Hodgson, 2003).

Flexor and extensor synergies are common patterns of discoordination post stroke. The flexor synergy pattern consists of shoulder retraction and elevation, external rotation and abduction, elbow flexion and supination of the forearm. For the extensor synergy, the pattern consists of shoulder adduction and internal rotation, elbow extension and pronation of the forearm (Brunnstrom, 1970). This abnormal muscle coordination is suggested to receive a contribution from reflex pathways (Trumbower, Ravichandran, Krutky, & Perreault, 2008); specifically, the neural coupling between shoulder and elbow muscles can be modulated by voluntary drive (Sangani, Starsky, McGuire, & Schmit, 2009).

Weakness, spasticity and abnormal synergy contribute to impairments of arm movement in people with post-stroke hemiparesis. The integrity of movement control can be quantified by movement smoothness. The trajectory of normal reaching is characterized as straight line with a bell-shaped speed profile (Flash & Hogan, 1985). Post-stroke hemiparesis reaching trajectories often lack of smoothness, as manifested by a multi-peak velocity profile during point-to-point reaching (Kamper, Mc-Kenna-Cole, Kahn, & Reinkensmeyer, 2002). The non-smooth movement originates from both peripheral deficits and an alteration in neuromotor control post-stroke. In the case of

multi-joint movement, the inability to coordinate movement is suggested to cause a non-smooth trajectory (Levin, 1996). However, non-smoothness of movement trajectory is also observed in a single-joint movement of the elbow (Taso & Mirbagheri, 2007), indicating the non-smooth movement of the paretic arm could be a consequence of deficits in global movement planning (Levin, 1996). In addition to the non-smooth endpoint trajectory, movement of the paretic arm often initiates in an inaccurate initial direction (Reinkensmeyer, McKenna-Cole, Kahn, & Kamper, 2002) because of the inability to control the interaction torques required to initiate multijoint movements (Beer, Dewald, & Rymer, 2000).

1.3 ARM STABILITY IN POST-STROKE HEMIPARESIS

Control of posture and movement has been hypothesized to use either separate controllers (Scheidt & Ghez, 2007) or a single controller (Feldman & Levin, 1995). Both theories have supporting evidences in neurophysiology for either distinct centers for movement and stabilization (Kurtzer, Herter, & Scott, 2005) or common centers (Sergio, Hamel-Paquet, & Kalaska, 2005). For motor control experiments, supportive evidence has been found for both separate controllers (Scheidt & Ghez, 2007; Burdet et al, 2006) and a single controller (Pilon, De Serres, & Feldman, 2007; Foisy & Feldman, 2006). The study of stability of the arm has been done mostly in the context of a stabilizing task in a force field to determine the ability to maintain a stable endpoint in the destabilizing force field.

Motor control strategies to stabilize arm posture include a strategy to appropriately increase the limb impedance through muscle coactivation (Gribble & Ostry, 1998) and a strategy to adjust the arm posture in the direction that minimizes instability (Franklin et al., 2007). Increased co-contraction has been associated with an increase in the overall stretch reflex threshold (Milner, Cloutier, Leger, & Franklin, 1995). A decreased stretch reflex threshold is observed in spastic hemiparetic subjects (Levin & Feldman, 1994). In fact, muscle weakness and lack of reflex adaptation are believed to contribute to functional joint instability post stroke (Meskers et al., 2009). Regarding motor adaptation, specifically to a novel force field, Scheidt and Stoeckmann (2007) has found that stroke subjects are less effective than healthy subjects at adapting reaches to perturbations, even though they use the same compensatory strategy as healthy subjects. Trajectory adaptation and final position regulation deficits are significantly dependent on the integrity of limb proprioception and the amount of time post stroke (Scheidt & Stoeckmann, 2007).

1.4 THE ROLE OF PROPRIOCEPTION IN MOVEMENT AND STABILITY

1.4.1 Proprioception

The sensorimotor system consists of afferent, efferent and central integration and processing components. Proprioceptive information is encoded by a neural population of receptors and transferred to the CNS (Aimonetti, Hospod, Roll, & Ribot-Ciscar, 2007) which ascends via either the dorsal lateral tract or the spinocerebellar tract. The dorsal

lateral tract conveys the "conscious proprioception" (i.e. touch, pressure and vibration) and the spinocerebellar tract conveys the "nonconscious proprioception" (i.e. limb position, joint angles and muscle length and tension) that is used for reflexive, automatic and voluntary activities (Riemann & Lephart, 2002). Receptors for nonconscious proprioception include joint receptors and muscle spindles. Muscle spindles are sensitive to muscle length change and speed (group Ia-afferents from the primary endings) and muscle length change alone (group II-afferent from the secondary endings). Therefore the primary endings are believed to contribute to the sense of limb position and movement while the secondary endings contribute only to the sense of limb position (Matthews, 1972). Cutaneous receptors are responsible for conscious proprioception (Kandel, James, & Thomas, 2000).

Proprioception is associated with different regions of the brain in both hemispheres and at both cortical and subcortical levels. Regions in contralateral primary motor cortex (M1), primary sensory cortex (S1), the dorsal premotor cortex (PMD), caudal parts of the supplementary motor (SMA) and cingulate motor areas (CMA) are involved in the processing of the proprioceptive feedback. Within the premotor cortical region, the bilateral rolandic operculum and contralateral supplementary motor area have been linked with proprioception (Naito et al., 2007). As for the subcortical regions, the ipsilateral cerebellum and contralateral putamen are also mentioned in connection with proprioception (Niessen et al., 2008).

Proprioceptive information plays a major role in arm motion and ability to maintain a stable arm posture. According to Sarlegna and Sainburg (2009), proprioception is critical for the transformation of a motor plan into motor commands

that are sent to the arm muscles. It is used to update the internal model of limb mechanics, anticipating impending mechanical interactions. Proprioception also provides initial information about limb posture essential for motor planning, as when limb proprioception is altered (by means of vibration) in the absence of visual feedback, the final position is systematically altered (Larish, Volp, & Wallace, 1984). Specifically, terminal errors have also been shown to increase when the initial limb position is not correctly determined from altered proprioception (Larish et al., 1984; Sarlegna & Sainburg, 2009).

1.4.2 Proprioception deficit post stroke

Proprioception and tactile sensation impairments are frequently found in people post stroke. Sensory impairment has been associated with weakness and degree of stroke severity (Tyson, Hanley, Chillala, Selley & Tallis, 2008). Recovery of somatosensory modalities, particularly the proprioceptive sense, has been observed in longitudinal studies and corresponds with enhanced functional ability (Winward, Halligan, & Wade, 2007).

The integrity of limb proprioception is believed to contribute to abnormal movement post-stroke (Scheidt and Stoeckman, 2007). Improved proprioception may improve the movement post stroke. Niessen et al. (2008) found that shoulder proprioception is deteriorated in individuals post-stroke, and that deterioration is found in both arms, which is indicative of the problem of central integration and processing of

proprioception. As reviewed previously, the sites associated with proprioception integration and processing within the brain are dispersed in several locations.

1.5 SENSORY MANIPULATION

1.5.1 Tendon vibration

Tendon vibration at a constant low amplitude (0.2-0.5mm) is known to activate muscle spindles, specifically Ia-afferents fire harmonically with vibration frequency up to 80 Hz (Roll, Vedel, & Ribot, 1989). This selective characteristic of tendon vibration has been used as a technique to study the effect of Ia-afferent firing and altered proprioception, since tendon vibration can cause a proprioceptive illusion of the vibrated joint (Cordo, Gurfinkel, Bevan, & Kerr, 1995). Vibration also affects proximal joint stability when applied distally. Shirahashi and colleagues (2007) reported a case of applying vibration to the palm, which enhanced shoulder stability in hemiparetic arm. In 2D planar supported movement, vibration applied at the wrist flexor has found to increase shoulder stability in stroke subjects, which is not likely to originate from increased arm stiffness due to no systematic changes in arm stiffness in response to tendon vibration (Conrad, Scheidt, & Schmit, 2011).

1.5.2 Electrical stimulation

Cutaneous electrical stimulation has a positive effect in chronic stroke patients, as demonstrated in the limb sensation and the configuration of somatic evoked potential (SEP) of the paretic limb (Peurala, Pitkanen, Sivenius, & Tarkka, 2002). Electrical stimulation of the median nerve increases the pinch strength (Conforto, Kaelin-Lang, & Cohen, 2002) and improves performance of functional hand training (Conforto, Cohen, dos Santos, Scaff, & Marie, 2007), which could result from altered corticomotor excitability after electrical stimulation on the median nerve (Ridding, Brouwer, Miles, Pitcher, & Thompson, 2000).

1.6 SPECIFIC AIMS

The purpose of this dissertation was to understand how the common deficits post stroke (i.e. weakness, spasticity and abnormal synergy) affect movement in three-dimensional space of people with post-stroke hemiparesis. Comprehensive analysis of three dimensional movement (i.e. end point trajectory, joint kinematic and electromyography) was performed in order to see the commonality of impairments in different 3D movement tasks. As previously stated, arm trajectory and hand final position might be controlled separately. Thus, characterizing movement and stability was done in 3 specific study aims. First, the reaching trajectory was studied (Aim 1), followed by study of an arm stabilizing task (Aim 2) and finally examining a task involving the combination of movement and stability (Aim 3). Tendon vibration, as a possible intervention to improve arm stability post-stroke, and electrical stimulation of the median nerve, as an sensory-augmented strategy to improve the hand function, were

applied to the subjects in order to examine the role of sensory manipulation on 3D arm control in people with post-stroke hemiparesis. The work of this study will contribute to a better understanding of the sensorimotor characteristics of people with post-stroke hemiparesis.

1.6.1 Aim 1

The goal of the first aim (Chapter 2) was to characterize 3D unsupported targeted reaching post stroke. Subjects were instructed to make a rapid reach to one of six targets appearing in front of the subject. Targets were located beyond the reach. Reaching trajectory smoothness, joint kinematics and electromyography during reaching were quantified to characterize 3D targeted reaching post-stroke in comparison to reaching made by neurologically intact subjects. We hypothesized that reaching in stroke subjects might contain both preserved and impaired characteristics.

1.6.2 Aim 2

In the second aim (Chapter 3), we examined the ability of stroke subjects to stabilize the arm at different locations in 3D space. The objective was to characterize the stability of the paretic arm in different locations, therefore different postures, in the attainable workspace. The roles of tendon vibration and electrical stimulation on improving endpoint stability were also examined. Endpoint stability, joint kinematics and electromyography during stabilization were quantified. The endpoint instability in the 3D workspace for stroke subjects was hypothesized to be greater than the

neurologically intact subjects and tendon vibration was hypothesized to improve the endpoint stability of the paretic arm.

1.6.3 Aim 3

The objective of the study in the third aim (Chapter 4) was to investigate the motor performance of stroke subjects in a task that required simultaneous movement and stability of the arm. A 3D tracking task was selected so that subjects could simultaneously use fine control of movement to track a target on a screen using a laser pointer while stabilizing the arm in space. Similar to the studies in the previous aims, tracking trajectory performances, joint kinematics an electromyography were quantified. It was hypothesized that deficits in arm stability and fine motor control post stroke would be manifested in the task performance.

CHAPTER 2: CHARACTERIZING THREE-DIMENSIONAL TARGETED REACHING IN SUBJECTS WITH POST-STROKE HEMIPARESIS

2.1 INTRODUCTION

The development of effective rehabilitation approaches requires a fundamental understanding of the deficits underlying abnormal reaching movements in persons with hemiparesis in order to develop effective rehabilitation approaches. The purpose of this study was to characterize 3D targeted reaching in people with post-stroke hemiparesis. In general, characterizing the features of reaching movements post-stroke is essential for rehabilitation practice and research because reaching is a basic movement involved in many activities of daily living (McCrea, Eng & Hodgson, 2005). Thus, an improved understanding of the effects of stroke on the kinematics and muscle activity patterns of the stroke arm during reaching would be valuable in the development of new rehabilitation strategies for improving arm function.

Multijoint arm movement during 2D planar movement in stroke subjects is characterized by decreased endpoint velocity (Cirstea & Levin, 2000), limited elbow active range of motion (Beer et al., 2000), segmentation of movements (Krebs, Aisen, Volpe, & Hogan, 1999), discoordination (Beer, Dewald, Dawson, & Rymer, 2004) due to abnormal interaction torques (Beer et al., 2000) associated with the synergy patterns (Brunnstrom, 1970), and decreased trajectory smoothness (Rohrer et al., 2004). Similar to 2D arm-supported reaching, reaching in the 3D workspace is characterized by decreased endpoint velocity (Cirstea & Levin, 2000; Kamper et al, 2002), limited active

range of motion (Kamper et al, 2002), discoordination (Cirstea & Levin, 2000; Levin, 1996) while utilizing a compensatory strategy (Cirstea and Levin, 2000), increased trajectory curvature (Levin, 1996) and decreased trajectory smoothness (Kamper et al, 2002).

Straightness of arm trajectory is associated with motor recovery post stroke (Rohrer et al., 2002). Endpoint trajectory smoothness in post-stroke arm movement has been quantified by the number of speed peaks (Kamper et al, 2002), number of high-curvature transitions (Goldvasser, McGibbon, & Krebs, 2001), correlation of the actual velocity profile and the idealized bell-shape velocity profile (Daly et al, 2005), integrated absolute jerk (Goldvasser et al, 2001), the jerk metric (Rohrer et al, 2002) and normalized jerk score (Caimmi et al, 2008). Generally, the reaching trajectory post-stroke is observed to be less smooth than normal reaching, with velocity profiles that deviate from the symmetrical bell-shape velocity profile for straight line movement. Characterizing the trajectory of 3D targeted reaching in the current study was done using one of the minimum-jerk based metrics, the normalized jerk score, as it captures the basis of straight-line reaching (i.e. to minimize the jerk) and accounts for both curvature and fluctuation of the reaching trajectory. Since asymmetrical velocity profiles have been observed in several studies of normal reaching (Nagasaki, 1989; Lan & Crago, 1994; Wiegner & Wierzbicka, 1992) and post-stroke reaching (Krebs, Aisen, Volpe, & Hogan, 1999), quantifying the trajectory smoothness separately in acceleration and deceleration phases of the trajectories was done in the current study to examine the possible mechanisms underlying trajectory non-smoothness post stroke.

In summary, this study aimed to characterize the biomechanical and physiological features of post-stroke hemiparetic reaching in the 3D workspace in order to identify impairments and correlate them with the levels of clinical impairment post-stroke. The findings may have implications for identifying appropriate rehabilitation techniques and also for the study of motor control of normal reaching.

2.2 MATERIALS AND METHODS

2.2.1 Subjects

Eleven chronic stroke subjects with upper extremity hemiparesis (Mean ± SD, 57.6 ± 7.7 years) between 1 and 24 years post stroke (Mean ± SD, 9.7 ± 8. 6 years) and five age-matched neurologically intact control subjects (Mean ± SD, 51.0± 7.3 years) participated in this study (Table 2 -1). Inclusion criteria for participation in the study were that the subjects be at least 21 years of age and have a history of stroke (> 6 months) resulting in upper extremity hemiparesis. Exclusion criteria included: recent treatment using botulinum toxin injection in the upper extremity (< 2 months), a diagnosis of another neuromuscular disorder, the inability to give informed consent, apraxia, multiple strokes, chronic neck, shoulder or back pain, inability to complete minimum shoulder active range of motion (shoulder elevation of 30 degrees) and the inability to follow two –step commands. A licensed physical therapist conducted the upper-extremity Fugl-Meyer Assessment of Physical Performance (Fugl-Meyer 1975) prior to the experiment. The participants' upper extremity Fugl-Meyer score (FM score) ranged from 20 to 63

(Mean ± SD, 44. 4 ± 14.4). The study was initiated after subjects had given informed consent, in compliance with protocols approved by the Institutional Review Board of Marquette University.

Table 2-1 Subject information

Subject	Sex	Age (Years)	Paretic Side	Dominant Arm	Years after Incidence	FM Score[#]
1S	M	53	R	R	2	36
2S	F	57	L	R	3.5	50
3S	F	58	L	R	22	26
4S	F	57	R	R	18	57
5S	F	51	R	R	15	63
6S	F	75	R	R	8	20
7S	M	44	R	R	1	56
8S	M	56	R	R	9	42
9S	M	60	R	R	2	38
10S	F	62	R	R	24	38
11S	F	61	L	R	2	62
12C	F	43	-	L	-	-
13C	F	56	-	R	-	-
14C	F	57	-	R	-	-
15C	M	56	-	R	-	-
16C	M	43	-	R	-	-

[#] Based on Upper Extremity FM score; 0-66

2.2.2 Test Apparatus

The experimental apparatus consisted of six targets (5-mm diameter LEDs) aligned horizontally on a board in two rows (upper row at shoulder height and lower row at waist height), and vertically in three columns (medially, centrally and laterally) located with respect to the subject's paretic side as illustrated in Figure 2-1. The timing of the

LED sequence was controlled using a custom LabVIEW program and a data acquisition device (NI USB – 6229, NI Corporation, TX, USA).

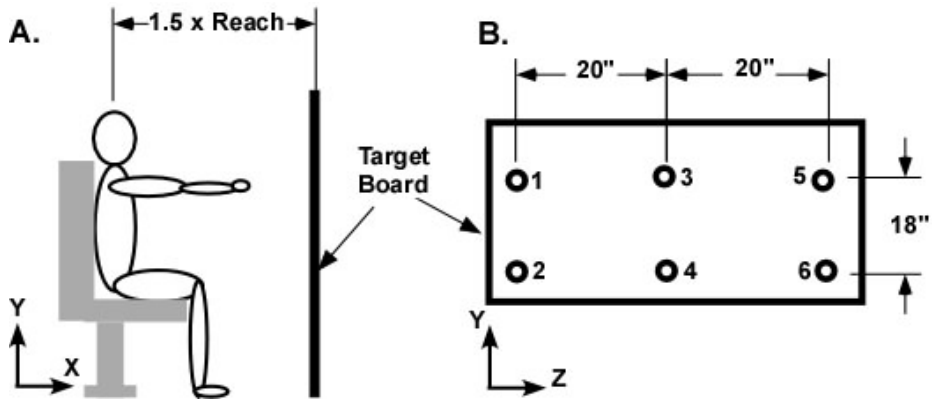

Figure 2-1: Experimental Set-Up. A. Sagittal view of the experimental set-up and **B.** frontal view of the target board with 6 LEDs arranged in 2 rows by 3 columns.

Surface electromyography (EMG) was collected at 1000 Hz from eight arm muscles: the pectoralis major (PECS), anterior deltoid (ADT), posterior deltoid (PDT), long head of biceps (BI), lateral head of triceps (TRI), brachioradialis (BRD), flexor carpi radialis (FCR) and extensor carpi radialis (ECR). Disposable Ag/AgCl electrodes (Vermed Medical, Bellows Falls, VT) were placed over the muscle bellies on lightly abraded skin and the signals were amplified (x1000) and low-pass filtered (500 Hz) prior to sampling (Bortec Medical AMT-16; Calgary, Alberta, CA). The EMG signals were recorded using a data acquisition device (NI USB – 6229, NI Corporation, TX, USA) and a custom-written LabVIEW program.

Kinematic data were collected at 100 Hz using a camera-based tracking system (OPTOTRAK 3020, Northern Digital, Ontario, Canada). The OPTOTRAK cameras track infrared emitting diode (IRED) markers, which were fastened to two flexible custom Aquaplast® (WFR-Aquaplast/Qfix Systems, Avondale, PA) orthoses. Eight and nine IRED markers were placed on the upper and lower arm orthoses, respectively, and served as the tracking markers (real markers). Markers on the orthoses were arranged so that a minimum of three markers could be seen by the camera at every angle of arm orientation throughout the experiment.

Prior to beginning the experiment, a static calibration was performed in order to register the bony landmark positions (virtual markers) to the local frames of reference of the tracking markers (real markers) on the orthoses. In other words, static calibration provided the relative positions of virtual markers to the real markers so that the Optotrak software could compute the virtual markers from the detected real markers. During the static calibration, the IRED markers were placed on the following bony landmarks – the acromion (AC), the medial and the lateral epicondyles of the humerus (EM and EL, respectively) and the styloid processes of the radius (RS) and ulna (US). The bony landmark markers were removed after the static calibration, which was done to obtain the relative position to the real markers and register them to the virtual markers. The virtual markers were then used to calculate the rigid body coordinates of the upper arm and lower arm. The AC virtual marker was used to approximate the glenohumeral joint rotation center (GH) by translating the AC position 14 mm laterally, 37 mm downward and 8 mm to the front (Wang, 1999).

The rigid body of the upper arm consisted of the virtual GH, EM, EL and the cluster of 8 real markers attached at the upper arm. The lower arm segment consisted of the virtual EM, EL, RS and US markers and the 9 real markers placed on the forearm. The real markers at each frame of data collection were used to calculate the position of the virtual markers using Toolbench® v. 1.1 (Northern Digital, Ontario, Canada). Missing marker positions were filled by cubic spline interpolation and then the 3D position data were low-pass filtered (cutoff frequency = 5 Hz) using a 2nd order zero-phase Butterworth filter.

2.2.3 Experimental Protocol

Before beginning the experiment, each subject performed isometric maximum voluntary contractions (MVCs) of the paretic arm muscles for shoulder flexion/extension, elbow flexion/extension and wrist flexion/extension. Subjects were given manual resistance to the arm in positions consistent with the standard Manual Muscle Testing procedures (Kendall, McCreary, & Provance, 1993). EMG during MVCs was recorded over approximately three seconds of maximum effort. The EMG measured during the MVC was used to assess the ability to activate each muscle group for each subject.

All subjects performed a series of fast reach and hold tasks. The stroke subjects were tested with their paretic arm while the control subjects were tested with their dominant arm. Subjects were seated in an armless stationary chair and positioned approximately 1.5 x arm length away from the target board (Figure 2A). At the beginning of the experiment, the subject's arm rested on a height-adjustable table with

the elbow flexed to 90 degrees and the shoulder in 0 degree ("home position"). A trunk strap was fastened around the waist to limit trunk movement and help trunk stabilization. The subjects were cued to reach by an auditory tone that sounded when one of the six LED targets was lit on the board. Subjects were instructed to reach with a loose fist "as fast as possible" from the resting home position towards the lit LED target and were asked to hold their arm at the end of the reach so that the fist blocked the light from their vision. No instruction on accuracy was given. The LED target remained lit for five seconds and subjects were asked to hold the arm at the final position. When the LED turned off and another audible cue sounded, the subject was to bring the arm back to the home position and wait for the next trial. If a subject could not move to the final position during the initial movement, the subject was allowed to continue to moving towards the target until the stop cue was sensed. There was enough time between trials to allow time for muscle relaxation before the next trial, which was randomized between 5-7 seconds to minimize movement in anticipation of the next trial. Practice trials for each target were given prior to the experiment. The subjects were allowed to practice as many times as they wanted to until they were comfortable with the task. Generally, the subjects were comfortable with the task after one reach toward each of the six targets. After practice, at least a 5 – minute break was allowed before the experiment.

The data used in this study were taken from a longer, more complex unpublished experiment that evaluated the effect of electrical stimulation on arm movements in post-stroke hemiparesis. Only the non-stimulation trials were analyzed for the present study. The data were obtained from 2 experimental protocols – a block design and a random design. The block protocol was applied to Subjects 1S-5S and the continuous protocol

was applied to Subjects 6S-11S and 12C-16C. In the block protocol, there were 5 blocks with 12 reaches each, including blocks of 'stimulation' and 'non-stimulation' for each target; both the order of the target position and application of stimulation were randomized. Between each of the 5 blocks the subjects were allowed to take a 1-2 minute break. For the random protocol, there were 30 randomized reaches in one block consisting of 5 reaches to each of 6 targets. The data were carefully analyzed for the effect of different experimental protocols, as explained in 'Data Analysis' section, to assure appropriate use of the non-stimulation trials from both protocols to characterize the reaching movement in people with post-stroke hemiparesis.

2.2. 4 Data Analysis

The smoothness of the wrist segment trajectory (which was calculated from the midpoint between the US and RS virtual markers) was quantified using the normalized jerk score (NJS). This measure has been used extensively in motor control studies to quantify movement smoothness (Teulings, Contreras-Vidal, Stelmach, & Adler, 1997; Seidler, Alberts, & Stelmach, 2001; Tsao & Mirbagheri, 2007) and is shown in the equation 2-1.

$$NJS = \sqrt{\frac{1}{2} * \int \left(\left(\frac{d^3x}{dt^3} \right)^2 + \left(\frac{d^3y}{dt^3} \right)^2 + \left(\frac{d^3z}{dt^3} \right)^2 \right) dt * \left(t^5 / l^2 \right)} \quad (2\text{-}1)$$

where NJS = Normalized Jerk Score,

(x, y, z) = position coordinates,

t = movement time (ms),

l = movement amplitude (mm).

NJS is the integrated squared jerk (the 3rd derivative of position) normalized by the corresponding time interval and movement amplitude. The squared tangential jerk was integrated over the entire reach period. The reach period ($t = t_{off} - t_{on}$) was defined using the peak tangential velocity (V_{max}) where the movement onset (t_{on}) and offset (t_{off}) occurred at the points in time when the tangential velocity exceeded and fell below 20 % of V_{max}, respectively. NJS was also computed separately during the acceleration (from onset to V_{max}) and deceleration (from V_{max} to offset) portions of the movement. High NJS indicates non-smooth and curved trajectory.

Joint angles (shoulder elevation, shoulder plane of elevation, humeral rotation and elbow flexion) were calculated from the positions of the virtual markers of the specified bony landmarks (GH, EL, EM, US and RS) as described in Appendix A. They were used to quantitatively describe the dynamic motion of the arm in joint space and the range of motion in terms of the joint angle at the final position. Joint angles at the final position were defined as the angles at the end of the reach (t_{off}).

All the EMG signals were bandpass filtered (10-350 Hz) and then notch filtered to remove the line noise (58 -62 Hz) using a 4th order zero-phase Butterworth filter. The

root-mean-square (RMS) of the filtered data (EMG_{rms}) was calculated using a 50-ms moving window. The average EMG (EMG_{avg}) was obtained by integrating the EMG_{rms} over the specified period of time and dividing by its respective time period (between T_2 and T_1 in Equation 2-2), whether it was the reach, acceleration or deceleration periods.

$$EMG_{avg} = \frac{1}{T_2 - T_1}\int_{T_1}^{T_2}(EMG_{rms})\,dt \qquad (2\text{-}2)$$

To assure appropriate use of the non-stimulation trials from both random and block protocols, a 2-way (6 targets x 2 protocols) repeated measures ANOVA was performed with the FM score as a covariate factor to identify if a significant difference between protocols was present before combining all trials. When comparing the difference between subject group (stroke and control subjects), a two-level mixed-model nested ANOVA was performed to determine the significant main effect from subject groups reaching to six different target locations. A repeated measures ANOVA with paired-sample t-test was used to compare the difference of NJS and EMG_{avg} during the acceleration and deceleration phase of movement during reaches made toward each target location (2 phases x 6 targets x 2 subject groups). The Pearson correlation analysis was done to identify the relationship of FM score and final joint angles, NJS and EMG_{avg}. The level of significance was set at $\alpha = 0.05$. The statistical analysis was performed with the software package SPSS 16.0 (SPSS Inc., Chicago, USA).

2.3 RESULTS

2.3.1 Endpoint Reaching Trajectory

The endpoint trajectories of the stroke subjects, compared to the control subjects, were found to be more curved and non-smooth as illustrated in Figure 2-2B. The tangential velocity profiles of selected trials (indicated by the darkest trajectory reaching to target 1) of three representative subjects are shown in Figure 2-2A. The trajectories from a stroke subject with a high FM score, shown in Figure 2-2B middle panel, were similar to those from a representative control (Figure 2-2B left panel). Trajectories from a subject with a low FM score, shown in Figure 2-2B (right panel), were less smooth, and the low FM subject was more capable of reaching to the medial targets than to the lateral targets.

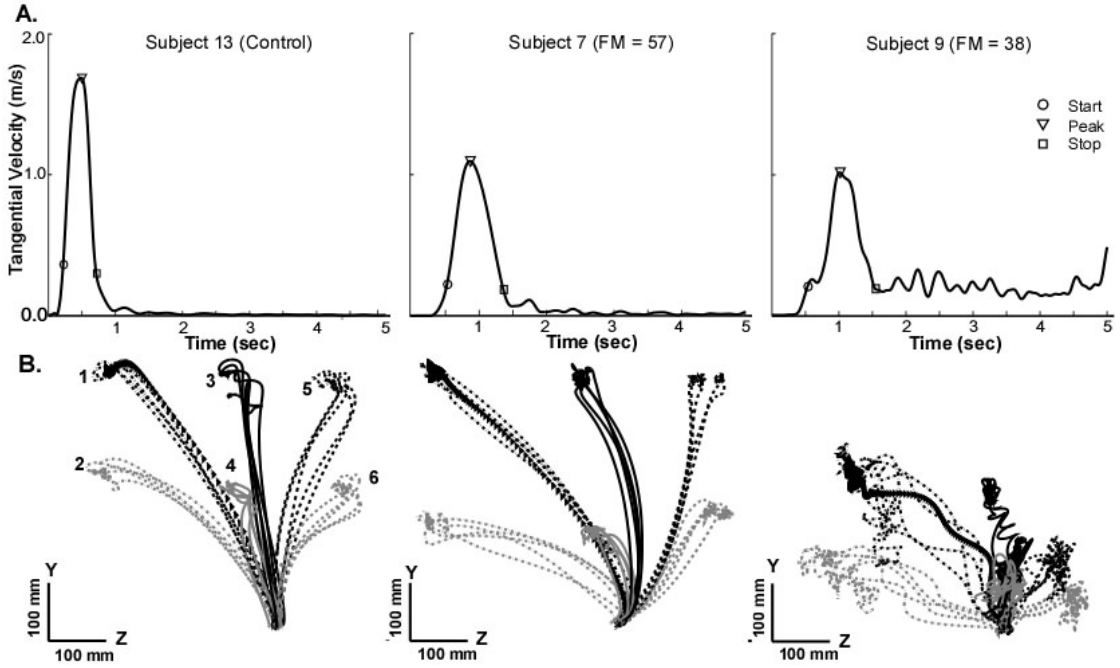

Figure 2-2: Endpoint Trajectory A) Tangential velocity profile selected from one of the trials from a control, a stroke subject with high FM score and a stroke subject with lower FM score. B) Coronal view of the endpoint trajectories of the selected subjects. The selected trials that are represented by the velocity profile are the darkest trajectories made to target 1.

2.3.2 Functional Range of Motion

The range of motion of shoulder elevation and elbow flexion/extension was significantly decreased in the stroke group for all targets. The shoulder elevation at the end of reaches in the control group was significantly higher than in the stroke subjects (Mean ± SE, control = 87.81 ± 2.55 degrees, stroke = 69.29 ± 1.73 degrees; $F_{1,84}$=106.291, $p<0.001$). For the plane of elevation, stroke subjects had a reduced range of motion as shown by the decreased plane of elevation at final position (Mean ± SE, control = 78.64 ± 2.45 degrees, stroke = 64.61 ± 1.16 degrees; $F_{1,84}$=545.209, $p<0.001$). For the elbow angle, stroke subjects had a significant decrease in range of motion,

considering that they could not move to full elbow extension, as the control subjects did (Mean ± SE, control = 147. 74 ± 4.86 degrees, stroke = 122.27 ± 3.31 degrees; $F_{1,84}$=393.348, p<0.001). There was no significant difference between the two groups in humeral rotation (Mean ± SE for all targets, control = -26.82 ± 2.95 degrees, stroke = -25.15 ± 2.01 degrees; $F_{1,84}$=0.352, p=0.579).

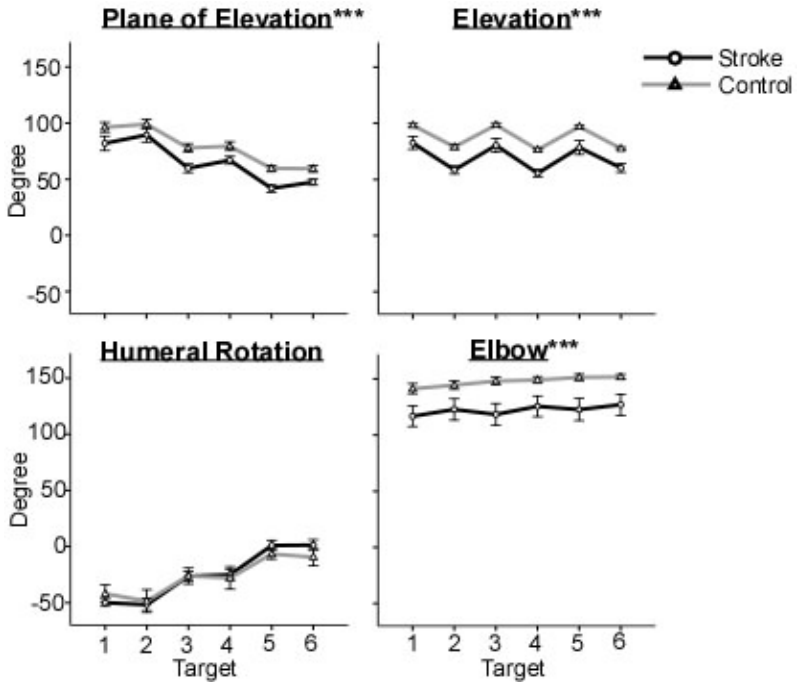

Figure 2-3: Joint angles at the final position. Functional range of motion was significantly reduced in stroke subjects (***, p<0.001) except in humeral rotation.

Even though the shoulder range of motions (elevation and plane of elevation) in stroke subjects was more limited than in the control subjects, the coordination of the shoulder joint was found to be similar. (Figure 2-4). That is, the joint angle trajectories for the stroke subjects tended to fall within the range of the controls.

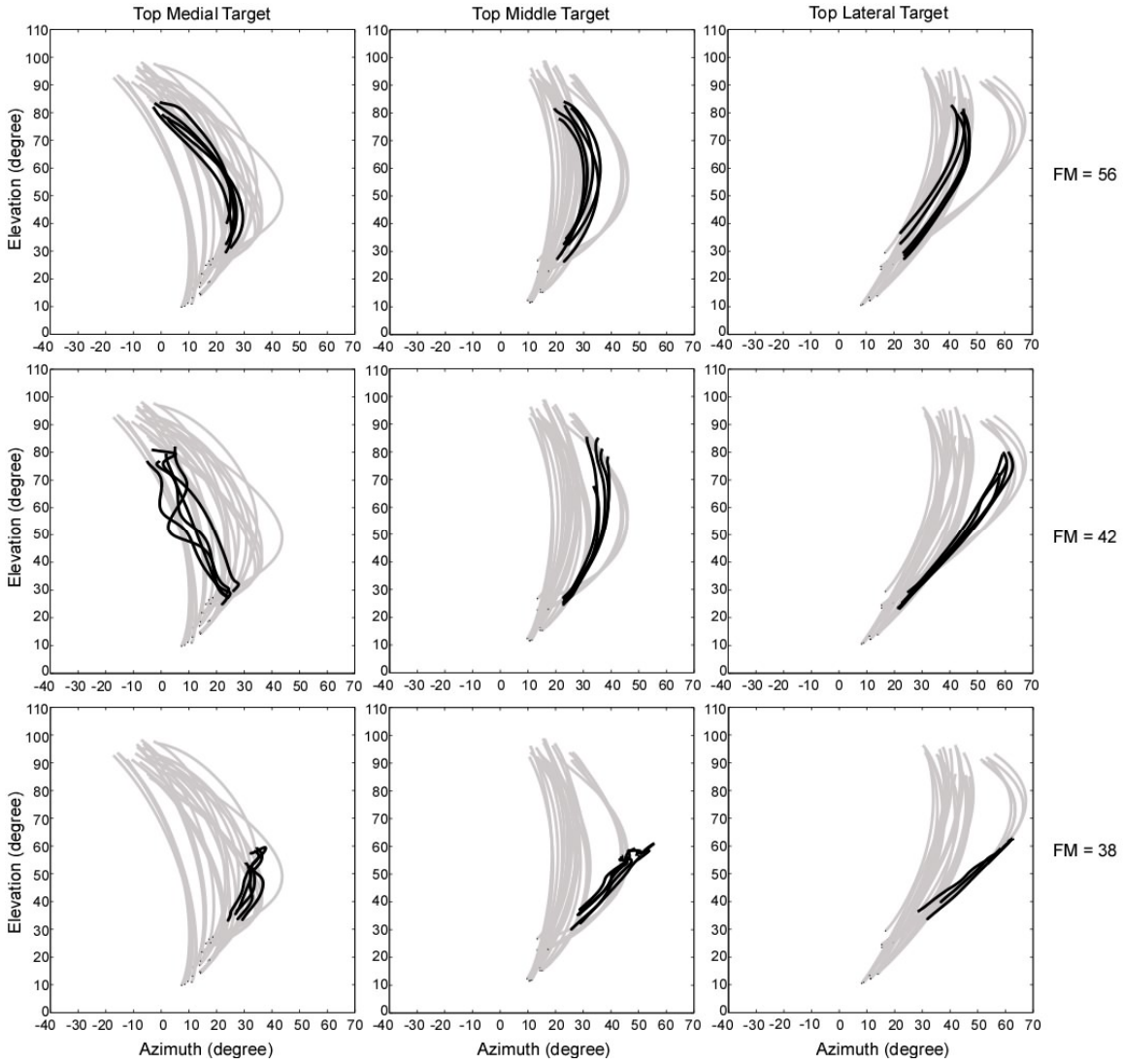

Figure 2-4: Plane of Elevation-Elevation Plot Plot of plane of elevation and elevation angles during reaches (5 reaches per target for each subject) made toward the top targets from 3 stroke subjects (black) is overlaid on the plot from all five control subjects (gray). Shoulder coordination of stroke subjects was within the normal range although the range of motion in shoulder elevation was particularly limited.

2.3.3 Muscle Activities during Reaching

Significant differences in muscle activity during reaching between the stroke and control groups were observed in all the recorded muscles except PDT (Mean ± SE, control = 0.048 ± 0.007 mV, stroke = 0.058 ± 0.005 mV; $F_{1,84}$ = 1.296, p = 0.258). During reaching, the stroke group had lower activity in the agonists and distal muscles but higher activities in the antagonists than the control group. Lower EMG_{avg} of the PECS (Mean ± SE, control = 0.067 ± 0.010 mV, stroke = 0.036 ± 0.007 mV; $F_{1,84}$ = 7.126, p=0.009), ADT (Mean ± SE, control = 0.136 ± 0.007 mV, stroke = 0.049 ± 0.004 mV; $F_{1,84}$ = 115.836, p < 0.001) and TRI (Mean ± SE, control = 0.152 ± 0.017 mV, stroke = 0.047 ± 0.011 mV; $F_{1,84}$=27.552, p < 0.001) was observed in the stroke group. Unlike the agonist muscles (PECS, ADT and TRI), the stroke group had significantly higher EMG_{avg} than in the control group for BI (Mean ± SE, control = 0.038 ± 0.010 mV, stroke = 0.073 ± 0.007 mV; $F_{1,84}$=8.220, p =0.005) and BRD (Mean ± SE, control = 0.024 ± 0.004 mV, stroke = 0.035 ± 0.002 mV; $F_{1,84}$=6.436, p =0.013). Lower activity of the distal muscles, ECR (Mean ± SE, control = 0.049 ± 0.005 mV, stroke = 0.017 ± 0.003 mV; $F_{1,84}$=30.581, p <0.001) and FCR (Mean ± SE, control = 0.048 ± 0.005 mV, stroke = 0.025 ± 0.003 mV; $F_{1,84}$=14.188, p <0.001), in the stroke group was also observed.

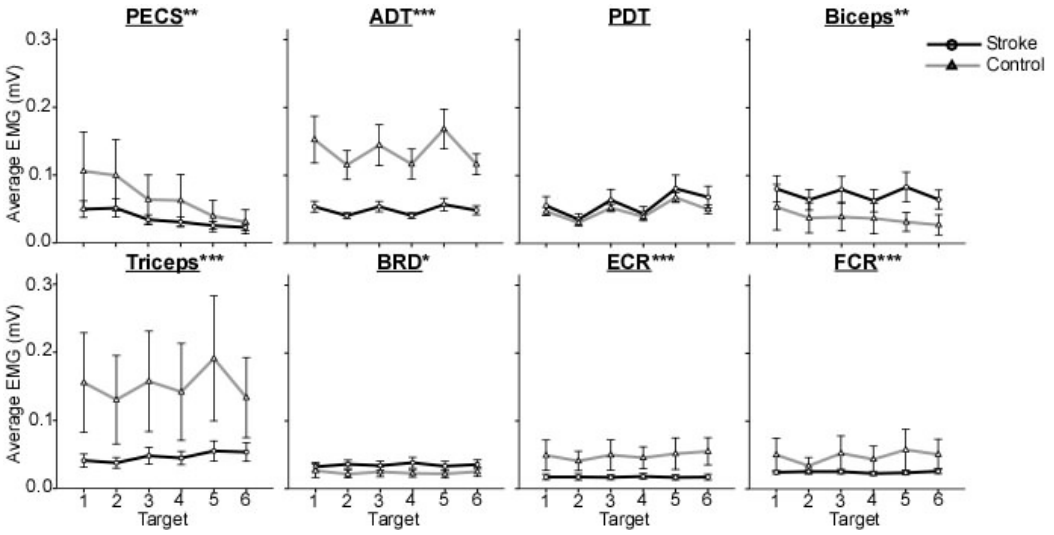

Figure 2-5: Average EMG during reaching. Stroke subjects had significantly lower activity of PECS (ANOVA, **p<0.01), ADT, Triceps, ECR and FCR (ANOVA, ***p<0.001) and significantly greater activity in the BI (ANOVA, **p<0.01) and BRD (ANOVA, *p<0.05) compared to the controls. No significant difference was found in PDT.

2.3.4 Acceleration-Deceleration Asymmetry

The NJS of stroke subjects was significantly higher than control subjects (Mean ± SE, control = 5.977 ± 4.897, stroke = 33.370 ± 3.301; $F_{1,84} = 236.662$, $p < 0.001$) regardless of the target location ($F_{5,84}=0.086$, $p=0.944$). The NJS of the deceleration phase of the reach was significantly higher than the acceleration phase ($F_{1,14}=5.488$, $p = 0.034$) for both stroke (Mean ± SE, acceleration = 6.282 ± 1.009, deceleration = 12.398 ± 1.599; post-hoc paired t-test, $t_{1,65}=-4.817$, $p < 0.001$) and control subjects (Mean ± SE, acceleration = 1.296 ± 0.103, deceleration = 1.714 ± 0.055; post-hoc paired t-test, $t_{1,29}=-4.942$, $p < 0.001$) regardless of the target locations ($F_{5,70}=0.492$, $p = 0.781$) as shown in Figure 2-6 I.

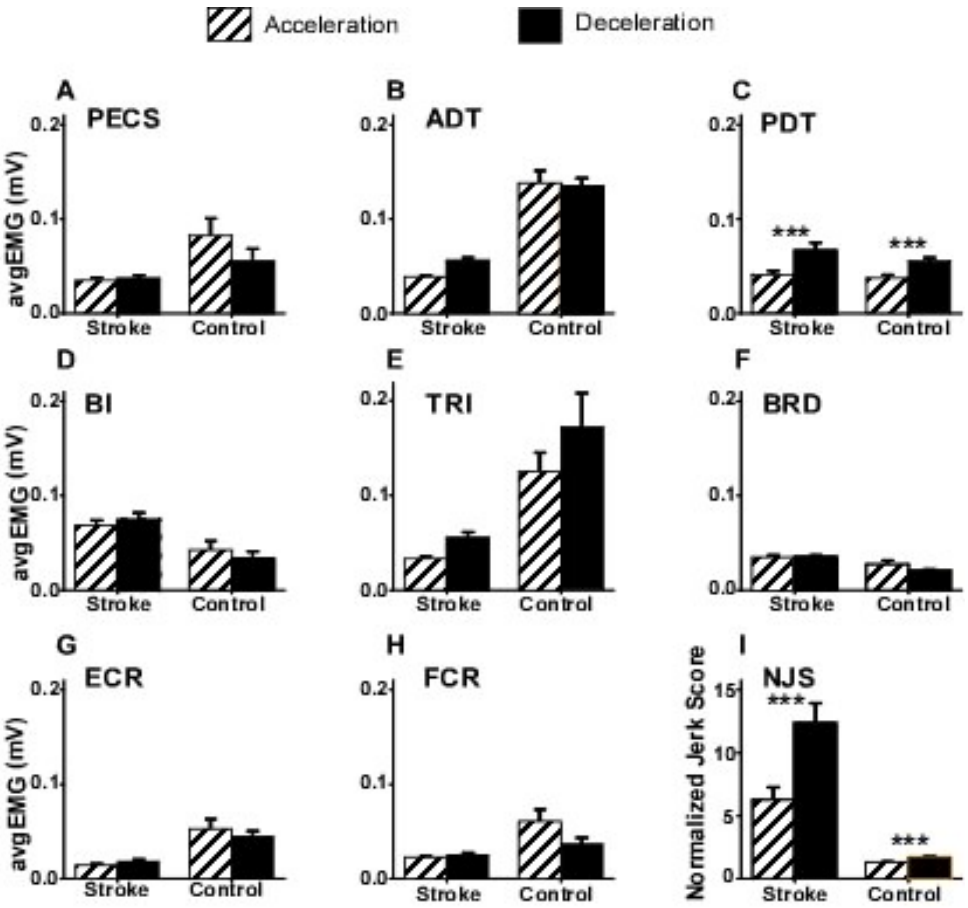

Figure 2- 6: Acceleration-Deceleration Asymmetry. A-E) Average muscle activities and **I)** average NJS for each subject group during acceleration and deceleration phases. PDT (Figure 2-6 C) and NJS (Figure 2-6 I) during deceleration was significantly higher than during acceleration for all subject groups (post-hoc paired sample t-test, $p<0.001$***) with no significant interaction from subject groups or target locations. Error bars are Mean ± SE.

Muscle activation during acceleration and deceleration of stroke and control subjects were not significantly different except for PDT. During the deceleration phase of reaching, both stroke (Mean ± SE, acceleration = 0.041 ± 0.004 mV, deceleration = 0.068 ± 0.007 mV; post-hoc paired t-test, $t_{1,65}$=-6.386, $p < 0.001$) and control subjects (Mean ± SE, acceleration = 0.038 ± 0.002 mV, deceleration = 0.056 ± 0.003 mV; post-

hoc paired t-test, $t_{1,29}$=-7.414, $p < 0.001$) significantly increased activation in PDT ($F_{1,14}$=9.314, $p = 0.009$) regardless of target locations ($F_{5,70}$=2.032, $p = 0.085$) as shown in Figure 2-6C.

2.3.5 Clinical Correlation

From the correlation analysis, only the shoulder elevation, elbow extension and the NJS were significantly correlated with the FM score for all targets as shown in Table 2-2, with all significant correlations for individual correlation tests shown in the shaded cells. Cells with a thicker border indicate significant differences after a Bonferroni correction was applied across targets ($p<0.05$). During reaching, subjects with lower FM score made more non-smooth movement and had limited functional range of motion in shoulder elevation and elbow extension. For reaching in the medial direction, stroke subjects with a higher FM score had a higher plane of elevation, which was likely due to higher activity of PECS. Stroke subjects with higher FM score had significantly higher activation of ADT and TRI in the lateral targets as well.

Table 2-2 Statistical results of the correlation analysis with FM score for stroke subjects

	Target 1 **Top Medial**	**Target 2** **Bottom Medial**	**Target 3** **Top Middle**	**Target 4** **Bottom Middle**	**Target 5** **Top Lateral**	**Target 6** **Bottom Lateral**
PECS	r = 0.667* p = 0.025	r = 0.679* p = 0.022	r = 0.664* p = 0.026	r = 0.573 p = 0.065	r = 0.526 p = 0.096	r = 0.549 p = 0.080
ADT	r = 0.479 p = 0.136	r = 0.288 p = 0.391	r = 0.589 p = 0.057	r = 0.350 p = 0.292	r = 0.660* p = 0.027	r = 0.635* p = 0.036
PDT	r = 0.284 p = 0.397	r = -0.072 p = 0.832	r = 0.349 p = 0.293	r = 0.064 p = 0.852	r = 0.477 p = 0.138	r = 0.339 p = 0.309
BI	r =- 0.218 p = 0.519	r = -0.284 p = 0.397	r = -0.202 p = 0.552	r = -0.363 p = 0.273	r = -0.224 p = 0.508	r = -0.163 p = 0.633
BRD	r = -0.011 p = 0.974	r = 0.021 p = 0.951	r = 0.008 p = 0.982	r = 0.084 p = 0.806	r = 0.069 p = 0.841	r = 0.104 p = 0.760
TRI	r = 0.563 p = 0.072	r = 0.367 p = 0.266	r = 0.611* p = 0.046	r = 0.314 p = 0.348	r = 0.634* p = 0.036	r = 0.654* p = 0.029
Plane of Elvation	r = 0.741** p = 0.009	r = 0.767* p = 0.010	r = 0.692* p = 0.018	r = 0.583 p = 0.060	r = 0.201 p = 0.554	r = 0.015 p = 0.965
Elevation	r = 0.812** p = 0.002	r = 0.686* p = 0.028	r = 0.829** p = 0.002	r = 0.770** p = 0.006	r = 0.803** p = 0.003	r = 0.835** p = 0.001
Elbow	r = 0.810** p = 0.002	r = 0.791** p = 0.006	r = 0.825** p = 0.002	r = 0.770** p = 0.006	r = 0.852** p = 0.001	r = 0.864** p = 0.001
NJS	r = -0.618* p = 0.043	r = -0.759** p = 0.007	r = -0.625* p = 0.040	r = -0.663* p = 0.026	r = -0.678* p = 0.022	r = -0.814** p = 0.002

2.4 DISCUSSION

2.4.1 Deficits in Multijoint Reaching Post Stroke

The fast reaching task in the current study required strong shoulder elevation and elbow extension, which was difficult for stroke subjects as evidenced by lower activity of the agonist muscles (ADT and TRI) and higher activity of antagonist muscles (BRD and BI) during a reach, compared to control subjects (Figure 2-5). Decreased shoulder joint motion (Figure 2-3) and decreased ADT activity with relatively comparable PDT activity during reach (Figure 2-5) in stroke subjects suggests shoulder weakness played an important role in reaching limitations. The shoulder flexor (ADT) is a prime mover in the reaching movement performed in the current study. Decreased activity of the ADT might have the direct effect of producing insufficient torque to accomplish the targeted reach (McCrea et al, 2003), resulting in a decrease in shoulder excursion at the end position.

Increased BI and BRD activities (Figure 2-5) and decreased range of elbow extension (Figure 2-3) suggests that the decreased range of elbow motion was from increased elbow stiffness due to the high activity of the antagonist elbow muscles (BI and BRD) during reach. This hyperactivity of elbow muscles, especially BI could reflect spasticity, originating from abnormal enhanced synaptic input to antagonistic motoneurons as the subjects were trying to extend their elbows (Mottram et al., 2009).

During multijoint forward reaching in stroke subjects, elbow flexion is often coupled with shoulder flexion, which has been described as a component of the classic

flexion synergy (Brunnstrom, 1970). In isometric tests, shoulder flexion has also been associated with secondary elbow flexion torques (Dewald & Beer, 2001; Lum, Burgar, & Shor, 2003; Dewald, Pope, Given, Buchanan, & Rymer, 1995; Beer, Ellis, Holubar, & Dawald, 2007). One contributing factor to this synergy pattern may be multijoint neural coupling at the spinal level, in which the stretch at the shoulder causes reflex activation in elbow flexors in people who are post-stroke, similar to the effect of elbow stretch on shoulder muscle activity (Sangani, Starsky, McGuire, & Schmit, 2009). The interjoint reflex coupling may contribute to deficits in joint individuation during voluntary movement (Zackaowski, Dromerick, Sahrmann, Thach, & Bastain, 2004) but has a minor effect on the targets location of reach (Kamper et al., 2002) which is seen only in the severely impaired subjects (Reinkensmeyer et al., 2002). The decrease in shoulder elevation and elbow extension that was correlated with the FM score of stroke subjects for all targets found in this study (Table 2-2) could be due to a deficit in joint individuation during voluntary movement.

Non-normalized EMG signals were used in the current study to assess muscle activity because of challenges in normalizing EMG in paretic muscles. Muscle activity as measured by EMG is often normalized due to variations in within-subject factors such as adipose tissue thickness (Kuiken, Lowery & Stoykov, 2003) and skin impedance (Perreault, Hunter & Kearney, 1993). Normalizing the raw EMG to the MVC (i.e. divided by MVC) is a popular method used by many studies (e.g. Conrad et al., 2011; Lehman & McGill 1999; David et al., 2000). However, in the case of hemiparetic subjects who cannot fully activate EMG during voluntary muscle contraction, the EMG measured during an MVC may not reflect full muscle activation and normalizing EMG to

MVC could give an inaccurate measure of the muscle activation. Interpolated twitch techniques have been used to identify full muscle activation for normalization of EMG (Horstman et al., 2008) but it is time consuming and often uncomfortable for subjects. Also, normalizing EMGs using an MVC at one joint angle can still result in errors during an unconstrained task (Mirka, 1991). In the current study, we attempted to account for some differences in amongst subjects by using age-matched controls. Also note that a systematic difference in EMGs was not observed across all muscles. The average rms value of the EMG reflected the proximal weakness (lower ADT activity) and distal spasticity (higher BI activity), consistent with previous findings (Gowland, deBruin, Basmajian, Plews, & Burcea, 1992; Kisiel-Sajewicz et al., 2011; Gracies, 2005).

The decreased muscle activity in some muscle groups (e.g. ADT) was likely a cause of the decreased reaching velocity in stroke survivors. Stroke subjects generally reach with slower speed than control subjects (Kamper et al, 2002). Subjects in the current study were instructed to make a fast reaching in which all subjects followed the instruction accurately. EMG activities during reaching reflected the muscle activities during maximum voluntary effort and are an indicator of weakness, especially of the shoulder.

2.4.2 Reaching Trajectory Post Stroke

Trajectory smoothness indicates the integrity of neural motor control of movement. From this study, trajectory smoothness as measured by NJS was higher in stroke subjects than control subjects and was significantly correlated with the level of

upper extremity motor impairment as measured by FM score (Table 2-2). This observation is consistent with a previous study reporting that 3D reaching trajectory smoothness (measured by number of speed peaks) and straightness (measured by path length) have highly significant linear trends with the arm portion of the Chedoke-McMaster stroke assessment scale (Kamper et al., 2002), suggesting a smoother and less curved movement trajectory indicates recovery after stroke (Rohrer et al., 2002). A non-smooth reaching trajectory post stroke could be due to the increased neuromotor noise. Execution noise is the noise accumulated from movement planning and transferred to execution that is thought to cause movement variability (van Beers, Haggard, & Wolpert, 2004). Increased neuromotor noise after stroke has consequences in both motor planning and execution, contributing to non-smooth movement (McCrea et al., 2005).

Based on the NJS during acceleration and deceleration phases, the trajectory during the deceleration phase was less smooth (higher NJS) than in the acceleration phase for both stroke and control groups, but was more pronounced in the stroke subjects (Figure 2-6I). This could be due to 1) secondary submovements in the deceleration phase were present to a greater extent in stroke subjects or 2) the impaired ability to regulate stretch reflexes during the deceleration phase, when the proprioceptive feedback was not centrally suppressed.

Secondary submovement during deceleration phase

The velocity irregularities from the smooth bell shape that are frequently observed during deceleration of pointing movements have long been interpreted as corrective submovements, which help to improve motion accuracy. Woodworth (1899) explained

these irregularities of velocity profile as the feedback-guided secondary submovements performed to improve the accuracy of the primary, ballistic movement. More recent studies also observe the presence of submovements in movements that have less demand for accuracy, in which submovements can be interpreted either as the motor command of movement (Rohrer et al., 2002; Novak, 2002) or motor output variability (Fradet, Lee, & Dounskaia, 2008). Increased NJS during the deceleration that was more pronounced in stroke subjects than in control subjects (Figure 2-6I), when explained in terms of submovements, could be either due to non-corrective submovements emerging from various sources of motor output variability (Fradet et al., 2008) or due to the inability to appropriately generate adequate submovements to blend into a smooth bell-shaped velocity profile (Rohrer et al., 2002).

Onset of proprioceptive feedback during deceleration phase

Proprioceptive feedback, as a part of an adaptive, feed-forward control mechanism, is used to improve the straightness and smoothness of the movement when there is an unexpected mechanical perturbation (Scheidt, Conditt, Secco, & Mussa-Ivaldi, 2005) by centrally modulating its gain in anticipation of a perturbation (Kimura, Haggard, & Gomi, 2006). The effect is reported to play a role in rapid reaching movements (Desmurget & Grafton, 2000) similar to those performed in the current study. Proprioceptive feedback is centrally suppressed at the beginning of the movement and turned on at a time when muscles are expected to generate maximum force (Shapiro, Niu, Poon, David, & Corcos, 2009), which in the case of fast reaching, is approximately the middle of the movement or about the peak velocity when the segmental reflex feedback is briefly facilitated (Shapiro, Gottlieb, Moore, & Corcos, 2002). Shapiro et al. (2009) has

proposed that the duration of feedback activity during movement has to be limited to stabilize the limb and is activated only to deliver a short powerful correction. Temporary suppression of feedback control can come from descending inputs to spinal interneurons and presynaptic inhibition in the segmental pathway (Shapiro et al., 2009).

Suppression of the proprioceptive feedback at the beginning of a movement may cause the trajectory during the acceleration phase to be smoother than during the deceleration phase. The release of proprioceptive feedback is suggested to characterize the onset of descending regulation of segmental reflexes (Shapiro et al., 2002), which could make the reaching trajectory less smooth even in the normal reaching. In stroke subjects, the less smooth trajectory (higher NJS) in the deceleration phase relative to control subjects (Figure 2-6I) could be related to the impaired ability to regulate reflex threshold (Levin & Feldman, 1994) or an altered stretch reflex coordination (Trumbower, Ravichandran, Krutky, & Perreault , 2010) during the deceleration phase when proprioceptive feedback is released.

2.4.3 Clinical Implications

As suggested from the clinical correlation (Table 2-2), the decreased ADT activation during reach in stroke subjects might affect reaching impairment more than the observed increased BI and BRD activation. Since weakness is the prominent impairment after stroke (Bohannon, 2007) and reduction of agonist activation has been found to cause movement impairment more than increased antagonist activation (Gowland et al., 1992), rehabilitation strategies aimed at strengthening the shoulder muscle, especially the ADT,

may be effective in restoring normal movement. Strength training post stroke has been found to improve upper-extremity strength and function without increasing spasticity (Harris & Eng, 2010). Improvement in multijoint coordination and a reduction in abnormal coupling of shoulder abduction and elbow flexion are also reported after a progressive strength training of the shoulder abduction (Ellis, Sukal-Moulton, & Dewald, 2009). Our study generally supports the concept of shoulder strengthening, but increased elbow flexor activity and NJS during deceleration suggest that reflex regulation also plays a role in impaired movements.

CHAPTER 3: ARM STABILITY OF SUBJECTS WITH POST-STROKE HEMIPARESIS IN THREE-DIMENSIONAL WORKSPACE

3.1 INTRODUCTION

The purpose of this study was to characterize arm stability of individuals with post-stroke hemiparesis in a 3D workspace and to examine the effect of wrist sensory stimulation on arm stability. Stabilization of the paretic arm is essential in daily living activities of post-stroke individuals, especially in bimanual tasks where an individual is likely to use the paretic hand to stabilize an object and the non-paretic hand to manipulate the object. This is similar to neurologically intact individuals who tend to use the non-dominant hand to stabilize and the dominant hand to manipulate (Kimmerle, Mainwaring, & Borenstein, 2003). We hypothesized that that the paretic arm is less stable than healthy subject's arm. Further, we anticipated that sensory stimulation applied at the wrist, which can improve arm stability in 2D planar movements (Conrad et al., 2011), might also improve arm stability in the 3D workspace. Note that arm stability is defined here as the ability to maintain the arm in a stable position after a point to point movement, not an ability to resist a perturbation (Perreault, Kirsch, & Crago, 2004) or reproducibility of motions and robustness to perturbations (Burdet, et al., 2006).

It has been suggested from 2D reaching and stabilizing studies that one stabilizes the arm by impedance control. That is, in order to stabilize the arm at the end of reach, endpoint impedance must increase (Hogan, 1985). Modifying the endpoint stiffness can be done either by increasing the co-contraction of antagonistic muscles (Franklin et al.,

2007) or by selecting an appropriate arm posture to maximize the stiffness of the direction of a perturbation (McIntyre, Mussa-Ivaldi, & Bizzi, 1996). In post-stroke hemiparesis, endpoint instability is often observed at the final position in 2D planar arm movement (Mihaltchev, Archambault, Feldman, & Levin, 2005). The instability of the endpoint in stroke survivors appears to result from an impaired ability to modulate the coactivation of opposing muscles at the final location, which depends on the proprioception integrity of the limb and amount of time post-stroke (Scheidt & Stoeckmann, 2007). Arm stability of neurologically intact subjects in the 3D workspace has also been studied in the framework of impedance control in response to the stochastic displacement perturbation. It is found that stretch reflex gain is increased to enhance limb stability and the modulation is directionally tuned to compensate for the external instability according to the mechanical properties of the limb (Krutky, Ravichandran, Trumbower, & Perreault, 2010), similar to what is found in 2D workspace. The aim of the current study was to investigate the strategy that stroke subjects use to stabilize the arm in 3D attainable workspace.

In order to characterize stabilization of the arm, we tested arm posture while subjects were instructed to maintain the hand at fixed positions within their attainable workspace. Previously (Chapter 2), we found that 3D reaching movements of stroke survivors are characterized by non-smooth trajectories and limited range of motion. When post-stroke subjects reach to the extent of their workspace, efforts to extend the arm further become indistinguishable from motion associated with instability. In order to evaluate arm stability in the current study, subjects were instructed to hold their hand at a position within the attainable workspace, avoiding the movements associated with

reaching efforts beyond their capable range of motion. The average final joint angles of stroke subjects obtained from Chapter 2 were used to design the target locations.

Tendon vibration and electrical stimulation are commonly used in clinical rehabilitation to provide sensory excitation. For example, tendon vibration applied at the wrist can improve endpoint stability in 2D planar movement in people post-stroke. (Conrad et al, 2011) Electrical stimulation of the medial nerve at the wrist prior to therapy increases hand grip strength (Conforto et al., 2002), improves hand function (Wu, Seo, & Cohen, 2006) and enhances training effects (Celnik, Hummel, Harris-Love, Wolk, & Cohen, 2007). However, the effect of electrical stimulation on arm stability has not been investigated. In this study, we investigated whether the stability improvements produced by wrist tendon vibration extend to the 3D workspace and whether similar effects could be produced using electrical stimulation of the median nerve.

3.2 MATERIALS AND METHODS

3.2.1 Subject Population

Ten chronic stroke subjects (age 54.2±7.3 years) with upper extremity hemiparesis and five age-matched neurologically intact subjects (age 57.0±10.6) participated in this study (Table 3-1). All stroke subjects were at least 21 years of age and had a stroke greater than six months prior to the experiment, which resulted in upper extremity hemiparesis. Exclusion criteria included: recent treatment using botulinum toxin injection in the upper extremity (< 2 months), a diagnosis of another neuromuscular

disorder, the inability to give informed consent, visual deficits, apraxia, multiple strokes, chronic neck, shoulder or back pain, and the inability to follow and focus on two –step commands. The participants' upper extremity Fugl-Meyer score (Fugl-Meyer, 1975) ranged from 26 to 66 (46. 6 ± 14.7). The assessment was conducted by a licensed physical therapist. Subjects whose upper extremity Fugl-Meyer score (FM score) was equal or greater than 40 were classified as high-FM and those less than 40 classified as low-FM. All subjects gave informed consent in compliance with protocols approved by the Institutional Review Board of Marquette University.

Table 3-1 Subject information

Subject	Sex	Age (Years)	Years after Incidence	Test Arm[#]	FM Score[##]	Subject Group*
1S	M	60	4	R	57	High
2S	F	59	5.5	L	50	High
3S	M	48	7.5	L	29	Low
4S	F	40	8	R	66	High
5S	F	54	17	R	63	High
6S	M	63	4	R	32	Low
7S	M	46	3	R	57	High
8S	M	55	4	R	36	Low
9S	M	57	32	L	26	Low
10S	F	60	20	R	50	High
11C	M	44	-	L	-	Control
12C	M	60	-	L	-	Control
13C	F	73	-	L	-	Control
14C	M	55	-	L	-	Control
15C	F	53	-	R	-	Control

[#] The control subjects were tested with the non-dominant arm and the stroke subject with the paretic arm.
[##] Based on Upper Extremity FM score; 0-66
* Control = age-matched control group, High = high FM subject group and Low = low FM subject group

3.2.2 Test Apparatus

Reach targets consisted of five LEDs (5-mm diameter) located central (25-30 cm in front of the sternum), medial (20 cm medial from the central target), lateral (20 cm. lateral to the central target), high (20-25 cm. in front of the glabella) and low (30-35 cm. in front of the umbilicus) with respect to the subject as illustrated (Figure 3-1A). All target locations were within the subjects' reachable and visible workspace. Timing and sequence of LEDs and auditory cues were controlled using a custom LabVIEW program and a data acquisition device (NI USB – 6229, NI Corporation, TX, USA).

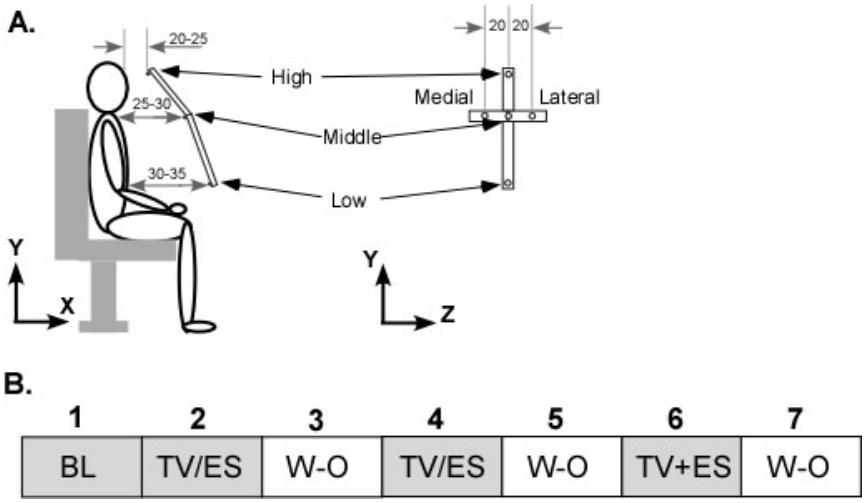

Figure 3-1: Experimental Set-Up. A. Subjects were seated on a comfortable chair with a 4-point harness to restrain trunk and shoulder movement. The targets were placed on crossbars in front of the subject with the dimensions specified in the figure. All dimensions are in cm. **B.** Experimental blocks. All subjects started with the baseline block (BL) without any stimulation followed by the stimulation blocks with the wash-out blocks (W-O) in between. Five stroke and 3 control subjects were given tendon vibration (TV) before electrical stimulation (ES) and 5 stroke and 2 control subjects were given ES before TV in the 2nd and 4th blocks (TV/ES). The 6th block was TV and ES simultaneously (TV+ES).

Kinematic data were collected using a camera-based tracking system (OPTOTRAK® 3020, Northern Digital, Ontario, Canada) sampled at a frequency of 100 Hz. The Optotrak cameras detected infrared emitting diode (IRED) markers which were attached to two flexible Aquaplast® orthoses, one on the upper arm (8 IRED markers) and one on the lower arm (9 IRED markers). Markers were arranged so that a minimum of three markers were visible to the camera during the whole arm movement. The acromion (AC), the medial (EM) and the lateral (EL) epicondyles of the humerus, and the styloid processes of the radius (RS) and ulna (US) were registered as the virtual markers by calibrating their positions with respect to the markers of the orthoses prior to the experiment. The glenohumeral joint rotation center (GH) was estimated by translating the AC position 14 mm laterally, 37 mm downward and 8 mm to the front (Wang, 1999). Markers on the orthoses were used to calculate the positions of virtual markers (GH, EM, EL,US and RS) for each frame of motion using Toolbench® v. 1.1 (Northern Digital, Ontario, Canada). These virtual markers' positions were used to compute the joint angles as described in Appendix A. Missing marker positions were filled by cubic spline interpolation and then the 3D position data were low-pass filtered (cutoff frequency = 5 Hz) using a 2^{nd} order, zero-phase Butterworth filter.

Surface electromyography (EMG) was collected at 1000 Hz from eight arm muscles: the pectorialis major (PECS), anterior deltoid (ADT), posterior deltoid (PDT), long head of biceps (BI), lateral head of triceps (TRI), brachioradialis (BRD), flexor carpi radialis (FCR) and extensor carpi radialis (ECR). Disposable Ag/AgCl electrodes (Vermed Medical, Bellows Falls, VT) were placed over the muscle bellies on lightly abraded skin and the signals were amplified (x1000) and low-pass filtered (500 Hz) prior

to sampling (Bortec Medical AMT-16; Calgary, Alberta, CA). The EMG signals were recorded using a data acquisition device (NI USB – 6229, NI Corporation, TX, USA) and the custom written LabVIEW program.

Tendon vibration was applied via a custom-made tendon vibrator which was placed on the forearm flexor (FCR) tendon and secured by a cohesive flexible bandage (CoFlex® Med, Andover™, Salisbury, MA). The tendon vibrator was made of an unbalanced mass (with maximum and minimum diameters of 1.27 cm. and 0.85 cm.) that rotated about a motor shaft (model 1319 TO12SR, Faulhaber, Clearwater, FL) with an integrated encoder (model IE2-400). Frequency of vibration was adjustable by changing the input voltage to the motor. The vibration frequency used in the experiment was 90 Hz, which activates Ia afferent firing harmoniously in a one-to-one manner (Roll et al, 1989). The motor with unbalanced mass was securely enclosed in a Teflon® sleeve of inner and outer diameter of 1.3 and 1.9 cm. respectively. A custom LabVIEW program was used to direct the controller (model MCDC 3006S, Faulhaber, Clearwater, FL) that controlled the vibrator.

Electrical stimulation was applied to the median nerve at the wrist using a bar electrode (two 9-mm diameter stainless steel disks with 30 mm spacing). Square pulse electric stimulation of 30 Hz, 0.5 duty cycle or pulse width of 1/60 second, and 80% of the motor threshold was delivered using a Digitimer® DS7A constant current electrical stimulator with a maximum voltage of 400 V. The motor threshold was determined by increasing the level of stimulation and detecting the electrical intensity value (mA) of the first thumb movement. If 80% of the motor threshold was not comfortable to the subjects, the electrical stimulation current (mA) was gradually reduced to the level that

was tolerable to the subjects, which was never below 50% of the motor threshold and always above the sensory threshold. The frequency and strength of electrical stimulation was selected as the strongest comfortable stimulation in a preliminary test in three young healthy adults. Information about the subjects' motor threshold and the strength of stimulation used are listed in Table 3-2.

Table 3-2 Experiment information

Subject	Experiment Group**	#Trials/ Target	Motor Threshold (mV)	Electrical Stimulation (mV)
1S	TV-ES	5	16.0	12.8
2S	ES-TV	5	11.0	8.8
3S	TV-ES	3	10.0	8.0
4S	TV-ES	5	4.3	3.4
5S	ES-TV	5	7.5	6.0
6S	ES-TV	3	16.0	12.8
7S	TV-ES	5	5.0	4.0
8S	ES-TV	3	12.0	9.6
9S	TV-ES	5	8.0	6.4
10S	ES-TV	5	5.0	4.0
11C	TV-ES	5	5.0	4.0
12C	TV-ES	5	10.0	8.0
13C	TV-ES	5	7.0	5.6
14C	ES-TV	5	19.0	13.6
15C	ES-TV	5	4.5	3.6

** TV-ES = tendon vibration block first and ES-TV = electrical stimulation block first

3.2.3 Experimental Protocol

Each subject was given practice trials with each target prior to the data collection. Subjects were allowed to practice until they were comfortable with the task. A one–minute break was allowed between each experiment block.

All subjects performed a series of the reach and position holding tasks. The stroke subjects were tested with their paretic arm while the control subjects were tested with their non-dominant arm. The "home position" for each reaching trial was on the lap where the arm was completely relaxed at approximately 90-100 degrees elbow flexion and 0 degree shoulder elevation. One of the five LED targets was randomly turned on with a simultaneous auditory cue. Subjects were instructed to initiate reach at the auditory cue to the lit LED target, and move the hand as close as possible to the target, but not touching. All the subjects could follow this instruction without problems with depth perception. Reaching was made at a comfortable speed with the hand held in a loose fist. The hand was maintained at the final position until another auditory cue was presented. The LED target remained lit for five seconds for each combined reach and hold trial. When the LED was turned off and an audible cue sounded, the subject brought the arm back to the home position and waited for the next trial. The time between trials was 6 seconds, which was enough to allow for muscle relaxation before the next trial.

A total of seven testing blocks were completed, and electrical and/or vibratory stimulation was applied during the second, fourth, and sixth blocks. Prior to the experiment, subjects were allowed to experience stimulation trains of 5 seconds on and 5 seconds off for vibration only (TV), electrical stimulation only (ES) and the combination

of vibration and electrical stimulation (TV+ES). Tendon vibration (TV) and electrical stimulation (ES) were randomly assigned in the 2nd or the 4th blocks. Subjects in TV-ES group were assigned with TV in the 2nd block and ES in the 4th block, while subjects in ES-TV group were assigned with ES in the 2nd block and TV in the 4th block. TV and ES were applied simultaneously in the 6th block. Each block contained 5 reaches per target, however, 3 reaches per target were allowed for subjects who expected to be fatigued by 5 reaches per target (see Table 3-2).

3.2.4 Data Analysis

Endpoint stability measures were quantified using stability error (m^2/s^2) and error frequency (Hz) similar to the stability measures used by Conrad (2009). Tangential velocity of the wrist (the midpoint of virtual US and RS markers) was used for analysis and a 1-second window after the end of reach (start of stabilization) was used to calculate the power spectral density (PSD). The area under the PSD curve between 1 and 5 Hz, was computed and defined as the stability error. Within the frequency band of 1 to 5 Hz, the frequency that divided the area under the PSD curve into halves (i.e. the half power frequency) was defined as the error frequency. Stability measures for shoulder and elbow joints were obtained similarly using the virtual GH marker and midpoint of the virtual US and RS markers.

Joint angles (shoulder elevation, plane of elevation, humeral rotation and elbow flexion) were calculated from the positions of the virtual markers of the specified bony landmarks (GH, EL, EM, US and RS) as illustrated in Appendix A. Markers were used

to quantify postures in terms of the joint angle at the final hold position. Joint angles at the final position corresponded to the average angles during 1 second period after reach. The end of reach was defined as the time when the tangential velocity profile was below 20% of maximum velocity.

All EMG signals were bandpass filtered (10-350 Hz) and then notch filtered to remove line noise (58 -62 Hz) and 90 Hz noise (from vibrator) using a 4^{th} order zero-phase Butterworth filter. The root-mean-square (RMS) of the filtered data (EMG_{rms}) was calculated using a 50-ms moving window. The average EMG (EMG_{avg}) was obtained by integrating the EMG_{rms} over the stabilization period, which was defined as the window of 1 second after the end of reach, where T_1 is the time at the end of reach and T_2 is 1 second after T_1 (Equation 2-2).

A repeated measures ANOVA was used to determine significant differences of parameters among the blocks (BL, VT, ES and VT+ES), considering the interaction of targets (Medial, Lateral, Middle, High and Low) and subject groups (Low, High, and Control). Targets and blocks were treated as the within-subject factors and subject groups as the between-subject factor. If the assumption of sphericity was not met (Mauchly's test, $p<0.05$), the p-value with a Greenhouse-Geisser correction was reported. For within-subject factors, if a significant difference was found, a post-hoc ANOVA was performed to determine significant differences in the fixed factors. If the assumption of equality of variance was met as shown by the Levene's test ($p<0.05$), the p-value from a Tukey post hoc test was reported on the different pairs, otherwise the p-value from the Games-Howell test was reported. For parameter comparison among the subject groups during the BL block, a two level (subject groups and targets) mixed-model nested

ANOVA was performed with Tukey post-hoc tests to determine significant differences between pairs of subject groups. A Pearson correlation analysis (2-tailed) was used to identify the relationship between the FM score and stability measures. Logarithmic scaling for stability error was done before the ANOVA and correlation analysis due to small amplitudes. The level of significance was set at $\alpha = 0.05$, with appropriate adjustment, for all statistical tests. The statistical analysis was performed with the software package SPSS 16.0 (SPSS Inc., Chicago, USA).

3.3 RESULTS

3.3.1 Endpoint Stability

The endpoint (wrist) trajectories to the Low target of three representative stroke subjects, 4S (FM score = 66), 1S (FM Score = 57) and 6S (FM Score = 32) are shown in Figure 3-2A. Corresponding tangential velocity profiles with an indication of stabilization period are shown in Figure 3-2B. During stabilization, subject 6S (Low FM Score) was less stable than subjects with higher FM score, evidenced by more fluctuation in the tangential velocity.

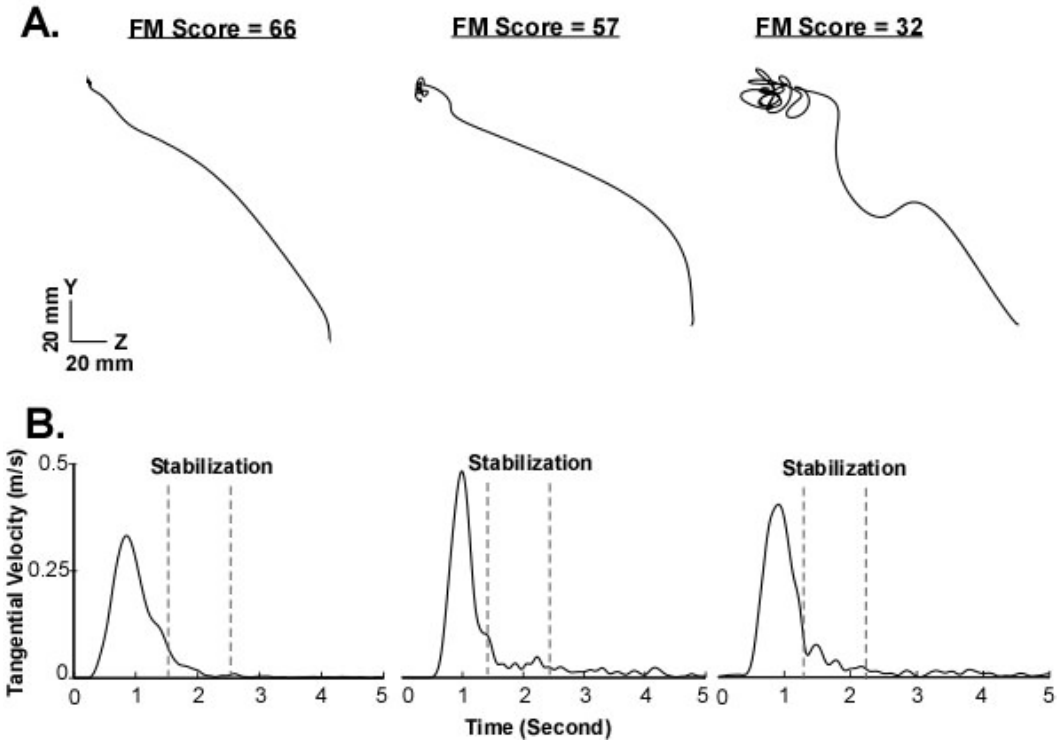

Figure 3-2: Endpoint Trajectory A. Endpoint (wrist) trajectories to the Low target and **B.** corresponding tangential velocity profiles of subject 4S (FM score = 66), 1S (FM Score = 57) and 6S (FM Score = 32). The stabilization period (1 second window after reach) is indicated.

The endpoint stability, quantified by stability error (logarithmic scaled due to very small amplitudes) and error frequency of all subjects performed during the BL block is illustrated in Figure 3-3. A nested ANOVA showed significant differences in stability error ($F_{2,54} = 43.601$, $p<0.001$) and error frequency ($F_{2,60} = 9.574$, $p=0.007$). Low-FM subjects had a significantly higher stability error ($p<0.001$, Tukey post-hoc) than both the high-FM and control subjects (Figure 3-3 A). For error frequency (Figure 3-3 B), low-FM subjects were significantly higher than high-FM ($p=0.039$, Tukey post hoc) and control subjects ($p<0.001$, Tukey post hoc). Pearson correlation analysis (Figure 3-3 C and D) showed that stability error and error frequency were significantly correlated with

FM score at Middle (stability error: r=-0.663, p=0.037; error frequency: r=-0.824, p=0.003) and High (stability error: r=-0.676, p=0.046; error frequency: r=-0.698, p=0.036) targets. Only stability error was found to be significantly correlated with FM score at the Lateral (r=-0.860, p=0.003) and Low target (r=-0.659, p=0.038). For the Medial target, no significant correlation of stability measures with FM score was found.

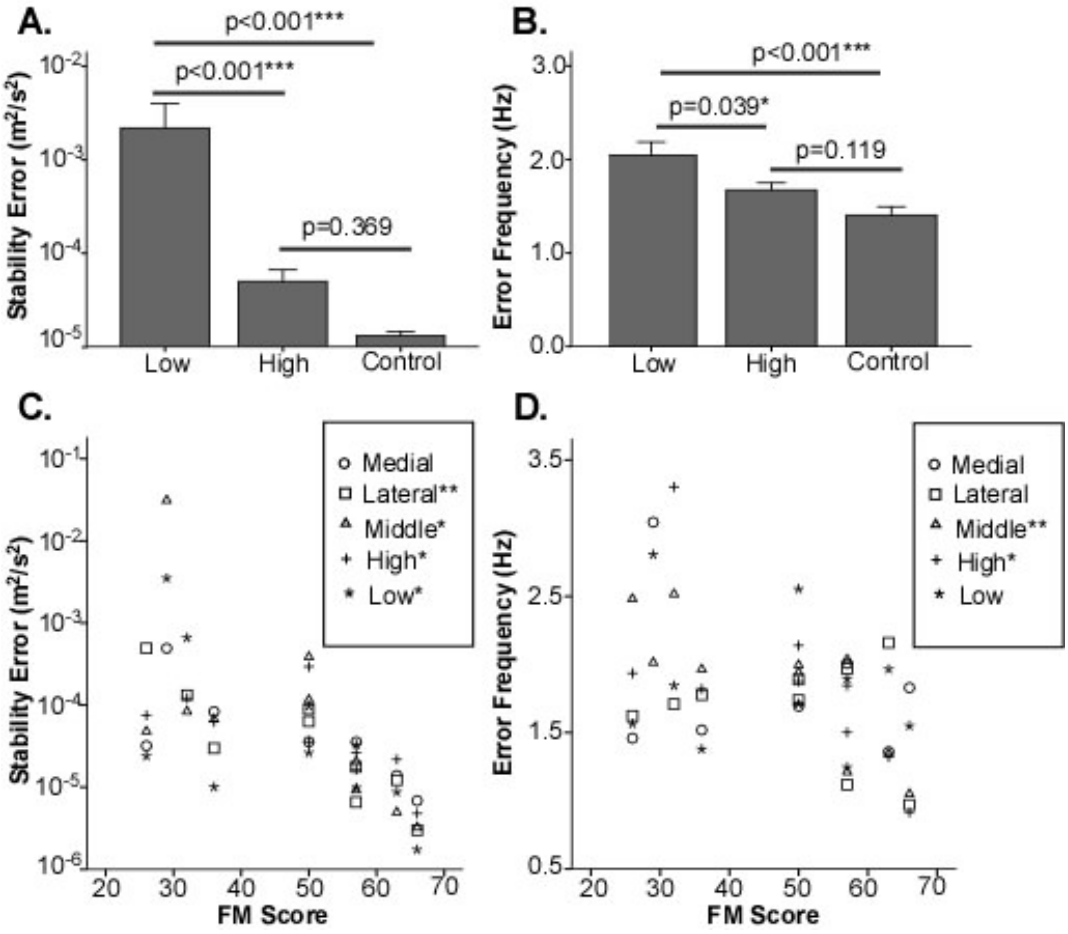

Figure 3-3: Endpoint Stability A. Stability error (log scale) and **B.** error frequency of the wrist during stabilization of each subject group for all targets. Low FM subjects had significantly higher stability error and error frequency than the high FM and control groups. Error bars indicate standard error. **C.** Stability error (log scale) and **D.** error frequency of the wrist correlation with the upper extremity Fugl-Meyer score (*p<0.05, **p<0.01).

3.3.2 Arm Posture during Stabilization

Joint angles at the final position, taken from the joint angles at the end of movement from the BL block, were used as a measure of the arm posture during stabilization for all subjects. A nested ANOVA showed a significant difference among subject groups only in the plane of elevation ($F_{2,60}$=69.433, $p<0.001$) with no significant difference among targets in all subject groups ($F_{8,60}$ = 0.339, p=0.947). A Tukey post-hoc analysis indicated that plane of elevation of low-FM subjects (mean±SE, 58.6±3.1 degree) was significantly lower than the control subjects (mean±SE, 76.8±2.7 degree) but not high-FM subjects (mean±SE, 66.9±2.5 degree) as illustrated in Figure 3-4.

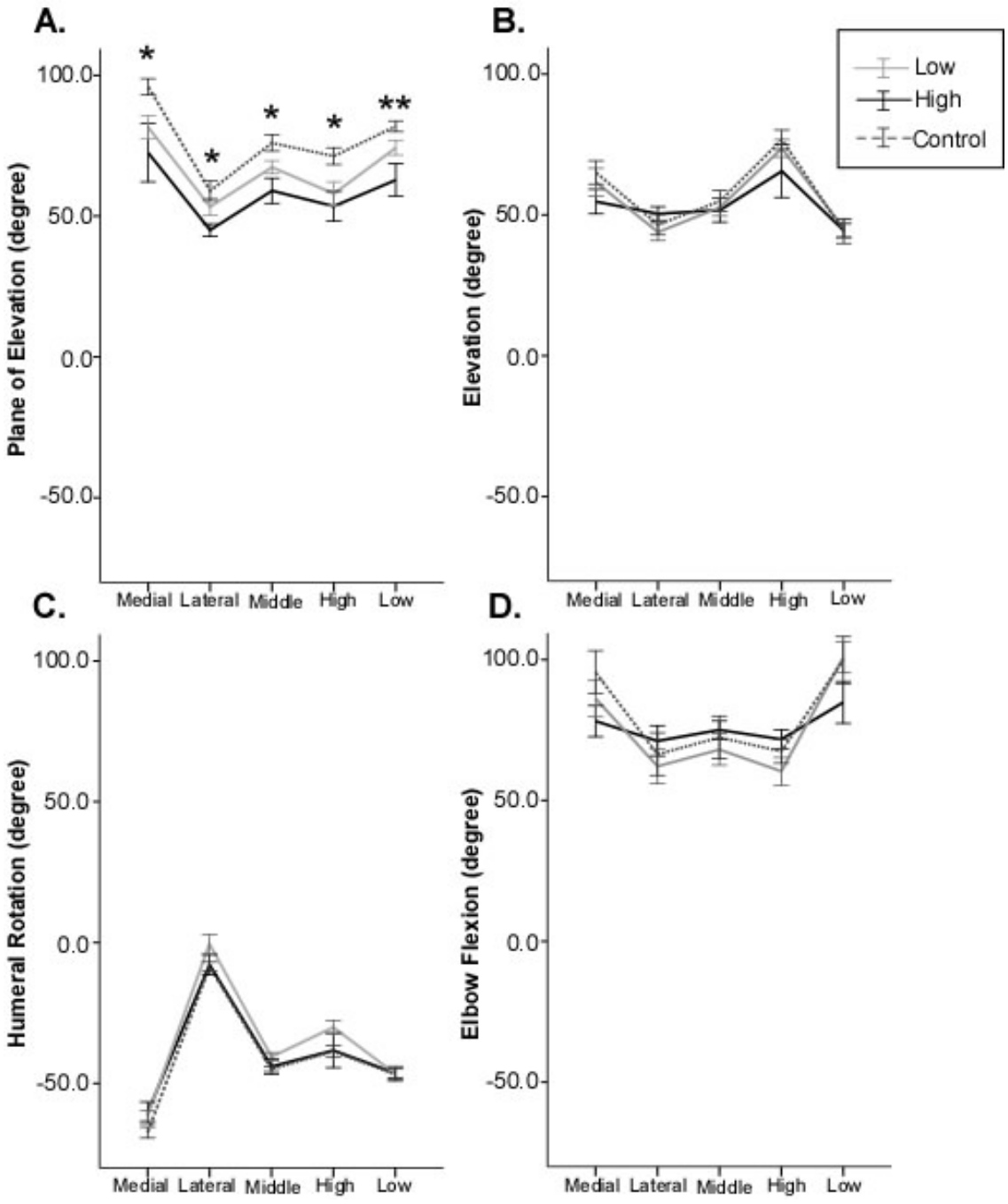

Figure 3-4: Joint angles at the final position. In the reachable workspace, stroke subjects had similar joint angles at the final position as the control subjects except for the plane of elevation. Low FM-score subjects had significantly more abduction (measured by the plane of elevation) than control subjects at all targets (*$p<0.05$, **$p<0.01$). Error bars indicate standard error.

The graphical presentation for the final posture of the selected subjects who were tested with the right arm (N_{Low} = 2, N_{High} = 5 and $N_{Control}$ = 1) is presented in Figure 3-5. More shoulder horizontal abduction, as measured by the plane of elevation, was observed in the stroke subjects for all targets.

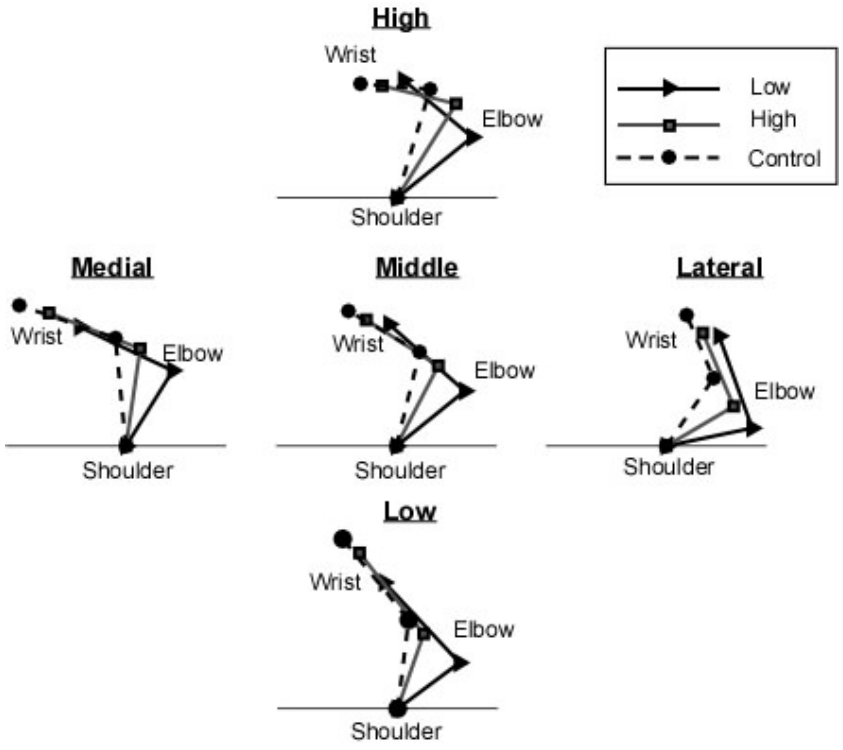

Figure 3-5: Graphical presentation of final arm posture from the top view for each subject group. The graphical presentation shows the average of the final positions of the shoulder, elbow and wrist of subjects tested with their right arm (N_{Low} = 2, N_{High} = 5 and $N_{Control}$ = 1). Stroke subjects horizontally abducted their upper arms more than the control subjects at all targets.

3.3.3 Muscle Activities during Stabilization

Stroke subjects had significantly lower ADT activity than control subjects during stabilization in the BL block ($F_{2,60}$ = 22.463, p=0.001) with no significant difference

among targets in all subject groups ($F_{8,60}$ = 1.054, p=0.407). Low FM subjects had a significantly higher PDT ($F_{2,60}$ = 6.763, p=0.019; target(subject group), $F_{8,60}$ = 0.589, p=0.783) and ECR ($F_{2,60}$ = 32.141, p<0.001; target(subject group), $F_{8,60}$ = 0.257, p=0.977) activations during hold than the high-FM and control groups. Significantly higher activity of BI ($F_{2,60}$ = 26.727, p<0.001; target(subject group), $F_{8,60}$ = 0.316, p=0.957) and FCR ($F_{2,60}$ = 9.229, p=0.008; target(subject group), $F_{8,60}$ = 0.440, p=0.892) were present in the low FM subjects compared to the control subjects. P-values from Tukey post-hoc test are reported in Figure 3-6, except for ECR (corrected p-value from Games-Howell).

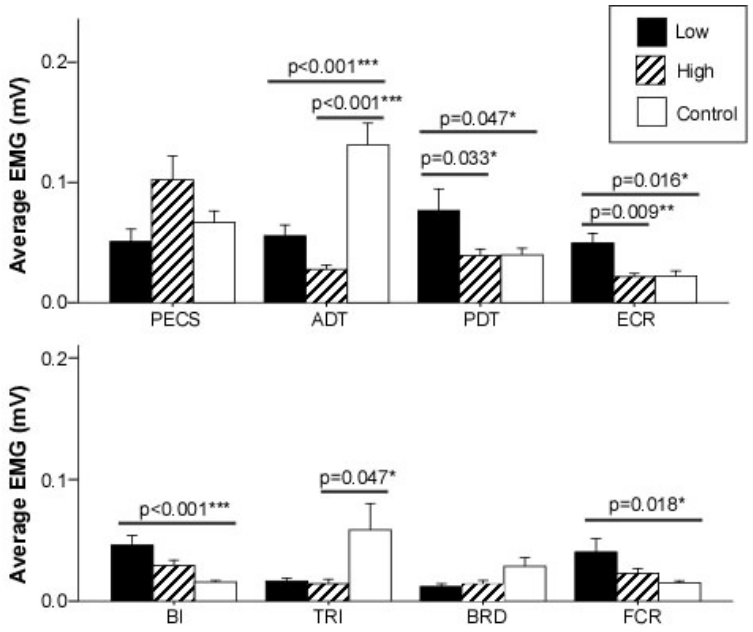

Figure 3-6: Muscle activities during stabilization. Stroke subjects had a different muscle activation pattern during stabilization than control subjects (ANOVA with the Tukey post-hoc test for all, except ECR, in which the corrected p-value from Games-Howell test was reported, ***p<0.001, **p<0.01, *p<0.05). Error bars indicate standard error.

3.3.4 Effects of Distal Sensory Manipulation on Arm Stability

When considering the effects of tendon vibration and electrical stimulation on arm stability, a three-way (3 subject groups x 4 blocks × 5 targets) ANOVA with repeated measures on the last two factors was performed in both stability error and error frequency to determine the main effect of experiment blocks and the interaction effect from target and subject group. Significant differences among blocks (main effect) was found in the logarithmic-scaled stability error ($F_{3,15}$=9.231, p=0.001) with a significant interaction effect between block and subject group ($F_{6,15}$=6.664, p=0.001) and between block and target ($F_{12,60}$=10.624, p<0.001). Separate post-hoc ANOVAs for each subject group and each target were done to determine the significantly different blocks, but no significant difference in stability error among blocks was found. Similar repeated measures ANOVAs were done with the error frequency, which revealed no significant differences among the experiment blocks ($F_{3,15}$=1.536, p=0.231) with no interaction effect from the subject group ($F_{6,15}$=1.413, p=0.251) and target ($F_{12,60}$=1.592, p=0.107). Figure 3-7 shows the individual data for all subjects. No systematic change in endpoint stability was observed with distal sensory manipulation. There appeared to be a possible trend in the low-FM subject group, with a lower mean stability error for the ES block. We conducted an additional two-way (4 blocks x 5 targets) ANOVA to check for effects within the low-FM group. No significant effects for block were observed ($F_{3,60}$ = 1.306, p=0.281), although the sample size was limited (n=4) for this group.

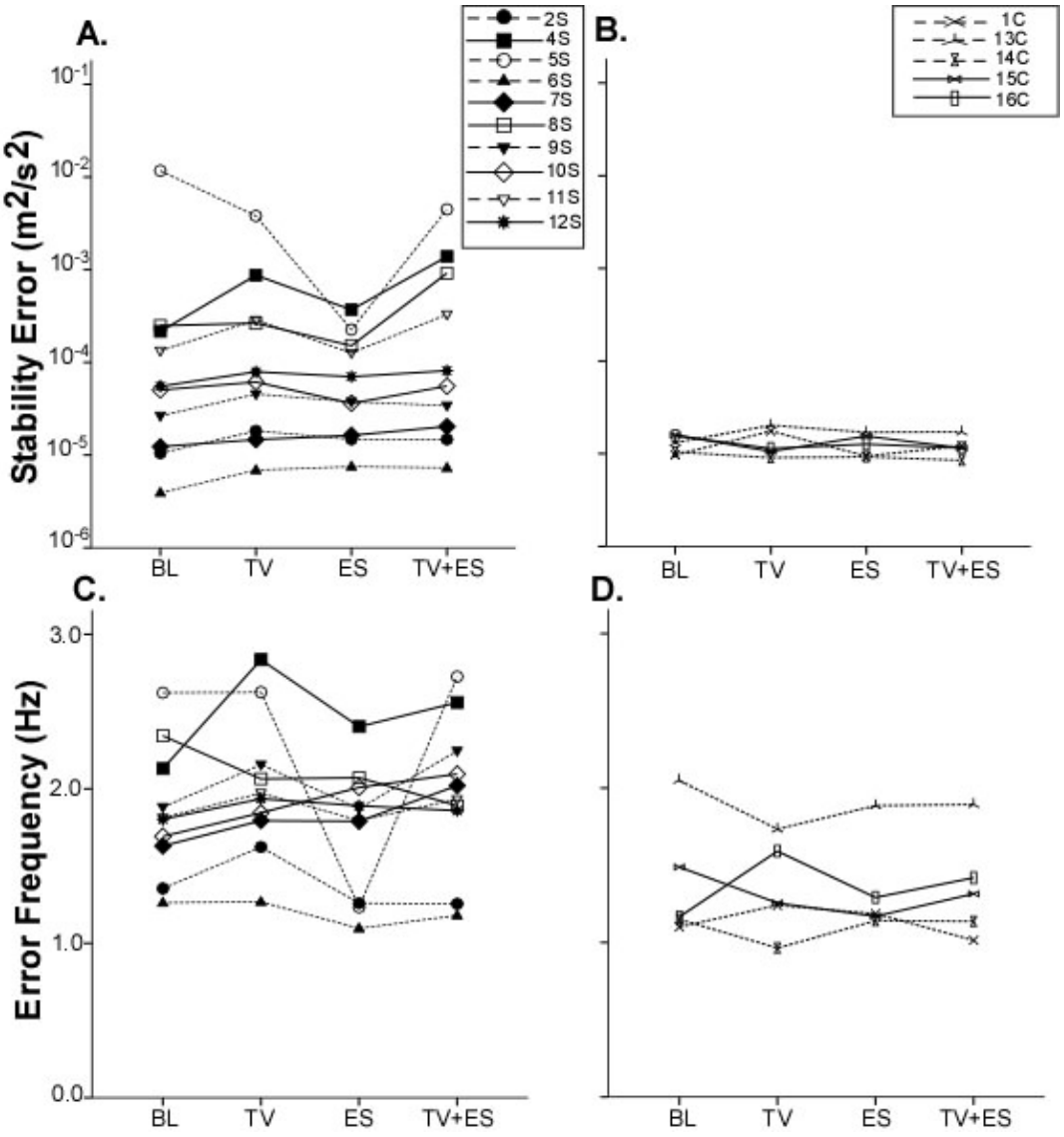

Figure 3- 7: Effects of distal sensory manipulation on stability measures. Stability error (A and B) and error frequency (C and D) of all subjects for BL, TV, ES and TV+ES blocks showed no systematic changes due to sensory stimulation. (Note that data are averaged across all 5 targets). Stability measures for stroke subjects are presented in the left panel (A and C) and for control subjects in the right panel (B and D) with the solid lines for subjects who were assigned ES block first (ES-TV) and dotted lines for those who were assigned TV block first (TV-ES). Among stroke subjects, the filled markers indicate high FM subjects and the open markers low FM subjects.

A three way (3 subject groups x 4 blocks × 5 targets) ANOVA with repeated measures on the last two factors was also done with all muscle activities during the

stabilization period. A significant difference among blocks was found only in the EMG_{avg} of FCR ($F_{1.57,18.79}$=5.957, p=0.014) with no interaction effect from subject group ($F_{3.31,18.79}$=2.199, p=0.120) or target ($F_{1.74,20.82}$=9.231, p=0.452). Post hoc ANOVAs showed that FCR activity in stroke subjects during stabilization of the TV+ES block was significantly higher than in the BL block (Tukey post-hoc, p=0.020) as illustrated in Figure 3-8.

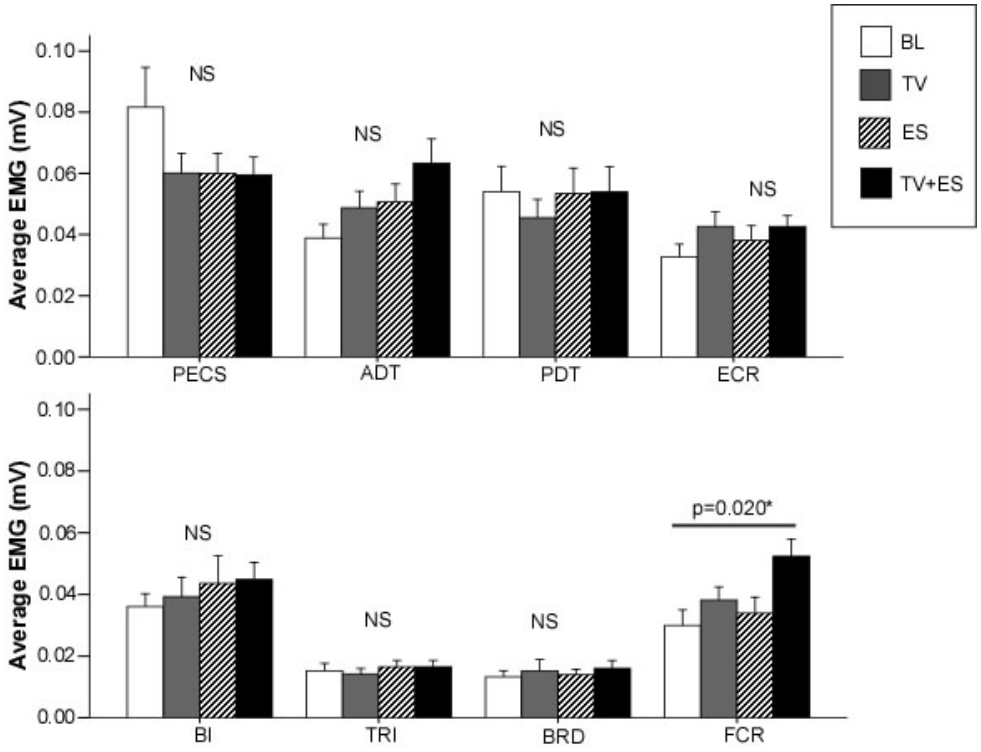

Figure 3- 8: Muscle activities during distal sensory stimulation in stroke subjects. No significant change in muscle activities with distal sensory stimuli was found except for the FCR. Significantly higher FCR activity was observed with the combination of tendon vibration and electrical stimulation (TV+ES) than the BL block. Error bars indicate standard error.

3.4 DISCUSSION

Stroke subjects had significantly greater endpoint instability than the control subjects, although the magnitudes of stability error were relatively low. The instability of the paretic arm was higher in the stroke subjects with low FM than in subjects with high FM and control subjects and was correlated with the level of sensorimotor impairment (FM score) except for the medial target. During endpoint stabilization, stroke subjects had significantly lower plane of elevation than control subjects with significantly lower activity of the ADT and higher activity of PDT. No significant effect on the arm stability from either tendon vibration or electrical stimulation on the arm stability was observed.

3.4.1 Endpoint Stability

Subjects with low-FM had significantly higher instability at the endpoint than high-FM stroke subjects and control subjects. This instability, as measured by the stability error, was significantly correlated with FM score except for the medial target. The strongest correlation was at the lateral target (Figure 3-3 C). This directional dependent stability that correlated with FM score could be linked to an abnormal synergy pattern post-stroke and/or a compensatory posture to stabilize the arm.

Endpoint stability of the arm is determined by endpoint impedance, which can be modulated either by muscle co-activation (Franklin et al., 2007) or by adjusting limb configuration (McIntyre et al., 1996). In post-stroke hemiparesis, the instability observed at the final position in 2D planar arm movement (Mihaltchev et al., 2005) is linked to the

impaired ability to modulate the co-activation of opposing muscles associated with the proprioception integrity of the paretic limb (Scheidt & Stoeckmann, 2007). Therefore, muscle co-contraction may not be a preferred strategy for stroke subjects to stabilize their arms, especially in the 3D workspace, compared to adjusting limb configuration.

3.4.2 Arm Postural Stability Strategy Post Stroke

Differences in arm posture could be associated with patterns of muscle activation traditionally classified as "synergy'. Synergy patterns in post-stroke patients (Brunnstrom, 1970) consist of flexor synergy (scapular adduction, elevation and shoulder abduction and external rotation, elbow flexion, forearm supination, wrist flexion and finger flexion) and extensor synergy (scapular abduction and depression, shoulder adduction and internal rotation, elbow extension, forearm pronation and wrist and finger flexion or extension). More horizontal abduction (Figure 3-4) and increased PDT activity (Figure 3-5) in stroke subjects could be associated with the flexion synergy pattern post-stroke. Synergy patterns have been suggested to possibly have the neural origin resulting from increased ipsilateral projection to the proximal arm muscle (Schwerin et al., 2008). Increased ipsilateral projection, specifically in the ipsilateral reticulospinal pathways, and multisegmental contralateralization of these pathways can coactivate shoulder abductors and elbow flexors (Matsuyama et al, 2004). Abduction and elbow flexion torque patterns in stroke subjects have been shown to be robust, regardless of changing position. This robust posture may be due to an inability to centrally modify the changing somatosensory input from the shoulder angle (Ellis, Acosta, Yao, & Dewald, 2007). During the

stabilization period of the experiment, stroke subjects may find a decreased plane of elevation, a portion of the flexion synergy, as a convenient posture to stabilize their arm.

The decreased plane of elevation in stroke subjects can also be explained in terms of a strategy to stabilize arm posture. Increased endpoint stiffness to maintain arm stability is generally associated with increased co-contraction of the antagonistic muscles (McIntyre et al., 1996). However, adjusting arm posture has been found to be more effective in modulating endpoint stiffness when stabilizing hand position than co-contraction, especially when the arm is in a position in which increased co-contraction can cause little effect in improving stability, e.g. the more extended elbow (Milner, 2002). For stroke subjects, where modulating co-contraction is difficult and weakness at the shoulder joint is problematic (especially in the anterior deltoid (Figure 3-6)), adjusting the arm posture by decreasing the plane of elevation may be preferable to co-contracting the arm muscles for stabilization. As all targets were in the reachable workspace, elbow extension was less demanding and should not be problematic for stroke subjects to reach towards each target. In order to stabilize their arms of subjects with low-FM who also had weak ADT but preserved strength of PDT, decreasing the elevation angle could reduce the required joint moment at the shoulder by decreasing of the moment arm between the shoulder joint and center of mass of the arm. Alternatively, decreasing plane of elevation in low-FM stroke subjects could be a strategy to compensate for ADT weakness.

3.4.3 Effects of Sensory Manipulation at the Wrist Level

Tendon vibration at the wrist flexors has been found to improve the endpoint stability in 2D planar movement (Conrad et al., 2011). However, no significant effect either from tendon vibration or electrical stimulation on improving arm stability in a 3D workspace was observed in the current study. One explanation would be that in 2D movement, the arm muscles activities are generally decreased (Prange et al., 2009) which leads to lower torque generation when reaching to a distal target compared to a proximal target (Beer et al., 2007). The difference in overall muscle activation might result in different characteristics of endpoint stability in 2D and 3D arm movements which would give different effects from tendon vibration. Decreased muscle activity associated with improved the 2D arm stability during wrist tendon vibration (Conrad et al., 2011) was not observed in the current study. A significant increase in FCR activity, which is independent of the whole arm stability, in the TV+ES block was hypothesized to be from muscle reflex response to stimulation.

3.4.4 Clinical Implication

The clinical contribution from this study is that the 3D arm stability was a deficit only in stroke subjects with low FM score in which they significantly decreased the plane of elevation, possibly to facilitate arm stabilization. In the free reaching and stabilizing, the limitation for stroke subjects was likely to be from the abnormal arm posture and limited functional range of motion. Even though abnormal shoulder abduction and elbow

flexion is a dominant characteristic of people with post-stroke (Brunnstrom, 1970), many studies have found that the paretic arm can be trained to extend the range of motion and break the synergy patterns, especially the flexor synergy associated with shoulder abduction and elbow flexion, through appropriate strength training (Ellis et al, 2009). This ability to move outside the flexor synergy pattern after the strength training could be due to a reduced need to compensate for shoulder weakness, rather than a change in fundamental synergy properties.

CHAPTER 4: ARM MOVEMENT AND STABILITY DURING DISCRETE AND CONTINUOUS TRACKING TASKS IN POST-STROKE HEMIPARESIS

4.1 INTRODUCTION

The simultaneous control of posture and movement in the paretic arm is an important component of functional movement in stroke survivors. Arm function in many activities of daily-life requires maintaining a stable arm posture while performing a hand movement task such as grasping an object off a table or writing on a pad of paper. These types of tasks require control of arm posture and simultaneous control of movement in distal joints to accomplish multiple features of the functional task. Even in the healthy nervous system, the simultaneous control of posture and movement is controversial in terms of whether the motor system uses distinct controls of posture and movement (Scheidt & Ghez, 2007) or a single robust control process (Feldman & Levin, 1995). Both motor control theories are supported by neurophysiologic evidence for either distinct centers for movement and stabilization (Kurtzer et al., 2005) or for common neural centers (Sergio et al., 2005). Similarly, experimental evidence has been presented on both sides of the issue. Some experimental results support the hypothesis of separate controllers (Scheidt & Ghez, 2007; Burdet et al., 2006) while other experiments that suggest a common controller provides a single control mechanism for both movement and stability (Pilon et al., 2007; Foisy & Feldman, 2006). Stroke survivors have enhanced movement errors, particularly for complex tasks and the nature of the impairments likely depend on the mechanisms of control. Investigations of simultaneous

control of postural stabilization and fine movement in stroke survivors is invaluable to understanding normal and impaired movement, and could provide valuable insight for developing assessments and therapies for recovery of function.

The primary motor control strategies implicated for stabilizing arm posture are 1) to appropriately increase limb impedance through muscle co-contraction (Gribble et al., 1998) and 2) to adjust arm posture in a direction that minimizes instability (Franklin et al., 2007). The co-contraction strategy may not be adequate for a task that requires simultaneous movement and stability, as it does not allow strength and stability of the limb to be modulated independently (i.e. increased co-contraction can increase limb stability but decrease the net force generation of the arm) (Perreault et al., 2004). An arm posture strategy, which is effective in stabilizing hand position, especially for postures in which co-contraction is compromised (Milner, 2002), could be a useful strategy to stabilize the arm while allowing appropriate force generation to perform a task. In stroke survivors, clinical observations suggest that arm postural stability is impaired; however, there is little published evidence of this instability, to date. A number of possible pathophysiologcal mechanisms could contribute to arm instability and similarly, stroke survivors might compensate for instability using co-contraction or postural adjustments.

Instability of the arm is a likely consequence of the motor impairments that occur after a stroke. Major impairments in people with post-stroke hemiparesis include weakness (Mercier & Bourbonnais, 2004; Meskers et al., 2009) and loss of fine control of movement (McCombe & Whitall, 2004). Weakness of the paretic arm may limit a co-contraction strategy, since some muscle groups might not generate enough force to provide adequate co-contraction to stabilize the arm, especially against gravity in a 3D

workspace. Conversely, spastic muscle activity could abnormally increase co-contraction and thus inadvertently increase arm stabilization. As an alternative strategy, adjustments to arm posture in people post-stroke may serve to improve arm stability. This may have other consequences, such that the arm is placed in unusual postures during functional tasks, thereby forcing changes to the control of a movement task at the distal joint. The impairment in fine motor control of the paretic arm during movement has been observed in 2D arm-supported conditions, where paretic arm movement is segmented (Roher et al., 2002), suggesting an inability to finely grade muscle movement after stroke (Canning, Ada, & O'Dwyer, 1999; Takahashi & Reinkensmeyer, 2003). This loss of ability to finely grade muscle contractions might interfere with arm postural stabilization, which is a task that requires small modulations in muscle activity to correct minor errors.

The aim of this study was to characterize arm instability during a task that required both arm postural stability and fine motor control. The task consisted of controlling a laser pointer while tracking a circular moving target. Discrete and continuous protocols of the circle tracking task in the vertical plane were used to investigate endpoint stability and movement post-stroke. The discrete tracking task allowed segmented movement with intermittent stabilization of arm posture along a circle. The task required features of endpoint stabilization and arm postural stability. The continuous tracking task required simultaneous control of stability of the arm and fine control of movement. The results demonstrated how people with post-stroke hemiparesis stabilize the affected arm and, from this stable posture, performed fine movement tasks.

4.2 MATERIALS AND METHODS

4.2.1 Subject Population

Ten chronic stroke subjects (age 56.6±6.8 years) with upper extremity hemiparesis and ten neurologically intact control subjects (age 68.2±13.1 years) participated in the study (Table 4-1). Inclusion criteria for the participation of stroke subjects in the study were that the subjects be at least 21 years of age and have a history of stroke (> 6 months) resulting in upper extremity hemiparesis. Exclusion criteria included: recent treatment of botulinum toxin injection in the upper extremity (< 2 months), a diagnosis of another neuromuscular disorder, the inability to give informed consent, apraxia, multiple strokes, chronic neck, shoulder or back pain, and the inability to follow and focus on two –step commands. Fugl-Meyer assessment (Fugl-Meyer, 1975) of the upper extremity was conducted by a licensed physical therapist before the experiment. The range of Fugl-Meyer scores was from 26 to 66 (46. 4 ± 14.2, N = 10) as listed in Table 4-1. The study was initiated after the subjects gave informed consent in compliance with protocols approved by the Institutional Review Board of Marquette University.

Table 4-1 Subject information

Subject	Sex	Age (Years)	First Tested Arm*	Dominant Arm#	Years after Incidence	FM Score##	Proprioception**
1S	M	53	R	R	3	40	Impaired
2S	F	61	L	R	25	26	Normal
3S	F	60	R	R	20	50	Impaired
4S	F	63	L	R	4	62	Normal
5S	M	63	R	R	4	42	Impaired
6S	M	58	R	R	7.5	29	Impaired
7S	M	55	R	R	4	36	Impaired
8S	F	59	L	R	8	50	Impaired
9S	F	54	R	R	17	63	Normal
10S	F	40	L	R	5.5	66	Impaired
1C	M	66	R	R	Control	-	Normal
2C	F	56	R	R	Control	-	Normal
3C	F	83	L	R	Control	-	Normal
4C	M	43	L	R	Control	-	Normal
5C	F	62	R	R	Control	-	Normal
6C	M	64	L	L	Control	-	Normal
7C	M	84	L	R	Control	-	Normal
8C	F	79	L	R	Control	-	Normal
9C	M	79	L	R	Control	-	Normal
10C	F	66	R	R	Control	-	Normal

Before the stroke incidence

Based on Motor Upper Extremity Fugl-Meyer score; 0-66

* First tested arm is the paretic arm for stroke subjects and was randomly selected (5 dominant and 5 non-dominant arms) for control subjects (see Table 4-2).

** Based on the Thumb Localizing Test

4.2.2 Test Apparatus

A series of the cursor targets (3-cm black dot) were projected onto a screen (black foam board) from a computer projector (NEC, model NP110, 2200 Lumens DLP Projector). The cursors were created using a custom LabVIEW program that controlled the timing and movement sequence of the cursor. The program also produced audio cues to indicate the start and stop of the cursor and synchronized the data collection of EMG

with data collection of a motion tracking system through a DAQ board (NI USB – 6229, NI Corporation, TX, USA).

The subjects tracked the projected targets using a green laser pointer (laser pointer module; model BO 798, 3VDC, 200mA, 5W) attached to a wrist splint. A high-speed digital camera (CASIO, model EX-FH100 high-speed camera) was used to record the motion of the laser pointer on the screen with a speed of 100 fps.

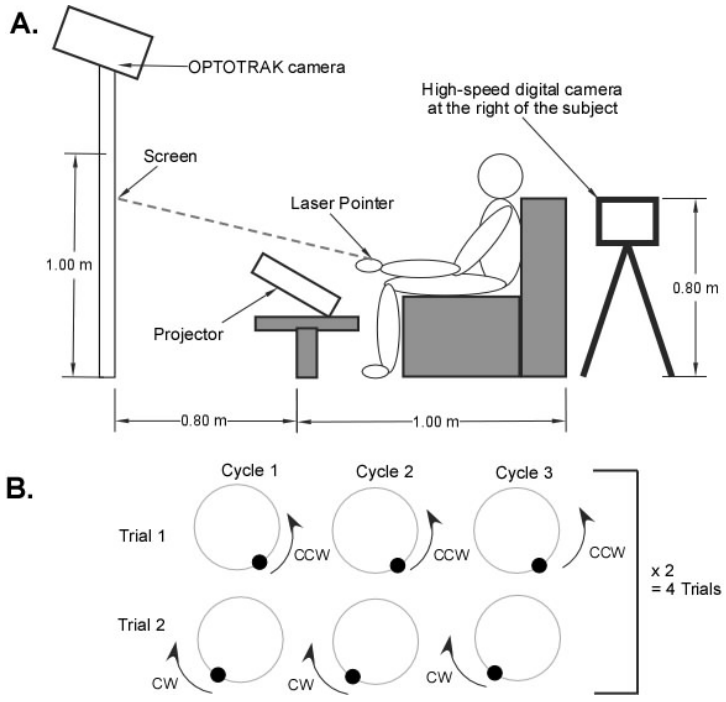

Figure 4-1: Schematic Diagram of the Experimental Set-Up. A. Subjects were seated on a comfortable chair with 4-point harness to restrain trunk and shoulder movement. An OPTOTRAK camera was used to measure arm motion. A digital camera was used to record the positions of the laser pointer and the target cursors on the screen in front of the subject. **B.** The diagram illustrates the target cursor presentation for discrete and continuous tasks that started with a counterclockwise (CCW) direction in the first trial (Trial 1), and was composed of 3 cycles. Black dots indicate the target cursors. Gray circles show the path, but were not actually present on the screen during the experiment.

Kinematic data were collected using a camera-based tracking system (OPTOTRAK 3020, Northern Digital, Ontario, Canada) with a sampling frequency of 100 Hz. The OPTOTRAK cameras detected infrared emitting diode (IRED) markers which were attached to two flexible Aquaplast® orthoses, one on the upper arm (6 IRED markers) and one on the lower arm (6 IRED markers) for both arms. Markers were arranged so that a minimum of 3 markers could be seen by the camera during the arm movement. The acromion (AC), the medial (EM) and the lateral (EL) epicondyles of the humerus, and the styloid processes of the radius (RS) and ulna (US) were registered as virtual markers by calibrating their positions with respect to the markers of the orthoses prior to the experiment. The glenohumeral joint rotation center (GH) was estimated by translating the AC position 14 mm laterally, 37 mm downward and 8 mm to the front (Wang, 1999). Markers on the orthoses were used to calculate the positions of virtual markers (GH, EM, EL,US and RS) for each frame of motion using Toolbench® v. 1.1 (Northern Digital, Ontario, Canada). These virtual markers' positions were used to compute the joint angles as described in Appendix A. Missing marker positions were filled by cubic spline interpolation and then the 3D position data were low-pass filtered (cutoff frequency = 5 Hz) using a 2^{nd} order zero-phase Butterworth filter.

Surface electromyography (EMG) was collected from four arm muscles of each arm: the anterior deltoid (ADT), posterior deltoid (PDT), biceps (BI) and lateral head of triceps (TRI). Disposable Ag/AgCl electrodes (Vermed Medical, Bellows Falls, VT) were placed over the muscle bellies on lightly abraded skin and the signals were amplified (x1000) and band-pass filtered (10 – 1000 Hz) prior to sampling (Bortec

Medical AMT-16; Calgary, Alberta, CA). The EMG signals were recorded using a data acquisition device (NI USB – 6229, NI Corporation, TX, USA) and the custom written LabVIEW program.

4.2.3 Experimental Protocol

The experiments consisted of two different tasks (discrete and continuous tracking tasks), performed in two blocks (Paretic and Non-Paretic for stroke subjects and Dominant and Non-Dominant for control subjects). In the first experiment block, five stroke subjects and five control subjects were randomly selected to perform the discrete tracking task while the other five of each group were randomly assigned to do the continuous tracking (see task sequence in Table 4-2). Stroke subjects were asked to perform the task, either continuous or discrete tracking, using the paretic arm (P) in the first block, then the non-paretic arm (NP) in the second block. For control subjects, the first tested arm was randomly assigned as dominant or non-dominant, as listed in Table 4-2 (first tested arm), followed by the other arm in the second block. The directions of target movement, clockwise (CW) and counterclockwise (CCW), were also randomly assigned among all subjects as shown in Table 4-2. Stroke subjects were called back for an additional session of the same protocol. Data from these two sessions were averaged in order to minimize the day-to-day variability. The protocols of the two tracking tasks are described below.

A. Discrete tracking task

Subjects were asked to place the laser pointer onto a cursor projected on the screen, with the cursor moving in a point-to-point manner. The cursor moved along nine segments, with points lying on a circle of 27 cm diameter. (The actual circle was not projected.) The nine points were defined by 9 arcs on the circumference of the circle, which consisted of three 60-degree arcs, three 45-degree arcs and three 15-degree arcs, which were placed in random order on the circle. The target cursors appeared one at a time, with an audible cue when each target appeared. The trial started with the projection of the cursor on the bottommost position on the circle, along with the audible cue. Subjects were instructed to move the laser pointer toward the cursor as fast as possible and stabilize the laser pointer within the boundary of the cursor. The time interval between the audible cues (and new cursor positions) was 3 s (i.e. the total 'on' period for each position). One block of tracking consisted of 4 cycles (2 clockwise and 2 counterclockwise directions) and each cycle consisted of movement involving 3 complete revolutions. The cursor moved discretely along the circle in either a clockwise or counterclockwise direction for 3 cycles (9x3 = 27 movements/cycle), with a 5 second pause when subjects were asked to relax before the new cycle started in the opposite direction.

B. Continuous tracking task

Subjects were instructed to track a continuously moving cursor with the laser pointer. The trial started with an audible cue and projection of the cursor at the bottom of the circle. The cursor was 3 cm in diameter and moved along a 27-cm diameter circle

(not projected) at a speed of 24 deg/s or 0.0565 m/s. The cursor started to move with an audible cue from the start position at the bottom of the circular trajectory, and disappeared with another audible cue when it reached the end position. The subjects were asked to follow the cursor continuously with the laser pointer, keeping the laser pointer within the boundary of the cursor. At the stop position, which was after the third full circle, when no black dot was present on the screen, subjects were asked to relax their arms at the home position and ready for the next trial. The cursor moved along the circle in either a clockwise or counterclockwise direction 3 times, with a 5-second pause following the third full circle of the cursor, as illustrated in Figure 4-1 B.

Table 4-2 Experiment information

Stroke Subjects	Control Subjects	Task Sequence[#]	Direction Sequence[##]	First Tested Arm (Control)[*]
1S	**1C**	D	CCW	D (R)
2S	**2C**	D	CCW	D (R)
3S	**3C**	C	CCW	ND (L)
4S	**4C**	C	CW	ND (L)
5S	**5C**	D	CW	D (L)
6S	**6C**	C	CCW	D (R)
7S	**7C**	C	CW	ND (L)
8S	**8C**	C	CCW	ND (L)
9S	**9C**	D	CW	ND (L)
10S	**10C**	D	CW	D (R)

[#] C= continuous tracking task first and D= discrete tracking task first
[##] CW= clockwise first and CCW= counterclockwise first
* D= dominant and ND= non-dominant arm. In parentheses, R= right and L=left.

4.2.4 Data Analysis

Data analysis in this experiment focused on the characteristics of tracking path, arm stability and posture and muscle activities. Three main analyses were arm kinematics, tracking trajectory and EMG.

Kinematic Analysis

Joint angles (shoulder elevation, plane of elevation, humeral rotation and elbow flexion) were calculated from the positions of the virtual markers of the specified bony landmarks (GH, EL, EM, US and RS) as illustrated in Appendix A. The mean joint angle during the discrete task was defined as the mean angle during the last 1 s window of the cursor 'on' period. For the continuous task, the angular motion traces of each tracking trial (3 cycles) were linearly detrended (*detrend* function in MATLAB), which yielded the linear trend and the residual signal. The mean joint angles (i.e. arm posture) during the continuous tracking task were the means of the linear trend, averaged over the four trials. The joint range of motion during continuous tracking was calculated as the average peak-to-peak amplitude (there were 3 maximums and 3 minimums) of the residual signal of each joint.

Tracking Trajectory Analysis

Time series of laser pointer locations were obtained from the positions of the laser pointer at each frame of the video recording (100 fps) during both tracking tasks. For each frame, the positions of the center of the laser pointer and the center of the cursor were defined by the centroids of the laser pointer image (*regionprops* function in

MATLAB). The laser pointer region was obtained by subtracting the current frame (I) from the background (B) image (I-B), in which B was the first frame of the tracking where there was no laser pointer or cursor present. The subtraction was used to enhance the contrast of the image and extract the green laser pointer object. Then, an appropriate color threshold was defined in order to obtain the binary image with a white region defined by the laser pointer and black otherwise. The cursor white region was obtained similarly except that, in order to extract the region of the cursor, the background image was subtracted by the current frame (B-I).

Tracking performance during discrete tracking was quantified by determining the covariance matrix of the laser pointer distribution during stabilization (i.e. during the 1-second window at the end of the cursor 'on' period), which was then visualized by a 95% confidence ellipse. Three parameters were calculated from the ellipse: orientation, area and aspect ratio. Orientation was defined by the angle between the first eigenvector, corresponding to the largest eigenvalue of the covariance matrix, and the vertical axis in either the left or right side, which basically quantified the deviation of the ellipse from the vertical line. Area was calculated from the product of the square root of the two eigenvalues and pi. Aspect ratio was the ratio of the square root of the larger eigenvalue by the smaller eigenvalue of the covariance matrix.

Performance parameters for continuous tracking were quantified as the root-mean-square error of the Euclidian distance between the laser pointer and desired cursor positions ($RMSE_{xy}$), average tracking velocity (Vavg) and standard deviation of the tracking velocity (Vstd). Tracking velocity was defined as the tangential velocity between 2 consecutive points.

EMG Analysis

The EMG signals were bandpass filtered (10-350 Hz) and then notch filtered to remove the line noise (58 -62 Hz) using a zero-phase 4th order Butterworth filter. The root-mean-square (RMS) of the filtered data (EMG_{rms}) was calculated using a 50 ms moving window. The average EMG area (EMG_{avg}) was obtained by integrating the EMG_{rms} over the specified period of time and was normalized by its respective time period (between T_2 and T_1 in Equation 2-2).

For discrete tracking, T1 and T2 were the stabilization time (1-second window at the end of the cursor 'on' period). EMGs from the discrete task during stabilization were obtained for the entire stabilizing period and finally averaged to obtain the average EMG during the discrete tracking task. For continuous tracking, T1 and T2 were defined as the period of the entire tracking trial (15 seconds). The average EMG during continuous tracking was obtained by averaging the values over the 4 trials.

Statistical Analysis

A repeated measures ANOVA was conducted to compare the effect of the arms of each subject group (i.e. paretic (P) and non-paretic (NP) arms of stroke subjects and dominant (D) and non-dominant (ND) arms of control subjects) on the measurement parameters. When a significant difference between the arms (within subject factor) was found, a post-hoc paired t-test was performed to determine the significant difference between P and NP, and D and ND. When a significant difference between subject group (between subject factor) was found, a post-hoc (4 arms x 2 subject groups) ANOVA with a Tukey post-hoc test was performed order to determine the difference between P and D

and between P and ND. For correlation analyses, Pearson correlation (2-tailed) were used to analyze the correlation with the Fugl-Meyer score. The level of significance was set at $\alpha = 0.05$ for all statistical tests. The statistical analysis was performed with the software package SPSS 16.0 (SPSS Inc., Chicago, USA).

4.3 RESULTS

4.3.1 Discrete Tracking Trajectories

Sample trajectories during one cycle of a discrete tracking trial from the paretic and non-paretic arm of a stroke subject (S7) and the dominant arm of a control subject (C4) are shown in Figure 4-2A for spatial illustration and Figure 4-2B for time series display. The 95% confidence ellipse during stabilization at the target for each case is illustrated in Figure 4-2C. More endpoint instability, based on the area of the ellipse (larger ellipse), was generally observed in the paretic arm.

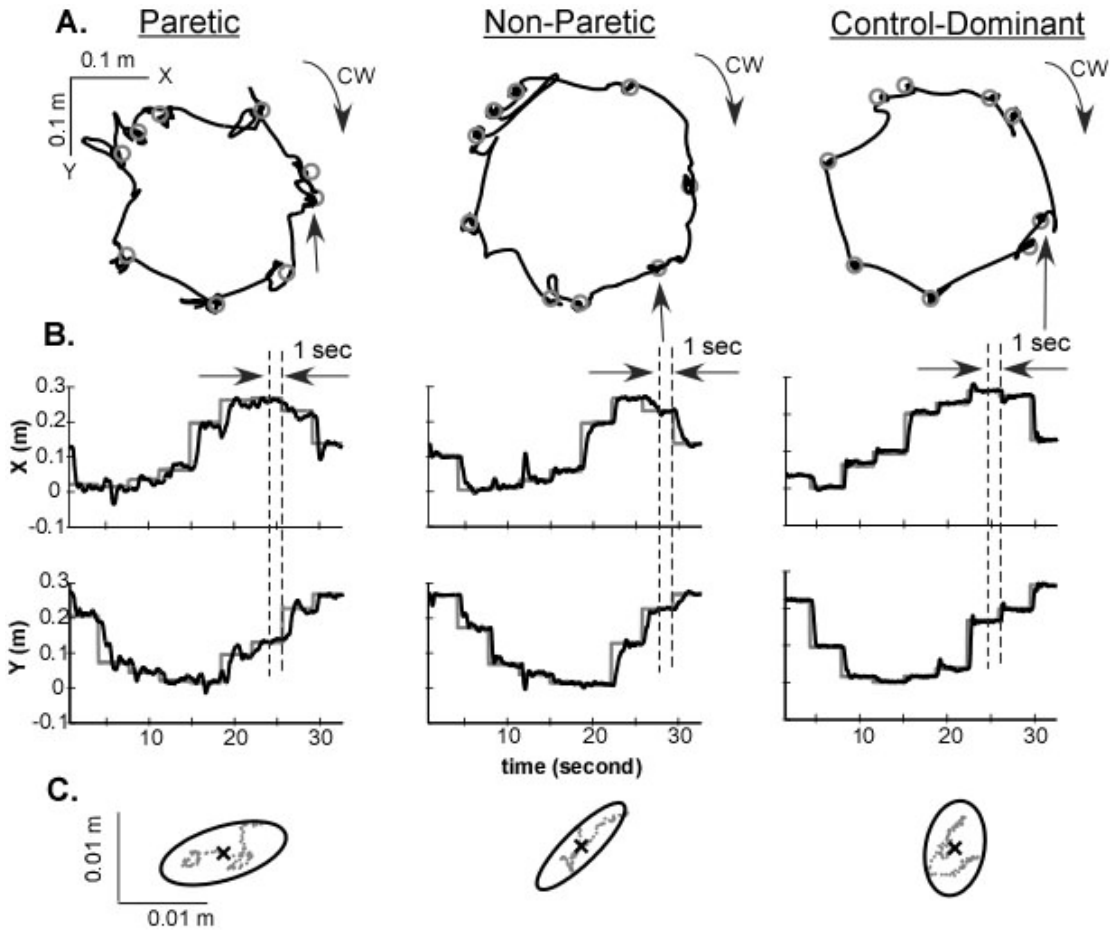

Figure 4-2: Discrete tracking trajectories A. Tracking trajectory traces (black) of the laser pointer during one cycle of a trial from paretic and non-paretic arm tracking of a stroke subject (S7) and the dominant arm tracking of a control subject (C4). Target cursors are displayed as gray open circles. **B.** Time series of X and Y positions during the same cycle trial. The stroke subject (S7) had shown higher endpoint instability than the control subject (C4). **C.** The 95% confidence ellipse of the endpoint trajectory during stabilization. Black crosses represent the mean positions during stabilization. Arrows from **A.** and **B.** indicate the target at which the laser pointer positions (100 points) during the 1-second window at the end of target appearance (stabilization phase) were used to determine the 95% confidence ellipses.

Endpoint stability measures determined from the characteristics of the 95% confidence ellipse, averaged over all trials of each subject during stabilizing period, are illustrated in Figure 4-3. The 95% confidence interval ellipses of the stroke subjects were significantly greater in the orientation angle ($F_{1,18} = 4.969$, $p=0.039$), aspect ratio ($F_{1,18} =$

7.400, p=0.014) and area ($F_{1,18}$ = 8.734, p=0.008) than control subjects. The post-hoc ANOVA revealed that the paretic arm was significantly higher in the orientation angle and area for dominant compared to non-dominant arms. For the aspect ratio, the only significant difference was found between the paretic and dominant arms (Figure 4-3A). Specifically, stroke subjects' endpoint instability was larger than control subjects with a direction of instability deviating more from the vertical axis and with the endpoint distribution more in a single axis during stabilization (more elongated 95% confidence ellipse). A significant correlation with the FM score was observed for the orientation (Pearson: r = -0.707, p = 0.022) and the area (Pearson: r = -0.743, p = 0.014) of the 95% confidence ellipse of the endpoint (Figure 4-3B).

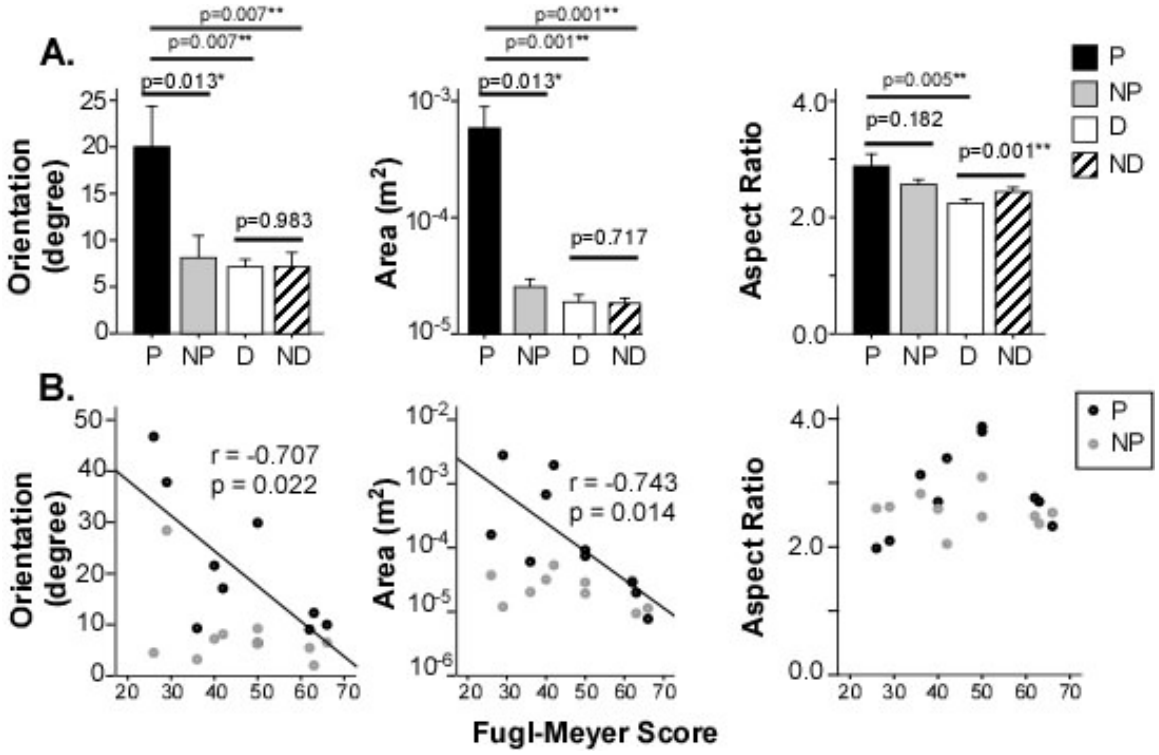

Figure 4-3: Discrete tracking performances A. Comparisons of orientation, area and aspect ratio of the 95% confidence ellipse of the endpoint variability during stabilization among paretic (P) and non-paretic (NP) arms of stroke subjects and dominant (D) and non-dominant (ND) arms of the controls subjects. Error bars represent ± 1SE. **B.** Correlation with the Fugl-Meyer score for the paretic (black) and non-paretic (NP) tracking.

4.3.2 Continuous Tracking Trajectories

Sample laser pointer trajectories during one cycle of a discrete tracking trial from the paretic and non-paretic arms of a stroke subject (S7) and the dominant arm of a control subject (C4) is shown in Figure 4-4A. Corresponding X and Y time series are plotted in Figure 4-4B.

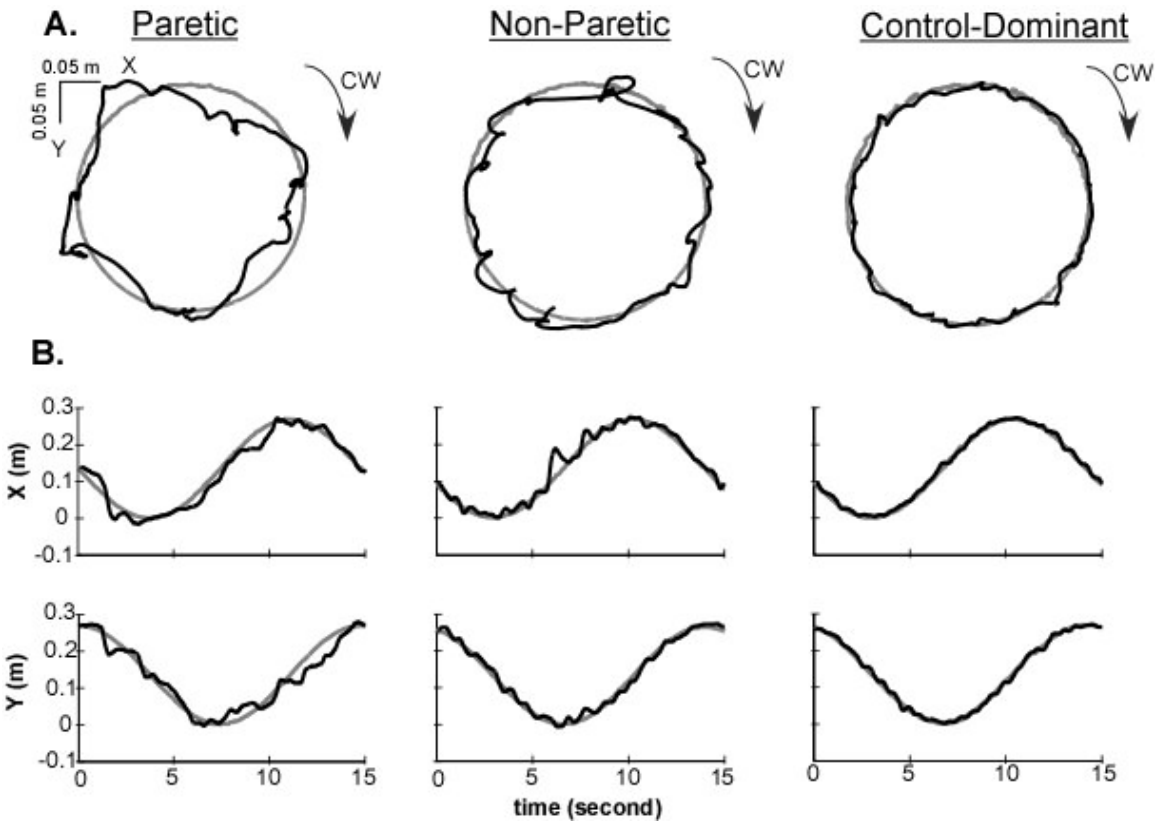

Figure 4-4: Continuous tracking trajectories A. Tracking trajectory traces (black) of laser pointer in 1 cycle of a trial from paretic and non-paretic arm tracking of a stroke subject (S7) and a dominant arm tracking of control subject (C4). Target cursor trajectories are displayed in gray. **B.** Time series of X and Y positions during the same cycle trial.

Performances in the continuous tracking task were quantified by the root mean square error of the laser pointer positions during tracking ($RMSE_{xy}$), average tracking velocity (Vavg) and standard deviation of the tracking velocity (Vstd). Stroke subjects had significantly larger $RMSE_{xy}$ ($F_{1,18} = 6.305$, $p=0.022$), Vavg ($F_{1,18} = 7.623$, $p=0.013$) and Vstd ($F_{1,18} = 8.184$, $p=0.010$) compared to control subjects. Post-hoc paired t-tests showed significant differences between the paretic and non-paretic arms in $RMSE_{xy}$ ($p=0.035$), Vavg ($p=0.023$) and Vstd ($p=0.029$), but not between the dominant and non-dominant arms. Post-hoc ANOVAs revealed that paretic arm tracking was significantly

different from dominant and non-dominant arms in $RMSE_{xy}$, Vavg and Vstd, as shown in Figure 4-5A. A significant correlation with the Fugl-Meyer score (Figure 4-5B) was found in RMSExy (Pearson: r = -0.710, p = 0.021), Vavg (Pearson: r = -0.658, p = 0.039) and Vstd (Pearson: r = -0.799, p = 0.006).

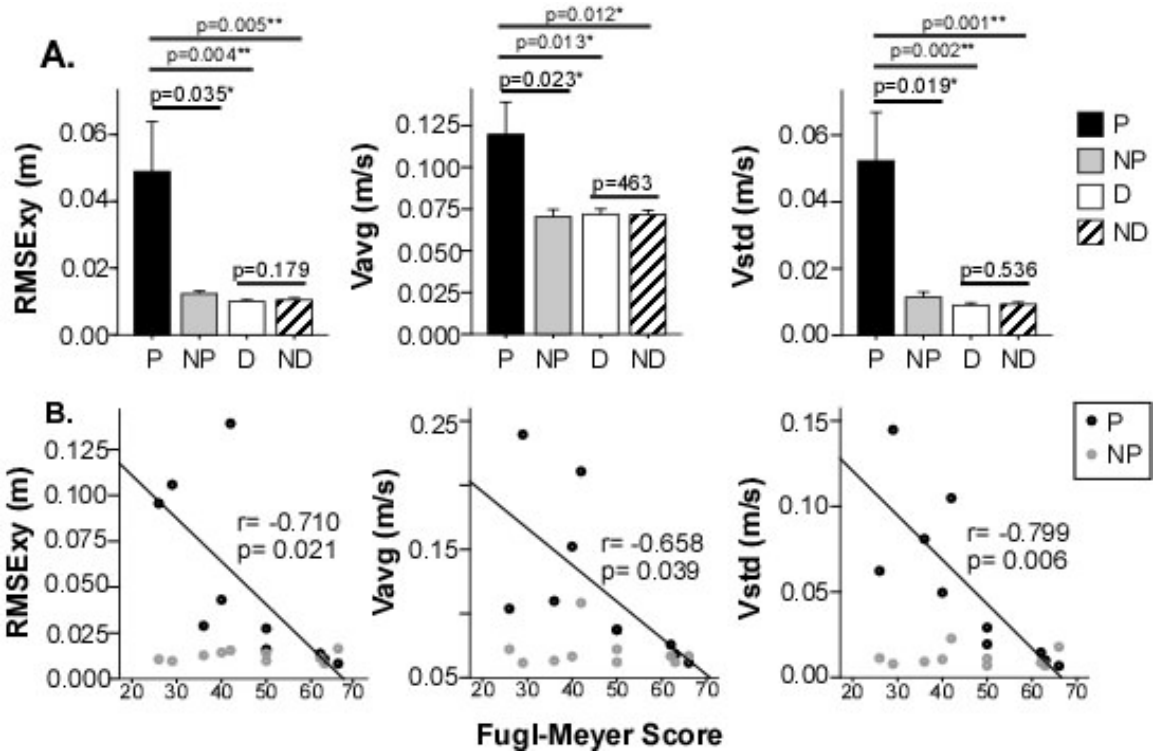

Figure 4-5: Continuous tracking performances A. Comparisons of root mean square error of tracking trajectory (RMSExy), average tracking velocity (Vavg) and mean standard deviation of tracking velocity (Vstd) among the paretic (P), non-paretic (NP) arms of stroke subjects and dominant (D) and non-dominant (ND) arms of the control subjects. Error bars represent ± 1SE. **B.** Correlation of RMSExy, Vavg and Vstd with the Fugl-Meyer score for the paretic (black) and non-paretic (NP) tracking.

4.3.3 Arm Posture during Tracking

Mean joint angles during tracking are illustrated in Figure 4-6. Stroke subjects had significantly decreased mean plane of elevation of the paretic arm during both discrete tracking ($F_{1,18}$ = 12.217, p=0.003) and continuous tracking ($F_{1,18}$ = 6.912, p=0.017). The mean elbow angle was also observed to be significantly decreased in paretic tracking for the discrete task ($F_{1,18}$ = 5.073, p=0.037) but not for the continuous task ($F_{1,18}$ = 4.073, p=0.059). For discrete tracking during stabilization, the paretic arm was significantly decreased in plane of elevation (post-hoc paired t-test, p = 0.020) and elbow extension (p=0.008) compared to the non-paretic arm. Similarly, non-dominant arms of control subjects also had significant decreases in plane of elevation (post-hoc paired t-test, p = 0.046) and elbow extension (p=0.012) compared to the dominant arms for discrete tracking.

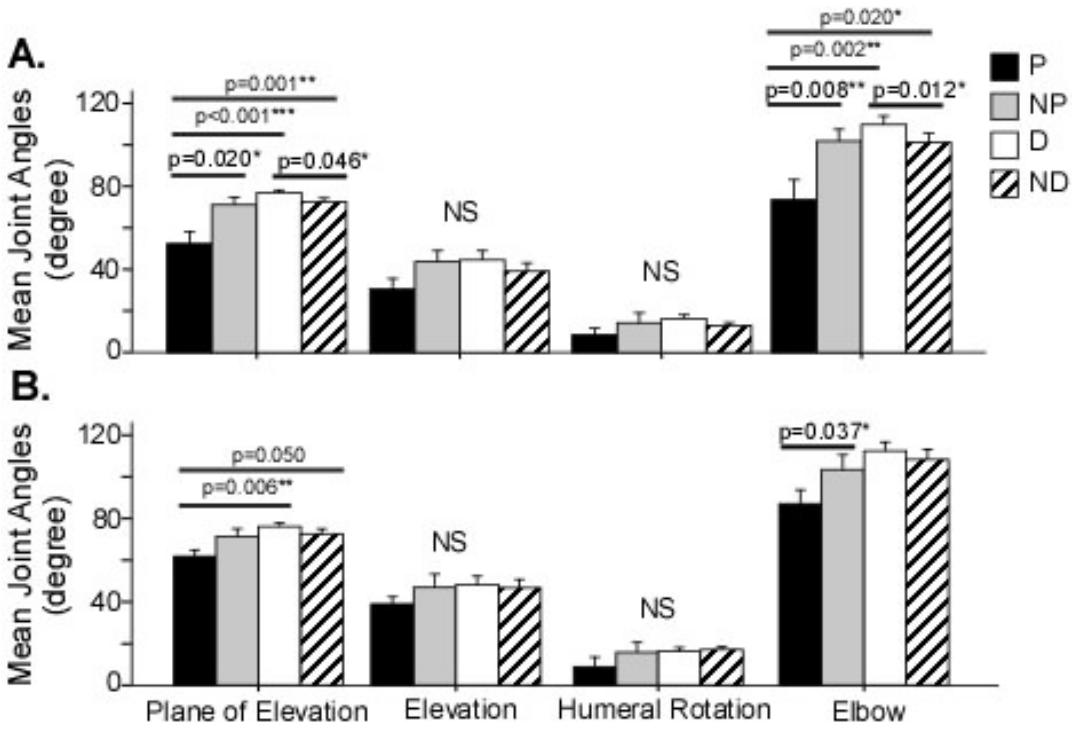

Figure 4-6: Mean joint angles during tracking Comparisons of joint angles during **A.** discrete tracking and **B.** continuous tracking among the paretic (P) and non-paretic (NP) arms of stroke subjects and the dominant (D) and non-dominant (ND) arms of control subjects. Stroke subjects significantly decreased their plane of elevation and elbow extension during both discrete and continuous tracking tasks. Error bars represent ± 1SE. Reported p-values were from the Tukey post-hoc test. Asterisks indicate the significant difference from the repeated measures test (* $p<0.05$).

The correlation of the Fugl-Meyer score and the mean joint angles of the paretic arms are illustrated in Figure 4-7. During the stabilization period of the discrete tracking task, a significant correlation of the Fugl-Meyer score was observed for the plane of elevation (Pearson: $r = 0.834$, $p = 0.003$) and elbow extension (Pearson: $r = 0.890$, $p = 0.001$). In the continuous tracking of the paretic arm, only elbow extension was significantly correlated with the Fugl-Meyer score (Pearson: $r = 0.751$, $p = 0.012$). No

correlation of arm posture and Fugl-Meyer score was found in the non-paretic arm during tracking.

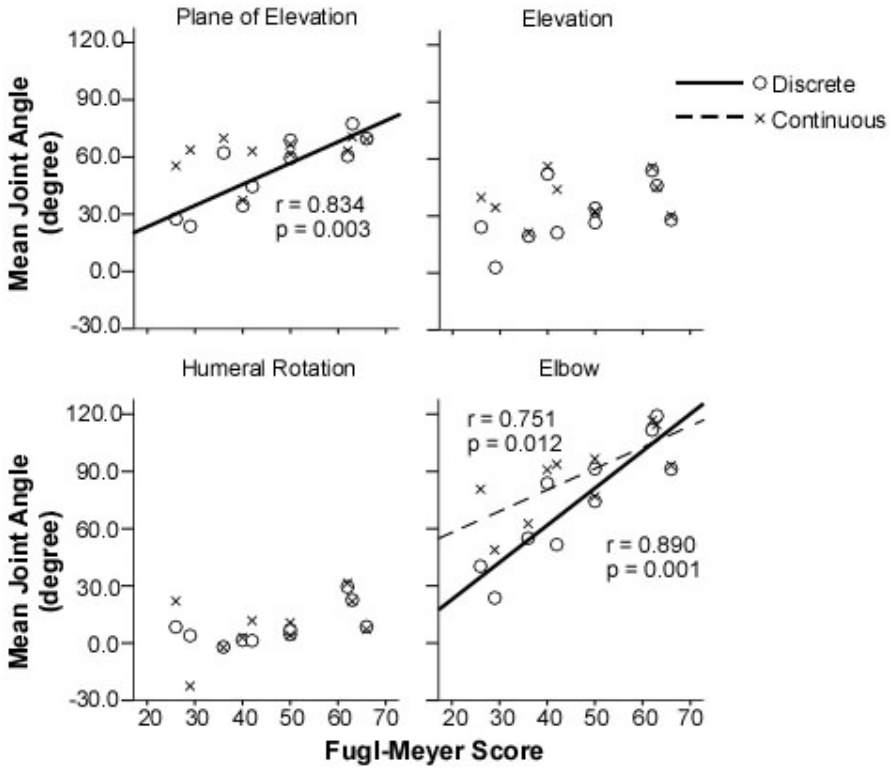

Figure 4-7: Correlation of the mean joint angles during tracking of the paretic arm with the Fugl-Meyer score. Elbow extension was significantly correlated with the FM score for both discrete and continuous tasks. Plane of elevation and humeral rotation were significantly correlated only in the discrete task. Elevation angles were not significantly correlated with the FM score. Lines show only the significant fit.

When considering the range of motion during continuous tracking (Figure 4-8), the paretic arm of stroke subjects showed a significantly larger range of motion in the plane of elevation ($F_{1,18} = 5.427$, $p=0.032$) and elbow ($F_{1,18} = 6.983$, $p=0.017$) than control subjects. Significant correlation with the Fugl-Meyer score was found only for

elbow extension (Pearson: r = 0.751, p = 0.012); specifically, subjects with lower Fugl-Meyer score had a significantly larger plane of elevation and elbow movement.

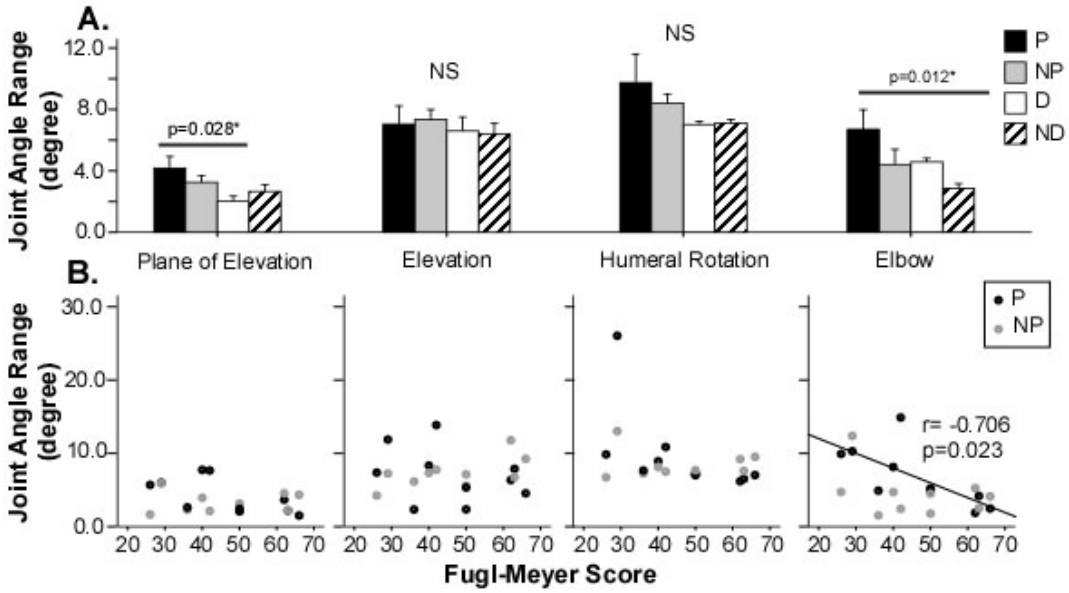

Figure 4-8: Joint angle range during continuous tracking A. Comparisons of joint angle ranges among the paretic (P) and non-paretic (NP) arms of stroke subjects and the dominant and non-dominant (ND) arms of control subjects. Stroke subjects had a significantly higher range of motion in the plane of elevation. Error bars represent ± 1SE. Reported p-values were from the Tukey post-hoc test. **B.** Correlation of the joint angle range with the Fugl-Meyer score during the paretic (black) and non-paretic (gray) tracking of all stroke subjects. Stroke subjects with lower Fugl-Meyer score had a significantly larger range of elbow motion during continuous tracking.

During both discrete and continuous tracking tasks, repeated measures ANOVA analyses did not show a significant difference in any muscle activities between the paretic and non-paretic arms of stroke subjects and the dominant and non-dominant arms of the control subjects for the continuous tracking task (Figure 4-9). Correlation with Fugl-

Meyer score was found only in the biceps for both discrete (Pearson: r = -0.736, p=0.015) and continuous tracking (Pearson: r = -0.807, p=0.005).

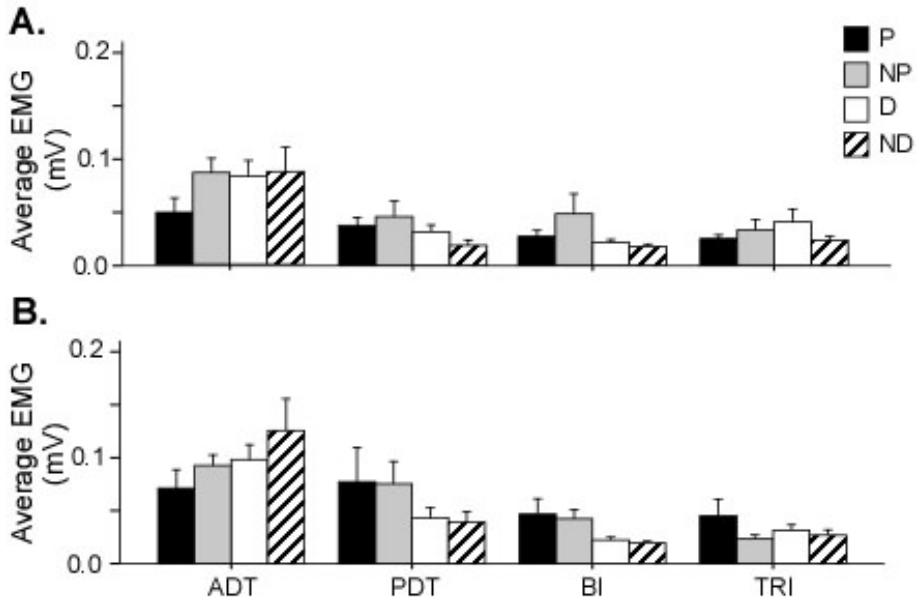

Figure 4-9: Average EMGs A. Comparisons of averaged EMGs during the stabilization period of the discrete tracking task and **B.** during the whole period of continuous tracking task. No significant difference among each tracking arm was found in all the averaged EMGs of both tasks.

4.4 DISCUSSION

Results from the current study provide documentation of the instability of the paretic arm during laser pointing tasks, which included combined postural and motion components, and demonstrated an arm postural strategy that stroke subjects used to stabilize their arms while performing tracking tasks. The postural strategy might be used

to compensate for weakness of the affected arm, or could be a consequence of motor impairments of the arm. Deficit in fine control of movement of the paretic arm was also evident, as the range of joint angular motion was greater than controls.

4.4.1 Arm posture during tracking

Stroke subjects appeared to use an arm postural strategy, which included decreasing the plane of elevation and decreasing elbow extension, to maintain stability of the arm. This strategy to maintain the paretic arm posture of stroke subjects may result from proximal weakness, abnormal stretch reflex gain of the paretic arm and/or the manifestation of muscle synergies post stroke.

Post-stroke weakness has been identified as a clinical impairment that directly affects movement integrity (Patten et al., 2004). Different arm postures during tracking using the paretic arm could be attributed to weakness, especially at the shoulder, since the posture consisted of a combined decrease in plane of elevation and elbow extension. This posture would reduce the joint moment required by the shoulder to counteract gravity by decreasing the moment arm (the distance between shoulder and center of mass of the arm). A similar pattern of arm posture during tracking was observed in the dominant and nondominant arms in control subjects. The relative strength differences of the dominant and nondominanat arms could affect the posture for the laser pointing task. The strength of the dominant arm is normally greater than the nondominant arm, especially in the shoulder (Chandler, Kibler, Stracener,, Ziegler, & Pace, 1992), although not necessarily at the elbow (Wittstein et al., 2010). Similar to stroke subjects, the

reduced plane of elevation and increased elbow flexion of the nondominant arm of control subjects might help reduce the joint moment at the shoulder, resulting in a more comfortable arm posture.

Abnormal stretch reflex gain post-stroke could make a co-contraction strategy during arm stabilization difficult for stroke subjects. Even though co-contraction is a strategy to increase limb stability, force generation and stability are independently regulated via co-contraction. Specifically, increased co-contraction can increase the limb stability, but compromise the force generation capacity of the arm (Perreault et al., 2004). In the tracking tasks of the present study, postural stability and movement were required simultaneously; thus, a co-contraction strategy could be difficult for stroke subjects. Since stabilization of the arm by means of co-contraction is accompanied by an increase in stretch reflex gain (Milner et al., 1995), decreased static and dynamic stretch reflex threshold and impaired regulation of stretch reflex threshold post stroke (Levin & Feldman, 1994; Schmit et al., 1999; Schmit & Rymer, 2001) may lead to deficits in the ability to appropriately co-contract antagonistic muscles during stabilization. Because of difficulty in modulating muscle contraction, a postural stability strategy may be more favored than co-contraction. For a postural strategy, the arm configuration is adjusted so that the direction of endpoint stiffness is aligned with the direction of instability, in order to stabilize the hand (Milner, 2002). Decreased plane of elevation and elbow extension is an arm posture that minimizes the moment arm of the endpoint (hand) and thus stabilizes the whole limb against gravity. Altered arm posture in stroke subjects may therefore be the strategy used by stroke subjects to stabilize their arm during tracking due to an

inability to regulate stretch reflex excitability, making modulation of co-contraction difficult.

Abnormal regulation of muscle 'synergy' patterns in stroke survivors could have contributed to differences in arm posture between the hemiparetic arm and controls. Decreased plane of elevation and elbow flexion are associated with a flexor synergy post stroke (Brunnstrom 1970; Dewald & Beer, 2001). In order for stroke subjects to accomplish the laser pointer task, they would have had to elevate the shoulder (to lift the laser). In the flexion synergy, active shoulder elevation is coupled with elbow flexion and shoulder abduction (i.e. equivalent to decreased plane of elevation), consistent with the posture observed in the current study. In addition, it is worth noting that the coupling of muscle activation within the flexor synergy is more robust and less sensitive to changing posture compared to the extensor synergy (Ellis et al., 2007). The posture associated with the flexor synergy might be the most comfortable or neutrally efficient posture for stroke subjects and thus stroke subjects could have used this posture during tracking for these reasons.

4.4.2 Endpoint stability during tracking

The current study demonstrated deficiencies in both static (i.e. the endpoint stabilization period of the discrete tracking task) and dynamic (i.e. the continuous tracking task) stability in stroke subjects. The static stability was defined by the trajectory variability during hold after the point-to-point movement and was quantified by the characteristics of the 95% confidence ellipse of the trajectory during stabilization,

including the deviation from 90 degrees of orientation of the principle axis, aspect ratio and area (Figure 4-3). Dynamic stability was characterized by the performance during continuous tracking (Figure 4-5) as in the trajectory error ($RMES_{xy}$), average tracking velocity (Vavg) and standard deviation of the tracking velocity (Vstd). Generally, stroke subjects demonstrated impairment in both static and dynamic instability during tracking which was correlated with the level of clinical impairment (Fugl-Meyer score). Possible underlying mechanisms for these instabilities include deficits in anticipatory control, an inability to finely grade muscle contraction, spasticity, weakness and limb posture.

Static instability of the arm, as measured by the characteristics of the 95% confidence ellipse of the trajectory during stabilization of the discrete task, demonstrated higher instability (larger ellipse area) than the controls with a direction of instability deviating more from the vertical axis (higher orientation angle) and with the endpoint distribution more in a single axis during stabilization (more elongated 95% confidence ellipse). Different orientation and shape of the ellipse was likely due to different arm posture of the paretic arm during stabilization (decreased plane of elevation and elbow extension) as the plane of elevation (Pearson: $r = -0.804$, $p=0.005$) and elbow (Pearson: $r = -0.693$, $p=0.025$) were significantly correlated with the orientation angle of the ellipse.

Dynamic instability of the paretic arm, as demonstrated by a larger $RMSE_{xy}$, higher tracking velocity (Vavg) and higher standard deviation of velocity (Vstd) than control subjects or the non-paretic arm could result from deficits in anticipatory control post stroke. During tracking, it is postulated that an internal model has to be updated using available sensory information (Vercher, Sares, Blouin, Bourdin, & Gauthier, 2003) and then implemented in the execution of a response to an external perturbation, (i.e. a

moving target that needs to be tracked in this case). It has further been suggested that stroke survivors have an impairment in anticipatory control due to the inability to implement an internal model fast enough (Takahashi & Reinkensmeyer, 2003). When tracking a continuously moving cursor, this impairment could result in larger spatial error, with higher and more fluctuating tracking velocity. Since the proprioceptive integrity of the paretic limb contributes significantly to the estimation of kinematic performance during updating of motor commands (Scheidt & Stoeckmann, 2007), dynamic instability during continuous tracking in stroke subjects could also result from impaired proprioception as measured by the thumb localizing test similar to the current study.

A larger range of motion during continuous tracking for the hemiparetic arm (Figure 4-8) likely reflected a deficit in fine motor control of movement post stroke. In addition to the supraspinal mechanism previously stated (i.e. involving the internal model), deficits in the ability to finely grade muscle contraction and relaxation post stroke could also contribute to the observed larger range of motion. Compromised rate of muscular force generation post stroke (Canning et al., 1999) and impairment in time to reduce and increase torque following stroke (McCrea et al., 2003) could affect the inability to finely grade muscle contraction in stroke subjects resulting in the higher range of motion in the plane of elevation and elbow during the fine motor control task of continuous tracking. Note that this could also have contributed to the differences in posture. The laser tracking required movement of the forearm to change the position of the laser pointer on the screen. The range of motion depends on the beginning arm posture, thus stroke subjects could have placed their arm in a posture such that movement

of the laser pointer involved greater joint angle ranges. If stroke subjects have an inability to finely grade movement, this larger range might make it easier to make small corrections in the laser pointer location. This strategy could have consequences to the stability of the laser pointer.

Trends in the dominant and nondominant arms of control subjects might reflect a similar adjustment to differences in fine motor control. Dominant and nondominant arms are specialized for different aspects of task performance, i.e. the dominant arm is specialized for maintaining the dynamic features of a movement while the nondominant arm is more specialized for stabilizing posture (Wang & Sainburg, 2007). This difference in the use of the dominant and nondominant arms likely affects how they are controlled during the laser pointing task, and differences in the ability to finely control movements in the arms could produce the same trend in posture and movement seen for the hemiparetic arm. That is, the posture, movement range and stability of the nondominant arm tended to be more similar to the paretic arm.

Spasticity and weakness of the paretic limb could also contribute to endpoint instability. The impaired ability to regulate descending stretch reflex threshold (Levin and Feldman, 1994) or altered stretch reflex coordination (Sangani et al., 2009; Trumbower et al., 2010) could contribute to the dynamic instability observed during discrete tracking. We observed a higher spatial error and tracking velocity in the hemipartic arm of stroke subjects compared to controls (Figure 4-5). During the stabilization periods of the discrete tracking task, there was also a larger area of the endpoint trajectory ellipse (Figure 4-3). These instabilities could arise from problems when a stretch at one joint causes a reflex response at a separate joint. The combined

reflex response could produce increases in endpoint error, rather than correcting errors as might normally occur in the reflex regulation of endpoint stability

The altered limb posture could have affected the characteristics of endpoint instability post stroke. The orientation of the ellipses of the endpoint trajectory during stabilization in the paretic limb of stroke subjects deviated from the vertical line more than the nonparetic limb and dominant and nondominant arms of control subjects. In general, the principle axis of the endpoint stiffness ellipse is tuned to the instability of the environment (Franklin et al., 2007) and is approximately perpendicular to the final portion of movement trajectory (van Beers et al., 2004). For the point-to-point movements of the current study, environmental instability due to gravity and inertia of limb movement in the direction of movement trajectory could explain the overall instability at the final position experienced by the subjects. Orientation of the endpoint trajectory ellipses of the more stable nonparetic limb and control subject limbs (Figure 4-3) followed the movement trajectory along the circle, resulting in a mean value of approximately 90 degrees. The difference in the hemiparetic arm could originate from the difference in posture during tracking (Figure 4-6 and 4-7), as the endpoint stiffness is limb configuration dependent (Lametti & Ostry, 2010). Alternately, errors in control may have altered the trajectory of the final portion of the movement, resulting in changes in ellipse orientation.

4.4.3 Clinical implications

This study documents instability of the hemiparetic arm in stroke survivors using a laser pointing task. Arm stability is important in the complete assessment of neural motor control since instability could contribute to deficits in movement. Assessment of stability could provide a better understanding of the post-stroke deficits in neuromotor control. For example, when assessing instability of the endpoint in 2D planar movement in the medial-lateral direction, increased arm postural instability in stroke subjects is likely to originate from abnormal regulation of muscle co-activation, rather than the abnormal control of intersegmental torques (Mihaltchev et al., 2005). Also, some interventions, e.g. tendon vibration applied at the wrist flexor, improve stability function but not movement (Conrad et al., 2011). It is therefore important to assess stability function as well as movement function post stroke, as has been done by using the instability index (Mihaltchev et al., 2005) and stability error and error frequency (Conrad et al., 2011). Assessing arm stability using a laser pointer as in the current experiment can increase the sensitivity of the stability measurement.

Strengthening of the shoulder might improve arm posture and stability in people post stroke. As stated previously, the decreased plane of elevation in stroke subjects could result from shoulder weakness. In addition, as proximal joints are more specialized in the control of force, which is the main component in providing the stability (Nisky, Baraduc, & Karniel, 2010), strengthening the shoulder joint might improve overall stability of the paretic arm. For the stability task that needs co-contraction of the deltoid muscles, shoulder strength training could help increase stability of the shoulder. There is

evidence that strength training improves strength and function of the upper-limb in stroke subjects without inducing spasticity (Harris & Eng, 2010) and it could be done in combination with robotic therapy, as robotic therapy has shown to improve the fine control movement (Fasoli et al., 2004). Since a significant improvement in function using robotic therapy is not evident by a meta-analysis study, which included contribution from proximal and distal arm training (Kwakkel, Kollen, & Krebs, 2008), a combination of proximal strength training with the robotic therapy may help improve the overall stability and movement in people with post-stroke hemiparesis.

CHAPTER 5: INTEGRATION OF RESULTS

5.1 SUMMARY OF RESULTS

The results in this dissertation provide insight into the control of paretic arm movement and stability in people with post-stroke hemiparesis. The primary results of the study suggest that limits to paretic arm range of motion are related to shoulder weakness and elbow stiffness, that static and dynamic stability of the paretic arm are notably decreased, that stroke subjects place the arm in different baseline postures during a variety of movement tasks and that people with stroke have difficulty producing the graded muscle contractions necessary for fine motor control of the arm. Characterization of reaching, stability and tracking in people with post-stroke hemiparesis is summarized in the following subsections.

5.1.1 Reaching post-stroke

Reaching of the paretic arm was characterized by a limited range of joint motion at both the elbow and shoulder, with a more curved and non-smooth endpoint trajectory compared to the neurologically intact subjects. Limited shoulder motion was likely due to weakness of the shoulder joint as we observed from the reduced activity of the anterior deltoid muscle. Conversely, limited elbow motion appeared to be due to an increase in dynamic stiffness of the elbow, which could be associated with spasticity of the elbow

flexors, making elbow extension more difficult. Limited range of joint motion was observed in reaches towards six different target locations, with no effect of high/low or medial/lateral target placement. Trajectory smoothness, as quantified by the normalized jerk score (NJS), was significantly higher in the paretic arm during reaching. Paretic reaching trajectories were less smooth in the deceleration phase of reach compared to the acceleration phase (higher NJS in the deceleration phase), an effect that was also observed in controls. This finding indicated that the basic motor control mechanisms are likely preserved post stroke.

5.1.2 Arm stability post-stroke

When stabilizing the arm in different target locations within the reachable workspace, stroke subjects utilized a different arm posture as compared to controls. A significantly decreased plane of elevation was observed in stroke subjects, especially those who had low Fugl-Meyer scores. This arm posture could be associated with an abnormal flexor synergy, as the elbow generally remained flexed during the task. Shoulder abduction is often associated with elbow flexion in the flexor synergy pattern. Again, weakness of the anterior deltoid might have contributed to the postural differences, as efforts to elevate the shoulder would have relied more on posterior deltoid activity, thereby changing the plane of elevation as well.

5.1.3 Arm posture and movement post-stroke

When performing a laser pointing task, which simultaneously required both arm stability and fine movement, stroke subjects stabilized their paretic arm by significantly decreasing the plane of elevation and flexing the elbow, which was the same tendency as the non-dominant arm of control subjects. Similar to the stabilization task, the stroke subjects demonstrated a posture of decreased plane of elevation and elbow flexion, again possibly due to shoulder weakness and elbow stiffness. Furthermore, stroke subjects also demonstrated a deficit in the fine control movement during tracking by moving with greater angular range of motion, especially in the plane of elevation and elbow. This increase in angular range of motion likely reflected an impaired ability to finely grade muscle activity.

5.3 CLINICAL CONTRIBUTION

Characterization of the paretic arms during reaching, stabilizing and tracking in a 3D workspace suggested that reduced ADT activity is a common deficit that deteriorates task performance. The shoulder is generally the arm stabilizing joint. In stroke subjects, reduced ADT activity could contribute to shoulder weakness and thus affected the stability of the paretic arm of the low-FM subjects, especially for the stabilizing posture task when the paretic arm was in the reachable workspace (Chapter 3). For the tasks that required movement and stability (Chapter 2 and 4), shoulder joint of the paretic arms had to serve as both a stabilizer and a mover to produce joint motion, since elbow motion was

more restricted than shoulder motion in stroke subjects. Reduced ADT activity could make the movement more difficult and less efficient for stroke subjects as observed in the less smooth reaching (Chapter 2) and tracking (Chapter 4) trajectories. Targeted shoulder or upper arm strength training might be recommended in people with post-stroke hemiparesis to improve the paretic arm function. Note that shoulder strength training has demonstrated improved upper-limb function without inducing spasticity of the elbow (Harris & Eng, 2010).

5.4 FUTURE RESEARCH

The findings from this study suggest further investigation of stability and movement post-stroke with different arm postures is warranted. As the self-selected posture for stroke subjects was a decreased the plane of elevation, an experimental task that restrains posture to a different plane of elevation is an interesting study that could further characterize the multijoint movement and stability of the paretic arm. Furthermore, in order to investigate the role of tendon vibration in stability improvement of the paretic arm in 3D workspace, it may be helpful to design an experiment that involves on-line movement correction without having to stabilize the posture of the arm so that movement performance can be distinguished from the ability to stabilize the arm. A tracking task in the vertical plane similar to this study, with a support at the elbow which would provide gravity compensation at the shoulder joint, while still allowing motion of the shoulder and elbow joints, is one possibility.

REFERENCES

Aimonetti, J. M., Hospod, V., Roll, J. P., & Ribot-Ciscar, E. (2007). Cutaneous afferents provide a neuronal population vector that encodes the orientation of human ankle movements. *The Journal of Physiology, 580*(Pt. 2), 649-658.

Andrews, A. W., & Bohannon, R. W. (2000). Distribution of muscle strength impairments following stroke. *Clinical Rehabilitation, 14*(1), 79-87.

Barker, R. N., Brauer, S., & Carson, R. (2009). Training-induced changes in the pattern of triceps to biceps activation during reaching tasks after chronic and severe stroke. *Experimental Brain Research.Experimentelle Hirnforschung.Experimentation Cerebrale, 196*(4), 483-496.

Beebe, J. A., & Lang, C. E. (2008). Absence of a proximal to distal gradient of motor deficits in the upper extremity early after stroke. *Clinical Neurophysiology : Official Journal of the International Federation of Clinical Neurophysiology, 119*(9), 2074-2085.

Beer, R. F., Dewald, J. P., Dawson, M. L., & Rymer, W. Z. (2004). Target-dependent differences between free and constrained arm movements in chronic hemiparesis. *Experimental Brain Research.Experimentelle Hirnforschung.Experimentation Cerebrale, 156*(4), 458-470.

Beer, R. F., Dewald, J. P., & Rymer, W. Z. (2000). Deficits in the coordination of multijoint arm movements in patients with hemiparesis: Evidence for disturbed control of limb dynamics. *Experimental Brain Research.Experimentelle Hirnforschung.Experimentation Cerebrale, 131*(3), 305-319.

Beer, R. F., Ellis, M. D., Holubar, B. G., & Dewald, J. P. (2007). Impact of gravity loading on post-stroke reaching and its relationship to weakness. *Muscle & Nerve, 36*(2), 242-250.

Bhakta, B. B. (2000). Management of spasticity in stroke. *British Medical Bulletin, 56*(2), 476-485.

Bobath, B. (1977). Treatment of adult hemiplegia. *Physiotherapy, 63*(10), 310-313.

Bohannon, R. W. (1995). Measurement, nature, and implications of skeletal muscle strength in patients with neurological disorders. *Clinical Biomechanics (Bristol, Avon), 10*(6), 283-292.

Bohannon, R. W. (2007). Muscle strength and muscle training after stroke. *Journal of Rehabilitation Medicine : Official Journal of the UEMS European Board of Physical and Rehabilitation Medicine, 39*(1), 14-20.

Bourbonnais, D., & Vanden Noven, S. (1989). Weakness in patients with hemiparesis. *The American Journal of Occupational Therapy.: Official Publication of the American Occupational Therapy Association, 43*(5), 313-319.

Brunnstrom, S. (1970). *Movement therapy in hemiplegia:A neurophysiological approach* (1st ed.). New York: Medical Dept., Harper & Row.

Burdet, E., Tee, K. P., Mareels, I., Milner, T. E., Chew, C. M., Franklin, D. W., et al. (2006). Stability and motor adaptation in human arm movements. *Biological Cybernetics, 94*(1), 20-32.

Canning, C. G., Ada, L., & O'Dwyer, N. (1999). Slowness to develop force contributes to weakness after stroke. *Archives of Physical Medicine and Rehabilitation, 80*(1), 66-70.

Canning, C. G., Ada, L., & O'Dwyer, N. J. (2000). Abnormal muscle activation characteristics associated with loss of dexterity after stroke. *Journal of the Neurological Sciences, 176*(1), 45-56.

Celnik, P., Hummel, F., Harris-Love, M., Wolk, R., & Cohen, L. G. (2007). Somatosensory stimulation enhances the effects of training functional hand tasks in patients with chronic stroke. *Archives of Physical Medicine and Rehabilitation, 88*(11), 1369-1376.

Chae, J., Yang, G., Park, B. K., & Labatia, I. (2002). Muscle weakness and cocontraction in upper limb hemiparesis: Relationship to motor impairment and physical disability. *Neurorehabilitation and Neural Repair, 16*(3), 241-248.

Chandler, T. J., Kibler, W. B., Stracener, E. C., Ziegler, A. K., & Pace, B. (1992). Shoulder strength, power, and endurance in college tennis players. *The American Journal of Sports Medicine, 20*(4), 455-458.

Cirstea, M. C., & Levin, M. F. (2000). Compensatory strategies for reaching in stroke. *Brain : A Journal of Neurology, 123 (Pt 5)*(Pt 5), 940-953.

Cirstea, M. C., Mitnitski, A. B., Feldman, A. G., & Levin, M. F. (2003). Interjoint coordination dynamics during reaching in stroke. *Experimental Brain Research.Experimentelle Hirnforschung.Experimentation Cerebrale, 151*(3), 289-300. doi:10.1007/s00221-003-1438-0

Conforto, A. B., Cohen, L. G., dos Santos, R. L., Scaff, M., & Marie, S. K. (2007). Effects of somatosensory stimulation on motor function in chronic cortico-subcortical strokes. *Journal of Neurology, 254*(3), 333-339.

Conforto, A. B., Kaelin-Lang, A., & Cohen, L. G. (2002). Increase in hand muscle strength of stroke patients after somatosensory stimulation. *Annals of Neurology, 51*(1), 122-125.

Conrad, M. O., Scheidt, R. A., & Schmit, B. D. (2011). Effects of wrist tendon vibration on targeted upper-arm movements in poststroke hemiparesis. *Neurorehabilitation and Neural Repair, 25*(1), 61-70.

Cordo, P., Gurfinkel, V. S., Bevan, L., & Kerr, G. K. (1995). Proprioceptive consequences of tendon vibration during movement. *Journal of Neurophysiology, 74*(4), 1675-1688.

Cordo, P., Gurfinkel, V. S., Bevan, L., & Kerr, G. K. (1995). Proprioceptive consequences of tendon vibration during movement. *Journal of Neurophysiology, 74*(4), 1675-1688.

Daly, J. J., Hogan, N., Perepezko, E. M., Krebs, H. I., Rogers, J. M., Goyal, K. S., et al. (2005). Response to upper-limb robotics and functional neuromuscular stimulation following stroke. *Journal of Rehabilitation Research and Development, 42*(6), 723-736.

Danckert, J., Goldberg, L., & Broderick, C. (2009). Damage to superior parietal cortex impairs pointing in the sagittal plane. *Experimental Brain Research.Experimentelle Hirnforschung.Experimentation Cerebrale, 195*(2), 183-191.

David, G., Magarey, M.E., Jones, M.A., Dvir, Z., Türker, K.S., & Sharpe, M. (2000). EMG and strength correlates of selected shoulder muscles during rotations of the glenohumeral joint. *Clinical Biomechanics*, *15*(2), 95-102.

Davidson, A. G., & Buford, J. A. (2006). Bilateral actions of the reticulospinal tract on arm and shoulder muscles in the monkey: Stimulus triggered averaging. *Experimental Brain Research.Experimentelle Hirnforschung.Experimentation Cerebrale, 173*(1), 25-39.

de Kroon, J. R., Ijzerman, M. J., Chae, J., Lankhorst, G. J., & Zilvold, G. (2005). Relation between stimulation characteristics and clinical outcome in studies using electrical stimulation to improve motor control of the upper extremity in stroke. *Journal of Rehabilitation Medicine : Official Journal of the UEMS European Board of Physical and Rehabilitation Medicine, 37*(2), 65-74.

Desmurget, M., & Grafton, S. (2000). Forward modeling allows feedback control for fast reaching movements. *Trends in Cognitive Sciences, 4*(11), 423-431.

Desmurget, M., & Prablanc, C. (1997). Postural control of three-dimensional prehension movements. *Journal of Neurophysiology, 77*(1), 452-464.

Dewald, J. P., & Beer, R. F. (2001). Abnormal joint torque patterns in the paretic upper limb of subjects with hemiparesis. *Muscle & Nerve, 24*(2), 273-283.

Dewald, J. P., Pope, P. S., Given, J. D., Buchanan, T. S., & Rymer, W. Z. (1995). Abnormal muscle coactivation patterns during isometric torque generation at the elbow and shoulder in hemiparetic subjects. *Brain : A Journal of Neurology, 118 (Pt 2)*(Pt 2), 495-510.

Dounskaia, N., Fradet, L., Lee, G., Leis, B. C., & Adler, C. H. (2009). Submovements during pointing movements in parkinson's disease. *Experimental Brain Research.Experimentelle Hirnforschung.Experimentation Cerebrale, 193*(4), 529-544.

Ellis, M. D., Acosta, A. M., Yao, J., & Dewald, J. P. (2007). Position-dependent torque coupling and associated muscle activation in the hemiparetic upper extremity. *Experimental Brain Research.Experimentelle Hirnforschung.Experimentation Cerebrale, 176*(4), 594-602.

Ellis, M. D., Sukal-Moulton, T., & Dewald, J. P. (2009). Progressive shoulder abduction loading is a crucial element of arm rehabilitation in chronic stroke. *Neurorehabilitation and Neural Repair, 23*(8), 862-869.

Fang, Y., Daly, J. J., Sun, J., Hvorat, K., Fredrickson, E., Pundik, S., et al. (2009). Functional corticomuscular connection during reaching is weakened following stroke. *Clinical Neurophysiology : Official Journal of the International Federation of Clinical Neurophysiology, 120*(5), 994-1002.

Fasoli, S. E., Krebs, H. I., Stein, J., Frontera, W. R., Hughes, R., & Hogan, N. (2004). Robotic therapy for chronic motor impairments after stroke: Follow-up results. *Archives of Physical Medicine and Rehabilitation, 85*(7), 1106-1111.

Feldman, A. G., & Levin, M. F. (1995). The origin and use of positional frames of reference in motor control. *Behavioral and Brain Sciences, 18*(04), 723.

Fishbach, A., Roy, S. A., Bastianen, C., Miller, L. E., & Houk, J. C. (2005). Kinematic properties of on-line error corrections in the monkey. *Experimental Brain Research.Experimentelle Hirnforschung.Experimentation Cerebrale, 164*(4), 442-457.

Flanders, M., & Soechting, J. F. (1990). Arm muscle activation for static forces in three-dimensional space. *Journal of Neurophysiology, 64*(6), 1818-1837.

Flash, T., & Hogan, N. (1985). The coordination of arm movements: An experimentally confirmed mathematical model. *The Journal of Neuroscience : The Official Journal of the Society for Neuroscience, 5*(7), 1688-1703.

Foisy, M., & Feldman, A. G. (2006). Threshold control of arm posture and movement adaptation to load. *Experimental Brain Research.Experimentelle Hirnforschung.Experimentation Cerebrale, 175*(4), 726-744.

Fradet, L., Lee, G., & Dounskaia, N. (2008). Origins of submovements during pointing movements. *Acta Psychologica, 129*(1), 91-100.

Franklin, D. W., Liaw, G., Milner, T. E., Osu, R., Burdet, E., & Kawato, M. (2007). Endpoint stiffness of the arm is directionally tuned to instability in the environment. *The Journal of Neuroscience : The Official Journal of the Society for Neuroscience, 27*(29), 7705-7716.

Franklin, D. W., Osu, R., Burdet, E., Kawato, M., & Milner, T. E. (2003). Adaptation to stable and unstable dynamics achieved by combined impedance control and inverse dynamics model. *Journal of Neurophysiology, 90*(5), 3270-3282.

Gabriel, D. A. (1997). Shoulder and elbow muscle activity in goal-directed arm movements. *Experimental Brain Research.Experimentelle Hirnforschung.Experimentation Cerebrale, 116*(2), 359-366.

Gemperline, J. J., Allen, S., Walk, D., & Rymer, W. Z. (1995). Characteristics of motor unit discharge in subjects with hemiparesis. *Muscle & Nerve, 18*(10), 1101-1114.

Goldvasser, D., McGibbon, C. A., & Krebs, D. E. (2001). High curvature and jerk analyses of arm ataxia. *Biological Cybernetics, 84*(2), 85-90.

Gordon, J., Ghilardi, M. F., & Ghez, C. (1995). Impairments of reaching movements in patients without proprioception. I. spatial errors. *Journal of Neurophysiology, 73*(1), 347-360.

Gowland, C., deBruin, H., Basmajian, J. V., Plews, N., & Burcea, I. (1992). Agonist and antagonist activity during voluntary upper-limb movement in patients with stroke. *Physical Therapy, 72*(9), 624-633.

Gracies, J. M. (2005). Pathophysiology of spastic paresis. II: Emergence of muscle overactivity. *Muscle & Nerve, 31*(5), 552-571.

Gribble, P. L., Mullin, L. I., Cothros, N., & Mattar, A. (2003). Role of cocontraction in arm movement accuracy. *Journal of Neurophysiology, 89*(5), 2396-2405.

Gribble, P. L., & Ostry, D. J. (1998). Independent coactivation of shoulder and elbow muscles. *Experimental Brain Research.Experimentelle Hirnforschung.Experimentation Cerebrale, 123*(3), 355-360.

Harris, J. E., & Eng, J. J. (2010). Strength training improves upper-limb function in individuals with stroke: A meta-analysis. *Stroke; a Journal of Cerebral Circulation, 41*(1), 136-140.

Hoffman, J. D. (1992). *Numerical methods for engineers and scientists*. New York: McGraw-Hill.

Hogan, N. (1985). The mechanics of multi-joint posture and movement control. *Biological Cybernetics, 52*(5), 315-331.

Horstman, A.M., Beltman, M.J., Gerrits, K.H., Koppe, P., Janssen, T.W., Elich, P., & de Haan, A. (2008). Intrinsic muscle strength and voluntary activation of both lower limbs and functional performance after stroke. *Clinical Physiology and Functional Imaging, 28*(4), 251–261.

Jaric, S., Gottlieb, G. L., Latash, M. L., & Corcos, D. M. (1998). Changes in the symmetry of rapid movements. effects of velocity and viscosity. *Experimental Brain Research.Experimentelle Hirnforschung.Experimentation Cerebrale, 120*(1), 52-60.

Kamper, D. G., McKenna-Cole, A. N., Kahn, L. E., & Reinkensmeyer, D. J. (2002). Alterations in reaching after stroke and their relation to movement direction and impairment severity. *Archives of Physical Medicine and Rehabilitation, 83*(5), 702-707.

Kamper, D. G., & Zev Rymer, W. (1999). Effects of geometric joint constraints on the selection of final arm posture during reaching: A simulation study. *Experimental Brain Research.Experimentelle Hirnforschung.Experimentation Cerebrale, 126*(1), 134-138.

Kandel, E. R., Schwartz, J. H., & Jessell, T. M. (2000). *Principles of neural science* (4th ed.). New York: McGraw-Hill, Health Professions Division.

Katz, R. T., Rovai, G. P., Brait, C., & Rymer, W. Z. (1992). Objective quantification of spastic hypertonia: Correlation with clinical findings. *Archives of Physical Medicine and Rehabilitation, 73*(4), 339-347.

Kendall, F. P., McCreary, E. K., & Provance, P. G. (1993). *Muscles, testing and function : With posture and pain* (4th ed.). Baltimore, Md.: Williams & Wilkins.

Kimmerle, M., Mainwaring, L., & Borenstein, M. (2003). The functional repertoire of the hand and its application to assessment. *The American Journal of Occupational Therapy.: Official Publication of the American Occupational Therapy Association, 57*(5), 489-498.

Kimura, T., Haggard, P., & Gomi, H. (2006). Transcranial magnetic stimulation over sensorimotor cortex disrupts anticipatory reflex gain modulation for skilled action.

The Journal of Neuroscience : The Official Journal of the Society for Neuroscience, 26(36), 9272-9281.

Kisiel-Sajewicz, K., Fang, Y., Hrovat, K., Yue, G.H., Siemionow, V., Sun, C.K., Jaskólska, A., Jaskólski, A., Sahgal, V., & Daly, J.J. (2011).Weakening of Synergist Muscle Coupling During Reaching Movement in Stroke Patients. *Neurorehabil Neural Repair, 25*(4), 359-368.

Krebs, H. I., Aisen, M. L., Volpe, B. T., & Hogan, N. (1999). Quantization of continuous arm movements in humans with brain injury. *Proceedings of the National Academy of Sciences of the United States of America, 96*(8), 4645-4649.

Krutky, M. A., & Perreault, E. J. (2007). Motor cortical measures of use-dependent plasticity are graded from distal to proximal in the human upper limb. *Journal of Neurophysiology, 98*(6), 3230-3241. doi:10.1152/jn.00750.2007

Krutky, M. A., Ravichandran, V. J., Trumbower, R. D., & Perreault, E. J. (2010). Interactions between limb and environmental mechanics influence stretch reflex sensitivity in the human arm. *Journal of Neurophysiology, 103*(1), 429-440.

Kuiken, T.A., Lowery, M.M.& Stoykov, N.S. (2003). The effect of subcutaneous fat on myoelectric signal amplitude and crosstalk. *Prosthetics and Orthotics International*, *27*(1), 48–54.

Kurtzer, I., Herter, T. M., & Scott, S. H. (2005). Random change in cortical load representation suggests distinct control of posture and movement. *Nature Neuroscience, 8*(4), 498-504.

Kwakkel, G., Kollen, B. J., & Krebs, H. I. (2008). Effects of robot-assisted therapy on upper limb recovery after stroke: A systematic review. *Neurorehabilitation and Neural Repair, 22*(2), 111-121.

Lametti, D. R., & Ostry, D. J. (2010). Postural constraints on movement variability. *Journal of Neurophysiology, 104*(2), 1061-1067.

Lan, N., & Crago, P. E. (1994). Optimal control of antagonistic muscle stiffness during voluntary movements. *Biological Cybernetics, 71*(2), 123-135.

Larish, D. D., Volp, C. M., & Wallace, S. A. (1984). An empirical note on attaining a spatial target after distorting the initial conditions of movement via muscle vibration. *Journal of Motor Behavior, 16*(1), 76-83.

Lehman, G.J., & McGill, S.M. (1999). The importance of normalization in the interpretation of surface electromyography: a proof of principle. *Journal of Manipulative and Physiological Therapeutics*, 22(7), 444-446.

Leonard, C. T., Gardipee, K. A., Koontz, J. R., Anderson, J. H., & Wilkins, S. A. (2006). Correlation between impairment and motor performance during reaching tasks in subjects with spastic hemiparesis. *Journal of Rehabilitation Medicine : Official Journal of the UEMS European Board of Physical and Rehabilitation Medicine, 38*(4), 243-249.

Levin, M. F. (1996). Interjoint coordination during pointing movements is disrupted in spastic hemiparesis. *Brain : A Journal of Neurology, 119 (Pt 1)*(Pt 1), 281-293.

Levin, M. F., & Feldman, A. G. (1994). The role of stretch reflex threshold regulation in normal and impaired motor control. *Brain Research, 657*(1-2), 23-30.

Lum, P. S., Burgar, C. G., & Shor, P. C. (2003). Evidence for strength imbalances as a significant contributor to abnormal synergies in hemiparetic subjects. *Muscle & Nerve, 27*(2), 211-221.

Massion, J. (1992). Movement, posture and equilibrium: Interaction and coordination. *Progress in Neurobiology, 38*(1), 35-56.

Matsuyama, K., Mori, F., Nakajima, K., Drew, T., Aoki, M., & Mori, S. (2004). Locomotor role of the corticoreticular-reticulospinal-spinal interneuronal system. *Progress in Brain Research, 143*, 239-249.

Matthews, P. B. C. (1972). *Mammalian muscle receptors and their central actions*. London: Edward Arnold.

McCombe Waller, S., & Whitall, J. (2004). Fine motor control in adults with and without chronic hemiparesis: Baseline comparison to nondisabled adults and effects of bilateral arm training. *Archives of Physical Medicine and Rehabilitation, 85*(7), 1076-1083.

McCrea, P. H., & Eng, J. J. (2005). Consequences of increased neuromotor noise for reaching movements in persons with stroke. *Experimental Brain Research.Experimentelle Hirnforschung.Experimentation Cerebrale, 162*(1), 70-77.

McCrea, P. H., Eng, J. J., & Hodgson, A. J. (2002). Biomechanics of reaching: Clinical implications for individuals with acquired brain injury. *Disability and Rehabilitation, 24*(10), 534-541.

McCrea, P. H., Eng, J. J., & Hodgson, A. J. (2003). Time and magnitude of torque generation is impaired in both arms following stroke. *Muscle & Nerve, 28*(1), 46-53.

McCrea, P. H., Eng, J. J., & Hodgson, A. J. (2005). Saturated muscle activation contributes to compensatory reaching strategies after stroke. *Journal of Neurophysiology, 94*(5), 2999-3008.

McIntyre, J., Mussa-Ivaldi, F. A., & Bizzi, E. (1996). The control of stable postures in the multijoint arm. *Experimental Brain Research.Experimentelle Hirnforschung.Experimentation Cerebrale, 110*(2), 248-264.

Medendorp, W. P., Crawford, J. D., Henriques, D. Y., Van Gisbergen, J. A., & Gielen, C. C. (2000). Kinematic strategies for upper arm-forearm coordination in three dimensions. *Journal of Neurophysiology, 84*(5), 2302-2316.

Mercier, C., Bertrand, A. M., & Bourbonnais, D. (2005). Comparison of strength measurements under single-joint and multi-joint conditions in hemiparetic individuals. *Clinical Rehabilitation, 19*(5), 523-530.

Mercier, C., & Bourbonnais, D. (2004). Relative shoulder flexor and handgrip strength is related to upper limb function after stroke. *Clinical Rehabilitation, 18*(2), 215-221.

Meskers, C. G., Koppe, P. A., Konijnenbelt, M. H., Veeger, D. H., & Janssen, T. W. (2005). Kinematic alterations in the ipsilateral shoulder of patients with hemiplegia due to stroke. *American Journal of Physical Medicine & Rehabilitation / Association of Academic Physiatrists, 84*(2), 97-105.

Meskers, C. G., Schouten, A. C., de Groot, J. H., de Vlugt, E., van Hilten, B. J., van der Helm, F. C., et al. (2009). Muscle weakness and lack of reflex gain adaptation predominate during post-stroke posture control of the wrist. *Journal of Neuroengineering and Rehabilitation, 6*, 29.

Mihaltchev, P., Archambault, P. S., Feldman, A. G., & Levin, M. F. (2005). Control of double-joint arm posture in adults with unilateral brain damage. *Experimental Brain Research.Experimentelle Hirnforschung.Experimentation Cerebrale, 163*(4), 468-486.

Milner, T. E. (2002). Contribution of geometry and joint stiffness to mechanical stability of the human arm. *Experimental Brain Research.Experimentelle Hirnforschung.Experimentation Cerebrale, 143*(4), 515-519.

Milner, T. E., Cloutier, C., Leger, A. B., & Franklin, D. W. (1995). Inability to activate muscles maximally during cocontraction and the effect on joint stiffness. *Experimental Brain Research.Experimentelle Hirnforschung.Experimentation Cerebrale, 107*(2), 293-305.

Mirka, G. A. (1991). The quantification of EMG normalization error. *Ergonomics, 34*(3), 343-352.

Morrison, S., & Newell, K. M. (2000). Limb stiffness and postural tremor in the arm. *Motor Control, 4*(3), 293-315.

Mottram, C. J., Suresh, N. L., Heckman, C., Gorassini, M. A., & Rymer, W. Z. (2009). Origins of abnormal excitability in biceps brachii motoneurons of spastic-paretic stroke survivors. *Journal of Neurophysiology,*

Muellbacher, W., Richards, C., Ziemann, U., Wittenberg, G., Weltz, D., Boroojerdi, B., et al. (2002). Improving hand function in chronic stroke. *Archives of Neurology, 59*(8), 1278-1282.

Musampa, N. K., Mathieu, P. A., & Levin, M. F. (2007). Relationship between stretch reflex thresholds and voluntary arm muscle activation in patients with spasticity. *Experimental Brain Research.Experimentelle Hirnforschung.Experimentation Cerebrale, 181*(4), 579-593.

Mussa-Ivaldi, F. A., Hogan, N., & Bizzi, E. (1985). Neural, mechanical, and geometric factors subserving arm posture in humans. *The Journal of Neuroscience : The Official Journal of the Society for Neuroscience, 5*(10), 2732-2743.

Nagasaki, H. (1989). Asymmetric velocity and acceleration profiles of human arm movements. *Experimental Brain Research.Experimentelle Hirnforschung.Experimentation Cerebrale, 74*(2), 319-326.

Naito, E., Nakashima, T., Kito, T., Aramaki, Y., Okada, T., & Sadato, N. (2007). Human limb-specific and non-limb-specific brain representations during kinesthetic illusory movements of the upper and lower extremities. *The European Journal of Neuroscience, 25*(11), 3476-3487.

Nielsen, J. F., & Sinkjaer, T. (1996). A comparison of clinical and laboratory measures of spasticity. *Multiple Sclerosis (Houndmills, Basingstoke, England), 1*(5), 296-301.

Niessen, M. H., Veeger, D. H., Koppe, P. A., Konijnenbelt, M. H., van Dieen, J., & Janssen, T. W. (2008). Proprioception of the shoulder after stroke. *Archives of Physical Medicine and Rehabilitation, 89*(2), 333-338.

Nisky, I., Baraduc, P., & Karniel, A. (2010). Proximodistal gradient in the perception of delayed stiffness. *Journal of Neurophysiology, 103*(6), 3017-3026.

Novak, K. E., Miller, L. E., & Houk, J. C. (2002). The use of overlapping submovements in the control of rapid hand movements. *Experimental Brain Research.Experimentelle Hirnforschung.Experimentation Cerebrale, 144*(3), 351-364.

Osu, R., Franklin, D. W., Kato, H., Gomi, H., Domen, K., Yoshioka, T., et al. (2002). Short- and long-term changes in joint co-contraction associated with motor learning as revealed from surface EMG. *Journal of Neurophysiology, 88*(2), 991-1004.

Parkinson, A., Condon, L., & Jackson, S. R. (2010). Parietal cortex coding of limb posture: In search of the body-schema. *Neuropsychologia, 48*(11), 3228-3234.

Patten, C., Lexell, J., & Brown, H. E. (2004). Weakness and strength training in persons with poststroke hemiplegia: Rationale, method, and efficacy. *Journal of Rehabilitation Research and Development, 41*(3A), 293-312.

Patton, J. L., Stoykov, M. E., Kovic, M., & Mussa-Ivaldi, F. A. (2006). Evaluation of robotic training forces that either enhance or reduce error in chronic hemiparetic stroke survivors. *Experimental Brain Research.Experimentelle Hirnforschung.Experimentation Cerebrale, 168*(3), 368-383.

Perreault, E.J., Hunter, I.W., Kearney, R.E. (1993) Quantitative analysis of four EMG amplifiers. *J Biomed Eng,* 15(5), 413–419.

Perreault, E. J., Kirsch, R. F., & Crago, P. E. (2004). Multijoint dynamics and postural stability of the human arm. *Experimental Brain Research.Experimentelle Hirnforschung.Experimentation Cerebrale, 157*(4), 507-517.

Peurala, S. H., Pitkanen, K., Sivenius, J., & Tarkka, I. M. (2002). Cutaneous electrical stimulation may enhance sensorimotor recovery in chronic stroke. *Clinical Rehabilitation, 16*(7), 709-716.

Pilon, J. F., De Serres, S. J., & Feldman, A. G. (2007). Threshold position control of arm movement with anticipatory increase in grip force. *Experimental Brain Research.Experimentelle Hirnforschung.Experimentation Cerebrale, 181*(1), 49-67.

Popescu, F., Hidler, J. M., & Rymer, W. Z. (2003). Elbow impedance during goal-directed movements. *Experimental Brain Research.Experimentelle Hirnforschung.Experimentation Cerebrale, 152*(1), 17-28.

Prange, G. B., Jannink, M. J., Stienen, A. H., van der Kooij, H., Ijzerman, M. J., & Hermens, H. J. (2009). Influence of gravity compensation on muscle activation patterns during different temporal phases of arm movements of stroke patients. *Neurorehabilitation and Neural Repair, 23*(5), 478-485.

Reinkensmeyer, D. J., McKenna Cole, A., Kahn, L. E., & Kamper, D. G. (2002). Directional control of reaching is preserved following mild/moderate stroke and stochastically constrained following severe stroke. *Experimental Brain Research.Experimentelle Hirnforschung.Experimentation Cerebrale, 143*(4), 525-530. doi:10.1007/s00221-002-1055-3

Ridding, M. C., Brouwer, B., Miles, T. S., Pitcher, J. B., & Thompson, P. D. (2000). Changes in muscle responses to stimulation of the motor induced by peripheral nerve stimulation in human subjects. *Experimental Brain Research, 131*(1), 135-143.

Riemann, B. L., & Lephart, S. M. (2002). The sensorimotor system, part I: The physiologic basis of functional joint stability. *Journal of Athletic Training, 37*(1), 71-79.

Rohrer, B., Fasoli, S., Krebs, H. I., Hughes, R., Volpe, B., Frontera, W. R., et al. (2002). Movement smoothness changes during stroke recovery. *The Journal of Neuroscience : The Official Journal of the Society for Neuroscience, 22*(18), 8297-8304.

Rohrer, B., Fasoli, S., Krebs, H. I., Volpe, B., Frontera, W. R., Stein, J., et al. (2004). Submovements grow larger, fewer, and more blended during stroke recovery. *Motor Control, 8*(4), 472-483.

Roll, J. P., Vedel, J. P., & Ribot, E. (1989). Alteration of proprioceptive messages induced by tendon vibration in man: A microneurographic study. *Experimental Brain Research.Experimentelle Hirnforschung.Experimentation Cerebrale, 76*(1), 213-222.

Sainburg, R. L., Ghilardi, M. F., Poizner, H., & Ghez, C. (1995). Control of limb dynamics in normal subjects and patients without proprioception. *Journal of Neurophysiology, 73*(2), 820-835.

Sangani, S. G., Starsky, A. J., McGuire, J. R., & Schmit, B. D. (2007). Multijoint reflexes of the stroke arm: Neural coupling of the elbow and shoulder. *Muscle & Nerve, 36*(5), 694-703.

Sangani, S. G., Starsky, A. J., McGuire, J. R., & Schmit, B. D. (2009). Multijoint reflex responses to constant-velocity volitional movements of the stroke elbow. *Journal of Neurophysiology, 102*(3), 1398-1410.

Sarlegna, F. R., Malfait, N., Bringoux, L., Bourdin, C., & Vercher, J. L. (2010). Force-field adaptation without proprioception: Can vision be used to model limb dynamics? *Neuropsychologia, 48*(1), 60-67.

Sarlegna, F. R., & Sainburg, R. L. (2009). The roles of vision and proprioception in the planning of reaching movements. In D. Sternad (Ed.), *Progress in motor control* (pp. 317-335) Springer US.

Scheidt, R. A., Conditt, M. A., Secco, E. L., & Mussa-Ivaldi, F. A. (2005). Interaction of visual and proprioceptive feedback during adaptation of human reaching movements. *Journal of Neurophysiology, 93*(6), 3200-3213.

Scheidt, R. A., & Ghez, C. (2007). Separate adaptive mechanisms for controlling trajectory and final position in reaching. *Journal of Neurophysiology, 98*(6), 3600-3613.

Scheidt, R. A., & Stoeckmann, T. (2007). Reach adaptation and final position control amid environmental uncertainty after stroke. *Journal of Neurophysiology, 97*(4), 2824-2836.

Schmit, B. D., Dhaher, Y., Dewald, J. P., & Rymer, W. Z. (1999). Reflex torque response to movement of the spastic elbow: Theoretical analyses and implications for quantification of spasticity. *Annals of Biomedical Engineering, 27*(6), 815-829.

Schwerin, S., Dewald, J. P., Haztl, M., Jovanovich, S., Nickeas, M., & MacKinnon, C. (2008). Ipsilateral versus contralateral cortical motor projections to a shoulder adductor in chronic hemiparetic stroke: Implications for the expression of arm synergies. *Experimental Brain Research.Experimentelle Hirnforschung.Experimentation Cerebrale, 185*(3), 509-519.

Schwerin, S., Dewald, J. P., Haztl, M., Jovanovich, S., Nickeas, M., & MacKinnon, C. (2008). Ipsilateral versus contralateral cortical motor projections to a shoulder adductor in chronic hemiparetic stroke: Implications for the expression of arm synergies. *Experimental Brain Research.Experimentelle Hirnforschung.Experimentation Cerebrale, 185*(3), 509-519.

Seidler, R. D., Alberts, J. L., & Stelmach, G. E. (2001). Multijoint movement control in parkinson's disease. *Experimental Brain Research.Experimentelle Hirnforschung.Experimentation Cerebrale, 140*(3), 335-344.

Sergio, L. E., Hamel-Paquet, C., & Kalaska, J. F. (2005). Motor cortex neural correlates of output kinematics and kinetics during isometric-force and arm-reaching tasks. *Journal of Neurophysiology, 94*(4), 2353-2378.

Shapiro, M. B., Gottlieb, G. L., Moore, C. G., & Corcos, D. M. (2002). Electromyographic responses to an unexpected load in fast voluntary movements: Descending regulation of segmental reflexes. *Journal of Neurophysiology, 88*(2), 1059-1063.

Shapiro, M., Niu, C., Poon, C., David, F., & Corcos, D. (2009). Proprioceptive feedback during point-to-point arm movements is tuned to the expected dynamics of the task. *Experimental Brain Research, 195*(4), 575-591.

Shirahashi, I., Matsumoto, S., Shimodozono, M., Etoh, S., & Kawahira, K. (2007). Functional vibratory stimulation on the hand facilitates voluntary movements of a hemiplegic upper limb in a patient with stroke. *International Journal of Rehabilitation Research.Internationale Zeitschrift Fur Rehabilitationsforschung.Revue Internationale De Recherches De Readaptation, 30*(3), 227-230.

Takahashi, C. D., & Reinkensmeyer, D. J. (2003). Hemiparetic stroke impairs anticipatory control of arm movement. *Experimental Brain Research.Experimentelle Hirnforschung.Experimentation Cerebrale, 149*(2), 131-140.

Teulings, H. L., Contreras-Vidal, J. L., Stelmach, G. E., & Adler, C. H. (1997). Parkinsonism reduces coordination of fingers, wrist, and arm in fine motor control. *Experimental Neurology, 146*(1), 159-170.

Trumbower, R. D., Ravichandran, V. J., Krutky, M. A., & Perreault, E. J. (2008). Altered multijoint reflex coordination is indicative of motor impairment level following stroke. *Conference Proceedings : ...Annual International Conference of the IEEE Engineering in Medicine and Biology Society.IEEE Engineering in Medicine and Biology Society.Conference, 2008*, 3558-3561.

Trumbower, R. D., Ravichandran, V. J., Krutky, M. A., & Perreault, E. J. (2010). Contributions of altered stretch reflex coordination to arm impairments following stroke. *Journal of Neurophysiology, 104*(6), 3612-3624.

Tsao, C. C., & Mirbagheri, M. M. (2007). Upper limb impairments associated with spasticity in neurological disorders. *Journal of Neuroengineering and Rehabilitation, 4*, 45.

Tyson, S. F., Hanley, M., Chillala, J., Selley, A. B., & Tallis, R. C. (2008). Sensory loss in hospital-admitted people with stroke: Characteristics, associated factors, and relationship with function. *Neurorehabilitation and Neural Repair, 22*(2), 166-172.

van Beers, R. J., Haggard, P., & Wolpert, D. M. (2004). The role of execution noise in movement variability. *Journal of Neurophysiology, 91*(2), 1050-1063.

Vercher, J. L., Sares, F., Blouin, J., Bourdin, C., & Gauthier, G. (2003). Role of sensory information in updating internal models of the effector during arm tracking. *Progress in Brain Research, 142*, 203-222.

Wang, J., & Sainburg, R. L. (2007). The dominant and nondominant arms are specialized for stabilizing different features of task performance. *Experimental Brain Research.Experimentelle Hirnforschung.Experimentation Cerebrale, 178*(4), 565-570.

Wang, X. (1999). Three-dimensional kinematic analysis of influence of hand orientation and joint limits on the control of arm postures and movements. *Biological Cybernetics, 80*(6), 449-463.

Wiegner, A. W., & Wierzbicka, M. M. (1992). Kinematic models and human elbow flexion movements: Quantitative analysis. *Experimental Brain Research.Experimentelle Hirnforschung.Experimentation Cerebrale, 88*(3), 665-673.

Winstein, C. J., Merians, A. S., & Sullivan, K. J. (1999). Motor learning after unilateral brain damage. *Neuropsychologia, 37*(8), 975-987.

Winward, C. E., Halligan, P. W., & Wade, D. T. (2007). Somatosensory recovery: A longitudinal study of the first 6 months after unilateral stroke. *Disability and Rehabilitation, 29*(4), 293-299.

Wisleder, D., & Dounskaia, N. (2007). The role of different submovement types during pointing to a target. *Experimental Brain Research.Experimentelle Hirnforschung.Experimentation Cerebrale, 176*(1), 132-149.

Wittstein, J., Queen, R., Abbey, A., & Moorman, C. T.,3rd. (2010). Isokinetic testing of biceps strength and endurance in dominant versus nondominant upper extremities. *Journal of Shoulder and Elbow Surgery / American Shoulder and Elbow Surgeons ...[Et Al.], 19*(6), 874-877.

Wolf, S. L., Catlin, P. A., Blanton, S., Edelman, J., Lehrer, N., & Schroeder, D. (1994). Overcoming limitations in elbow movement in the presence of antagonist hyperactivity. *Physical Therapy, 74*(9), 826-835.

Won, J., & Hogan, N. (1995). Stability properties of human reaching movements. *Experimental Brain Research.Experimentelle Hirnforschung.Experimentation Cerebrale, 107*(1), 125-136.

Woodworth, R. S. (1989). The accuracy of voluntary movement. *Journal of Nervous & Mental Disease, 26*(12), 743-752.

Wu, C. W., Seo, H. J., & Cohen, L. G. (2006). Influence of electric somatosensory stimulation on paretic-hand function in chronic stroke. *Archives of Physical Medicine and Rehabilitation, 87*(3), 351-357.

Yang, W. (2005). *Applied numerical methods using MATLAB*. Hoboken, N.J.: Wiley-Interscience.

Zackowski, K. M., Dromerick, A. W., Sahrmann, S. A., Thach, W. T., & Bastian, A. J. (2004). How do strength, sensation, spasticity and joint individuation relate to the reaching deficits of people with chronic hemiparesis? *Brain : A Journal of Neurology, 127*(Pt 5), 1035-1046.

Zorowitz, R. D., Chen, E., Tong, K. B., & Laouri, M. (2009). Costs and rehabilitation use of stroke survivors: A retrospective study of medicare beneficiaries. *Topics in Stroke Rehabilitation, 16*(5), 309-320.

APPENDIX A: 3D UPPER EXTREMITY JOINT KINEMATIC

Joint angles (elevation, plane of elevation, humeral rotation and elbow flexion) were calculated from the positions of the virtual markers of the specified bony landmarks (GH-glenohumeral joint, EL- lateral epicondyle, EM-medial epicondyle, US- styloid process of ulnar and RS-styloid process of radius). The local joint coordinate system is defined below.

A. Reference upper arm coordinate was obtained during calibration where the elevation is 0 degree, plane of elevation is 90 degrees, humeral rotation is 0 degree and elbow flexion is 90 degrees. The center of coordinate is at GH.

$$Y_H = \frac{(GH-Elbow)}{\|(GH-Elbow)\|}, Z_H = \frac{(GH-Elbow)\times(Wrist-Elbow)}{\|(GH-Elbow)\times(Wrist-Elbow)\|} \text{ and } X_H = Y_H \times Z_H,$$

where $Elbow = \frac{(EL+EM)}{2}$, and $Wrist = \frac{(US+RS)}{2}$.

B. Upper arm coordinate was obtained similarly to the reference upper arm coordinate except that GH,EL and EM were the positions during motion, not at the stationary calibrate position. The center of coordinate is at Elbow.

$$Y_h = \frac{(GH-Elbow)}{\|(GH-Elbow)\|}, Z_h = \frac{(GH-Elbow)\times(Wrist-Elbow)}{\|(GH-Elbow)\times(Wrist-Elbow)\|} \text{ and } X_h = Y_h \times Z_h$$

C. Lower arm coordinate was obtained from the EL, EM,US and RS positions during the arm motion, defined as following. Center of coordinate is at Wrist.

$$Y_f = \frac{(Elbow-Wrist)}{\|(Elbow-Wrist)\|}, Z_f = \frac{(GH-Elbow)\times(Wrist-Elbow)}{\|(GH-Elbow)\times(Wrist-Elbow)\|} \text{ and } X_f = Y_f \times Z_f,$$

where $Elbow = \frac{(EL+EM)}{2}$, and $Wrist = \frac{(US+RS)}{2}$.

Definition of each joint angle is as following.

1) Elevation (θ) was defined as the angle between the upper – arm (Y_h) and the body which approximately coincided with the vertical reference vector (Y_H). Elevation is equivalent to clinical shoulder flexion.

2) Plane of elevation (α) is the angle between the horizontal projection of the upper –arm (Y_h') and the reference vector pointing to the right side of the body (Z_H for the right arm and $-Z_H$ for the left arm) which is equivalent to the clinical shoulder horizontal abduction/adduction. Increase in the plane of elevation is equivalent to the horizontal adduction and decreased in the plane of elevation is equivalent to the motion of horizontal abduction.

3) Humeral rotation (γ) is calculated from the angle between the projection of the lower – arm on the cross –sectional plane of the upper –arm (Z_f') and the cross product of Y_h and Z_h (X_h). Positive value is the external rotation and negative value is the internal rotation.

4) Elbow angle (β) is the angle between the upper-arm (Y_h) and the lower-arm ($-Y_f$) which is equivalent to the elbow flexion/extension angle.

Calculation equations are described in Table A-1.

Table A-1 Calculation of joint angles

Joint Angles	Calculation
(Humeral) Elevation (θ) 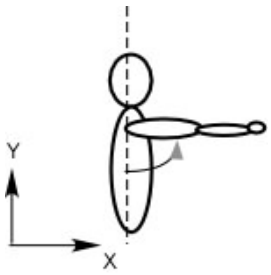 	$\theta = \cos^{-1}\left(\frac{Y_H * Y_h}{\lvert Y_H \rvert \lvert Y_h \rvert}\right)$
Plane of Elevation (α) 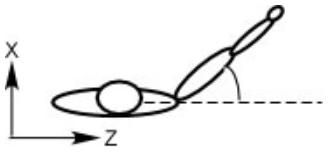 	$\alpha = \cos^{-1}\left(\frac{Z_H * Y_h^{'}}{\lvert Z_H \rvert \lvert Y_h^{'} \rvert}\right)$ Note: For the left arm, Z_H is replaced by $-Z_H$
Humeral Rotation (γ)	$\gamma = \sin^{-1}\left(\frac{X_h * (-Y_f')}{\lvert X_h \rvert \lvert (-Y_f') \rvert}\right)$, where $+\gamma$ = external rotation $-\gamma$ = internal rotation
Elbow (β)	$\beta = \cos^{-1}\left(\frac{Y_h * Y_f}{\lvert Y_h \rvert \lvert Y_f \rvert}\right)$

APPENDIX B: SENSORY STIMULATION POST-STROKE

Sensory stimulation, i.e. tendon vibration, applied at the wrist of the paretic arm improves stability of the paretic arm in 2D planar movement (Conrad et al, 2011). However, the effect of improved arm stability with wrist vibration was not observed in the 3D tasks of the present study. Since increased Ia afferent feedback associated with vibration can cause a proprioception illusion of the vibrated joint (Cordo et al., 1995), changes in joint angles with vibration are likely to be observed. A difference in humeral rotation posture with wrist vibration was observed only in the tracking tasks (Chapter 4 experiment), but not in the stabilization task (Chapter 3 experiment). That is, tendon vibration at the wrist flexors could alter proprioception of the forearm and thus result in more internal rotation of the shoulder, an effect that was also seen in subjects with impaired proprioception. This conclusion needs further investigation since the joint movement in the current studies was self-selected and the sample size of normal and impaired proprioception subjects was small.

B.1 Effect of vibration and electrical stimulation on arm posture during stabilization

An analysis on the arm posture of the stroke subjects (see experimental setup and methods in Chapter 3) during tendon vibration and electrical stimulation was conducted to determine whether wrist stimulation had any impact on the manner in which stroke subjects attempted arm stabilization at five targets. A 3-way (2 subject groups x 5 targets

x 4 blocks) ANOVA with repeated measures on the last two factors was used to compare the final joint angles among the four experiment blocks of baseline (B), wrist vibration (V), median nerve electrical stimulation at the wrist (E) and the combination of vibration and electrical stimulation (V+E). The results are shown in Figure B-1.

During stabilization, tendon vibration, electrical stimulation or the combination of them did not significantly affect the arm posture in either stroke or control subjects. No significant difference among experiment blocks was found in plane of elevation, elevation, humeral rotation or elbow flexion without any interaction effect from target location (plane of elevation: $F_{12,156} = 0.665$, $p=0.783$; elevation: $F_{12,156} = 0.794$, $p=0.657$; humeral rotation: $F_{12,156} = 0.954$, $p=0.495$; elbow: $F_{12,156} = 1.003$, $p=0.449$) or from subject group (plane of elevation: $F_{3,39} = 2.411$, $p=0.081$; humeral rotation: $F_{3,39} = 0.954$, $p=0.495$; elbow: $F_{3,39} = 1.003$, $p=0.449$) except for the elevation (elevation: $F_{3,39} = 2.982$, $p=0.043$). Separate analysis for each subject group did not find a significant difference among blocks for either stroke ($F_{3,27} = 1.816$, $p=0.168$) or control subjects ($F_{3,12} = 1.823$, $p=0.197$).

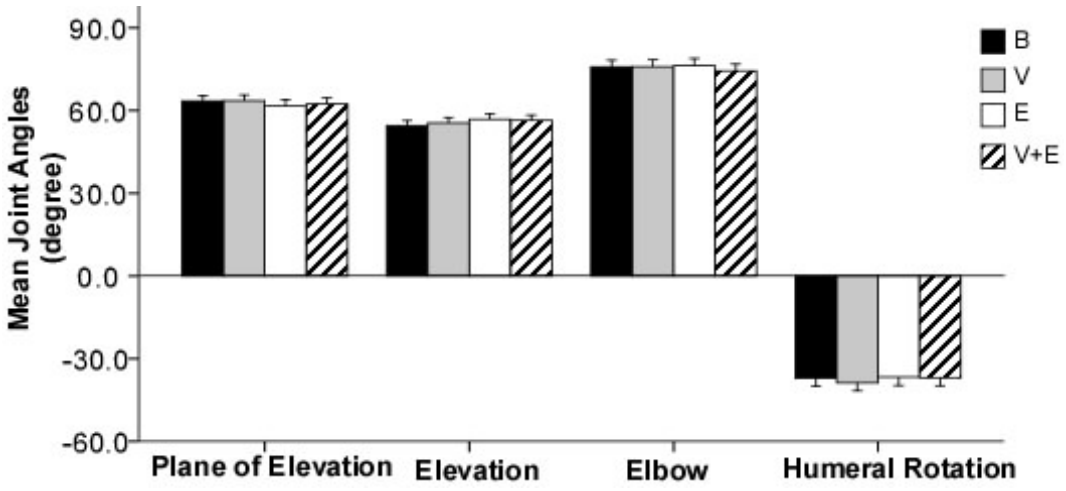

Figure B-1: Mean joint angle at the end position for each experiment block in post-stroke hemiparesis. Electrical stimulation (E) caused a significantly decreased plane of elevation and a significant increase in shoulder elevation compared to the baseline (B). Tendon vibration (V) caused significantly more internal humeral rotation.

B.2 Effect of vibration on arm posture during discrete and continuous tracking

Although the stability of the arm during tracking tasks using a laser pointer was not significantly improved with wrist vibration, postural effects similar to those associated with stabilizing the arm in space were observed. The experimental protocols for discrete and continuous tracking tasks are described in Chapter 4. We also conducted a test in which the second experimental block (non-paretic arm for stroke subjects and the second tested arm for control subjects) was followed by a vibration block. Vibration (90 Hz, <0.5 mm amplitude) was applied at the wrist flexor tendon (FCR) when the LED targets were present. In the vibration block, the vibrator was applied to the wrist flexor of the first tested arm (paretic arm for stroke subjects and randomly, the dominant or nondominant arm for control subjects) and the vibration was turned on for the entire time that the cursor was present on the screen. For stroke subjects, additional sessions of

placebo vibration were conducted (>1 week later). The measurements in the placebo vibration session were the same as the actual vibration session except that the stroke subjects were convinced that they received special vibration that they could not feel, but gave the same effect. During the vibration block of the placebo session, the vibrator was secured over the wrist flexors, similar to the true vibration session, without turning the vibrator on. All stroke subjects were convinced that they received tendon vibration that they could not perceive.

Comparison of the mean joint angles during tracking between the paretic block (first tested arm for control) and the vibration block was conducted using a one-way (3 blocks) repeated measures ANOVA. In discrete tracking, increased internal humeral rotation with vibration was observed in both control ($F_{1,9}$=51.574, p<0.001) and stroke subjects during the actual vibration session ($F_{1,9}$=7.049, p=0.038) but not in the placebo session ($F_{1,9}$=0.990, p=0.346). Significant decreases in shoulder elevation ($F_{1,9}$=20.566, p=0.001) and elbow extension ($F_{1,9}$=17.449, p=0.002) were also observed in the control subjects. Likewise, significantly more internal humeral rotation was found with vibration during continuous tracking in both control ($F_{1,9}$=5.977, p=0.037) and stroke subjects ($F_{1,9}$=9.251, p=0.016) but not in the placebo session ($F_{1,9}$=0.524, p=0.487). Decreased elbow extension with vibration was also observed during the continuous tracking task in both control ($F_{1,9}$=6.100, p=0.036) and stroke subjects ($F_{1,9}$=10.958, p=0.011). Shoulder elevation was consistently decreased in the vibration block for the control subjects ($F_{1,9}$=6.986, p=0.027). No significant differences were found with tendon vibration during tracking for the mean joint angles of the placebo session.

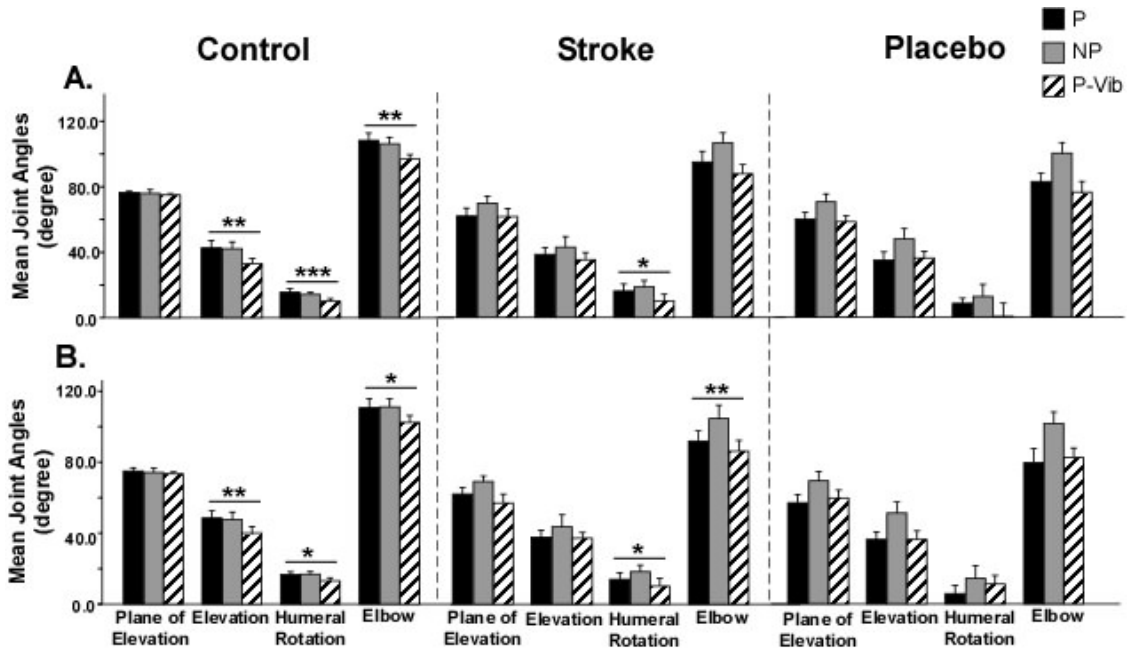

Figure B-2: Effects of tendon vibration on arm posture during tracking A. In the discrete tracking task, both control and stroke subjects had significantly more internal rotation with vibration, which was not observed in the placebo session. Significant decreases in shoulder elevation and elbow extension with vibration were also observed in control subjects. **B.** In continuous tracking, significantly greater internal humeral rotation and greater elbow flexion were observed with vibration in both control and stroke subjects, which was not observed in the placebo session. A significant decrease in shoulder elevation with vibration was also observed in the control subjects. P is the paretic arm for stroke subjects and the first tested arm for control subjects. NP is the nonparetic arm (stroke) or the second tested arm (control). P-Vib is the vibration trial block for the tested arm in P block. The statistical test was a repeated-measures ANOVA between P and P-Vib groups (*$p<0.05$, **$p<0.01$, ***$p<0.001$).

The results suggested that tendon vibration applied at the wrist level produced an increase in internal humeral rotation, as it was consistently observed in both control and stroke subjects, but not in the placebo trials. Even though it was confirmed from the placebo trials that the arm posture did not change with wrist tendon vibration, the effect of the tendon vibration on humeral rotation needs further investigation, since arm posture in this experimental protocol was self-selected, with minimum constraint. At this point, it

is unclear if the increased internal rotation with tendon vibration was compensation for an illusion effect at the wrist, or an arbitrary change for comfortable posture.

B.3 Effects of proprioceptive impairment

The effects of a proprioception deficit in the paretic arm of the stroke subjects on laser pointer tracking were examined with the notion that proprioceptive impairment may cause impaired subjects to have a different arm posture than subjects with normal proprioception. Proprioceptive impairment was assessed using the thumb localizing test (Hirayama, 1999) and classified as 'normal' or 'impaired' (Table B-1). There were 3 subjects with normal proprioception and 7 subjects with impaired proprioception. The mean Fugl-Meyer score for the normal (mean 50.33, standard deviation 21.08) and the impaired (mean 44.71, standard deviation 11.98) proprioception was not significantly different ($F_{1,8}$=0.303, p=0.597).

Table B-1 Summary of subject sample

Subject	Sex	Age (Years)	Paretic Side	FM Score[#]	Proprioception
1S	M	53	R	40	Impaired
2S	F	61	L	26	Normal
3S	F	60	R	50	Impaired
4S	F	63	L	62	Normal
5S	M	63	R	42	Impaired
6S	M	58	R	29	Impaired
7S	M	55	R	36	Impaired
8S	F	59	L	50	Impaired
9S	F	54	R	63	Normal
10S	F	40	L	66	Impaired

Subjects performed the discrete and continuous laser pointer tracking tasks (as in Chapter 4) with their paretic arms for day 1 and day 2 (>1 week apart). The mean joint angles during the baseline blocks of both sessions were averaged (to minimize the day-to-day variability) for the comparison between the normal and impaired proprioception groups using a univariate ANOVA. Subjects with impaired proprioception had significantly greater internal humeral rotation than subjects with normal proprioception during both the discrete (ANOVA; $F_{1,8}=15.071$, $p=0.005$) and continuous ($F_{1,8}=10.466$, $p=0.012$) tracking tasks. As this observation was done in groups with small and unequal number of subjects, further investigation is needed.

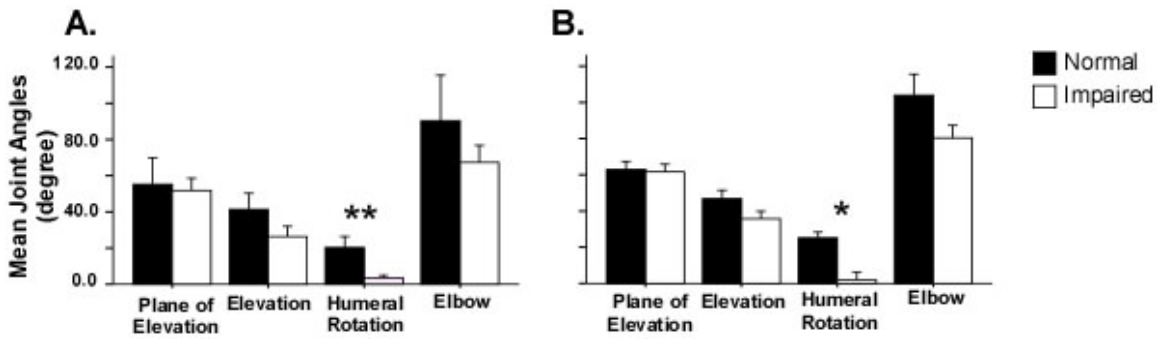

Figure B-3: Effects of proprioceptive impairment. Mean joint angles during **A.** discrete and **B.** continuous tracking tasks performed by the paretic arms of 10 stroke subjects (3 normal and 7 impaired proprioception subjects). Subjects with impaired proprioception had significantly more internal humeral rotation than subjects with normal proprioception (**$p<0.01$, *$p<0.05$).